Iron Release in Microelectrolysis Treatment for Arsenic Removal from Landfill Gas Condensate and Its Use to Predict Arsenic Removal Efficiency

Wanyu Mao

A thesis

submitted in partial fulfillment of the

requirements for the degree of

Master of Science

University of Washington

2024

Committee:

Gregory Korshin

Jessica Ray

Program Authorized to Offer Degree:

Civil and Environmental Engineering

University of Washington

Abstract

Iron Release in Microelectrolysis Treatment for Arsenic Removal from Landfill Gas Condensate and Its Use to Predict Arsenic Removal Efficiency

Wanyu Mao

Chair of the Supervisory Committee

Gregory Korshin

Department of Civil and Environmental Engineering

Abstract

Arsenic poses a significant threat as a highly hazardous contaminant. Its concentrations are particularly high in landfill gas (LFG) condensate, a byproduct of landfill gas purification, and landfill leachate generated at sites with combined LFG and renewable natural gas (RNG) production. This thesis addresses several aspects of the utilization of micro-electrolysis (ME) techniques for arsenic removal from LFG-derived condensate, specifically focusing on the release of iron solutes and colloidal particles from zero-valent iron (ZVI), a key component of ME treatment. The study encompasses multiple experiments aimed at quantifying and optimizing the ME process, with the objective of exploring alternative options for arsenic removal monitoring, and maximizing resource utilization. Another aspect of this study is that ME treatment is accompanied by release of high concentrations of iron whose presence may lead to challenges in post-treatment scenarios such as the formation of voluminous solids and contamination due to the presence of excessively high iron levels. To tackle this issue, a thorough analysis was conducted

to characterize iron content, particle sizes, ZVI weight loss, and other parameters relevant to ME treatment and its effluent properties.

Experiments reported in this thesis further explored the kinetics of iron release during the ME treatment process and compared the results using different analytical methods. The findings from this study suggest that field-enabled spectrophotometric (or color) measurements of iron concentrations can be used as a sufficiently reliable surrogate parameter with which to predict the removal of arsenic and co-occurring elements such as antimony in ME treatment under most circumstances. While the performance of this parameter needs to be explored for a wider range of ME treatment conditions (i.e., varying doses of ZVI and GAC, different types of the active media), this approach to monitor the efficiency of As removal by ME treatment can be employed when ME technology is deployed in pilot or full-scale applications.

Acknowledgments

As my time at the University of Washington draws to a close, I find myself reflecting on the incredible journey that has led me to this moment. I want to express my deepest appreciation to Dr. Gregory Korshin, for believing in me and offering me the opportunity to be part of his research team. Working alongside Dr. Korshin has been an enriching experience filled with memorable moments. I've cherished the times when he shared his personal stories, introduced us to captivating art, and even taught me to speak Italian. His ability to connect on a personal level while imparting knowledge has made our collaboration truly enjoyable. His unwavering support and invaluable guidance have not only shaped this thesis but have also influenced my academic and personal growth. I am also incredibly fortunate to have had my education sponsored by the King County Solid Waste Division. To Said Seddiki, Laura Belt, Kris McArthur, Joan Kenton, and all the staff at KC SWD, thank you for your support and trust in me to work on this special project. I'm grateful for the collaboration with WSP's consulting engineers, Karen Budgell, McBride Galt, and Scott Keen. Your expertise and insights have enriched this project and contributed to its success. A special mention goes to Dr. Jessica Ray for her time and dedication as a member of my thesis committee, and for her exceptional teaching. To not only my colleagues but also friends, thank you for your camaraderie, collaboration, and encouragement. Geneva Schlepp, your guidance and mentorship in the lab have been invaluable to me. Your passion and motivation for research and this industry and your excellent ability for problem-solving is truly inspiring. Annapaola Panico, my Italian sweetheart, your infectious energy and warmth have brightened every single day in the lab. You deeply impressed me with your execution and perfectionism at doing every single experiments. And Yak Yerbich-Louman, a reliable lab mate, your humor and laughter have made our workdays brighter and our collaborations stronger. I will miss your funny jokes and the experience we worked together. To my family and loved ones, words cannot express the depth of my gratitude for your unwavering love, support, and understanding. To my mom, dad, my boyfriend Chang, my aunt Jing, my cousin Pengyu, my grandparents, and all my friends, thank you for being my rock and for believing in me every step of the way. As I step into the next chapter of my journey, I carry with me the invaluable lessons learned, the cherished memories, and the meaningful relationships formed. Throughout my research journey, a song titled "How Far I'll Go" has been a constant companion, serving as a source of inspiration and motivation. With a curious spirit and unwavering self-belief, I eagerly embrace the adventures that lie ahead.

Table of Contents

List of abbreviations

1,10-phenanthroline - 1,10-Phen

AC – Activated Carbon

As - Arsenic

ASARCO - American smelting and refining corporation

BC - 3 L big column reactor

CHRLF - Cedar Hills regional landfill

Cr - Chromium

DLS - Dynamic Light Scattering

DMA - dimethylarsinic acid

EPA - Environmental Protection Agency

Fe - Iron

GAC - Granular Activated Carbon

HAPs - hazardous air pollutants

ICP-MS - inductively coupled plasma – mass spectrometry

ISO - International Organization for Standardization

KC - King County

KCEL - King County Environmental Laboratory

LFG - Landfill Gas

LPM - Liters per minute

MC - 250 mL mini Column reactor

ME - Micro Electrolysis

Mn - Manganese

MSW - municipal solid waste

MWD - Microwave Digestion

Ni – Nickel

ORP - oxidation-reduction potential

PAC - Powder Activated Carbon

PDF - Probability distribution function

PLA - polylactic acid

ppb - parts per billion

PPE - personal protective equipment

ppm - parts per million

RNG - renewable natural gas

Sb - Antimony

SEM - Scanning electron microscopy

SR - Sampling Round

SWD - Solid Waste Department

TDS - Total Dissolved Solids

VOCs - volatile organic compounds

WDOE - Washington State Department of Ecology

WM - Waste Management

XRD - X-ray diffraction

Zn - Zinc

ZVI - Zero Valent Iron

List of figures

List of tables

1. Introduction

Arsenic is a toxic element that has both geogenic and anthropogenic sources. Present in mineral ores, solutes in water, and gaseous arsines, arsenic's high toxicity and ubiquity emphasize the need for efficient treatment technologies to intercept this element and limit its exposures, as it is crucial for environmental and public health. This study delves into potential treatment methods for arsenic species in a municipal solid waste (MSW) landfill utility.

The site at which arsenic-containing landfill leachates and landfill gas condensates examined in this study come from is a local MSW landfill utility with a collocated gas plant separating methane from the other LFG components. This process produces high purity renewable natural gas (RNG) and also a stream of highly contaminated gas LFG condensate.

The collocated MSW landfill/RNG site has faced challenges due to elevated arsenic levels in its leachate stream. Prior examination of As loads in the landfill leachate produced at this site has established the occurrence of violations of arsenic maximum daily loads. While arsenic concentrations in the cover soils and waste material deposited at the site are not particularly high, the multi-year deposition of arsenic-containing spent landfill gas treatment solids (GTS) combined with the mobilization and at least fractional volatilization of the arsenic retained by them is deemed to have created a cyclic feedback loop, escalating arsenic concentrations in the leachate and gas condensate.

Removal of arsenic from leachate and LFG condensate is highly challenging due to the dominance of difficult to treat organo-As compounds in these matrixes. To address this challenge, the University of Washington group has developed a novel arsenic removal process referred to as Microelectrolysis (ME). While a number of fundamental aspects of reactions in ME processes remain to be ascertained, the major feature of ME is deemed to involve an electrochemical reaction between zero-valent iron (ZVI) and activated carbon (AC) that generates reactive intermediates that convert organo-As species in the condensate into extractable forms. The ME treatment has been repeatedly demonstrated to remove > 90% arsenic for at least 3 cycles of the use of the same ZVI/GAC media (Pinochet,2023; Schlepp, 2024).

This study addresses some of the challenges associated with the scaling-up and practical use of ME technology in pilot-scale and full-scale conditions. One such challenge is the need to have a

reliable method with which to estimate the removal of arsenic in field conditions when analytical data for actual As concentration in ME treated solutions may not be readily available and the turnaround time to obtain such data may be from several days to a few weeks. Given the novelty of ME technology and the need to optimize its performance in practical applications, the long turnaround time effectively limits options to optimize ME treatment without significant losses of time and other resources. On the other hand, because ME treatment is accompanied by the release of high amounts of iron solutes generated in anoxic conditions, it is also necessary to determine the stability of such solutes and solids formed upon the oxidation of ME-treated effluents in aerobic conditions expected for the environment. These aspects of ME treatment constitute the main thrust of this study whose results are present in the section that follow, starting with the discussion of general aspects of As occurrence and treatment.

2. Literature review

2.1. Sources of arsenic

Arsenic is ubiquitously present in the air, soil, water, plants, animals, and rocks (Matschullat et al., 2000). Historically, arsenic was notorious as a deadly poison, but it also has medicinal uses. It has been utilized in agriculture as a pesticide, textiles for dyeing, and cosmetics for skin treatments (American Cancer Society, 2023). Arsenic continues to have some industrial applications, primarily in the production of certain semiconductors and alloys.

In the environment, arsenic tends to be released through weathering, rock erosion, volcanic eruptions, and forest fires (Hughes et al., 2011). Human activities such as pesticide and fertilizer use, industrial processes, mining, and coal combustion also contribute significantly to arsenic pollution. (Mondal et al., 2006; Bundschuh et al., 2011).

Inorganic arsenic forms are considered to possess the highest levels of toxicity and carcinogenicity, leading to their classification as human carcinogens. Designated as a Group A human carcinogen by the US Environmental Protection Agency (EPA), arsenic is subject to stringent regulations aimed at mitigating potential health and environmental hazards associated with its use (EPA, 2003). The World Health Organization (WHO) has set a maximum guideline concentration of 0.01mg/L for As in drinking water (WHO 1993). Long-term As exposure may increase the risk of cancer (skin, lung, bladder, liver), cardiovascular disease, neurological effects, developmental issues in children, diabetes, and respiratory problems (Sahoo et al., 2013).

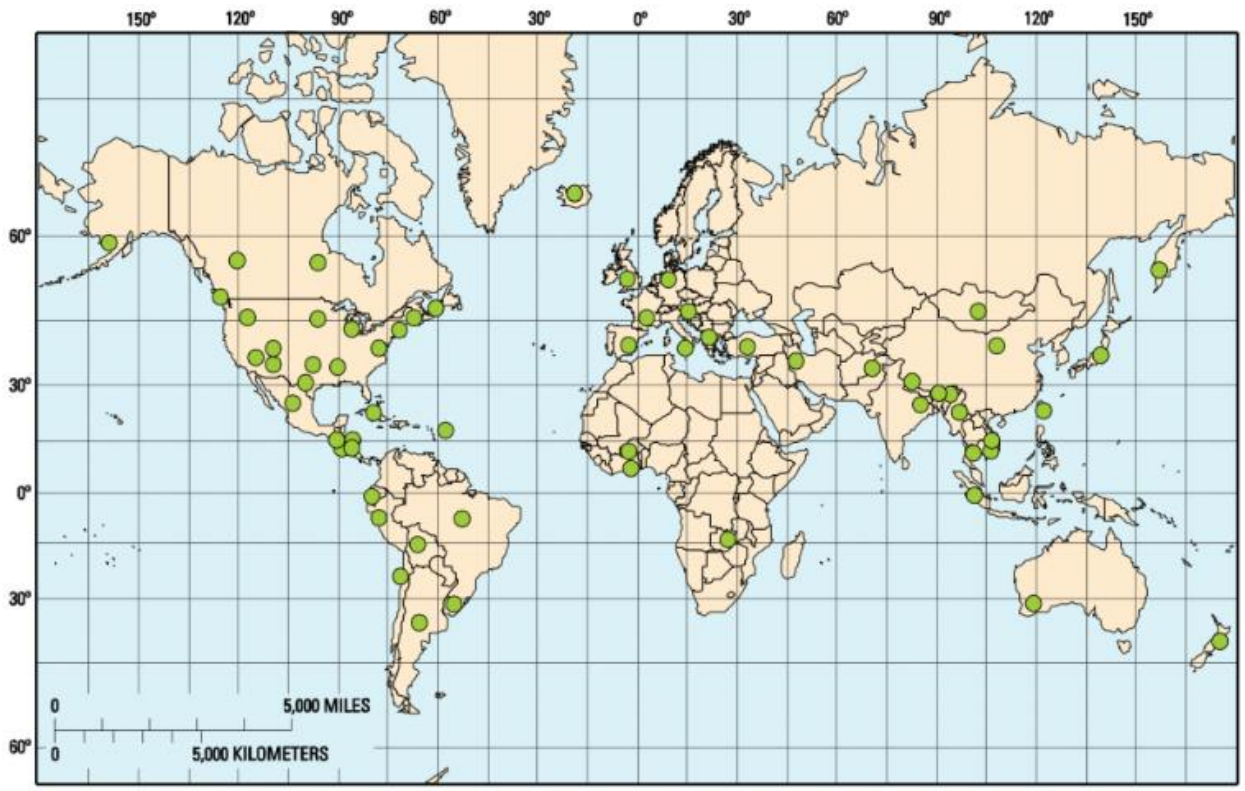

Fig 2-1 Worldwide distribution of areas with high concentrations of geogenic arsenic (Mosier et al., 2009)

As of 2012, arsenic contamination of groundwater resources has been detected in numerous regions worldwide, although awareness of the widespread extent of this issue has only recently gained traction. While localized sources of arsenic from human activities contribute to the problem, a significant portion of groundwater contamination with arsenic is attributed to natural geological (geogenic) sources. Groundwater affected by As contamination has been documented in countries across nearly every continent or major landmass although, as of now, no cases have been reported for Greenland and Antarctica.

Fig 2-1 shows the regions where arsenic concentrations in groundwater, including geothermal waters and water contaminated by mining, surpass the threshold of 10 micrograms per liter which is the standard recommended by the World Health Organization (WHO) in 1993. In most of the locations highlighted, arsenic concentrations exceed 50 micrograms per liter. The dots on the map represent these areas but are generalized spatially and do not pinpoint the exact locations of arsenic-contaminated waters.

2.2. Arsenic chemistry and mobilization

The toxicity, mobility, overall concentrations and fate of arsenic depend on pH, redox conditions, mineralogy, chemical speciation, and biological processes. In geochemical settings, arsenic exists primarily in +3 and +5 oxidation states frequently denoted as As (III) and As (V) (in solute forms, arsenite and arsenate, respectively), each exhibiting distinct chemical behavior and toxicity. Arsenic can also exist as As (-III) (as volatile arsines) and As (0) (Smedley et al., 2002). Arsenite is more mobile and toxic than arsenate under reducing conditions commonly found in anaerobic environments, while arsenate predominates in oxygen-rich environments. In addition to inorganic arsenic compounds, various organo-arsenic species exist in the environment, originating from both natural processes and human activities. These include arsenobetaine and arsenocholine found in marine organisms, as well as methylated arsenic compounds such as DMA and MMA formed through microbial methylation (Cullen et al., 1989). While inorganic arsenic compounds are typically more toxic, organo-arsenic species can also pose health risks depending on their concentration and chemical form.

Redox conditions quantified via the redox potential (Eh) that in many cases depends on the other master parameter pH play a crucial role in regulating the behavior of various major and minor species in natural aquatic environments, including arsenic (As) (Ronald et al., 2003). Under oxidizing conditions, the dominant species of arsenic vary with pH levels. At low pH values (less than approximately pH 6.9), the predominant species is $H_2AsO_4^-$, while at higher pH levels, $H_2AsO_4^-$ becomes prevalent. In extremely acidic conditions (pH<2), $H_3AsO_4^0$ may be present, whereas under strongly alkaline conditions, AsO_4^{3-} could be observed. Conversely, under reducing conditions and pH levels below pH 9.2, the uncharged arsenite species $H_3AsO_3^0$ predominates. At very low Eh values, AsH_3, arsine, may be formed. Arsine is a slightly soluble gas that tends to escape to the atmosphere. However, achieving redox equilibrium in the case of As reactions tends to occur slowly in the environment, with the redox potential typically influenced by predominant elements such as oxygen (O), carbon (C), nitrogen (N), sulfur (S), and iron (Fe). Minor and trace elements sensitive to redox changes, such as As, are responsive to these shifts but due to their low concentrations they do not exert direct control over them (Smedley et al., 2002). Despite the slow redox transformations, both arsenite and arsenate are commonly found in either redox environment. Arsenite is reported to be 25-60 times more toxic than arsenate and it is more mobile in the environment (Korte et al., 1991).

The distributions of the species as a function of pH are given in Fig 2-2 and Fig 2-3, respectively.

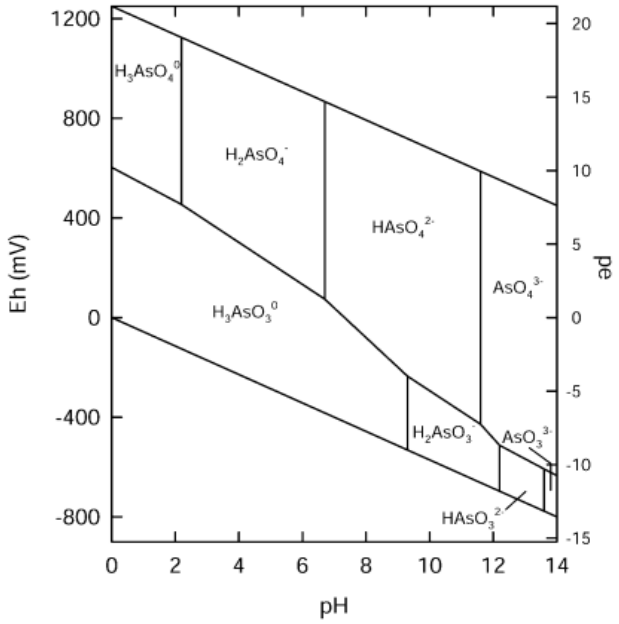

Fig 2-2 Eh-pH predominance diagram for aqueous As species at 25 ℃ and 1bar total pressure (Smedley et al., 2001)

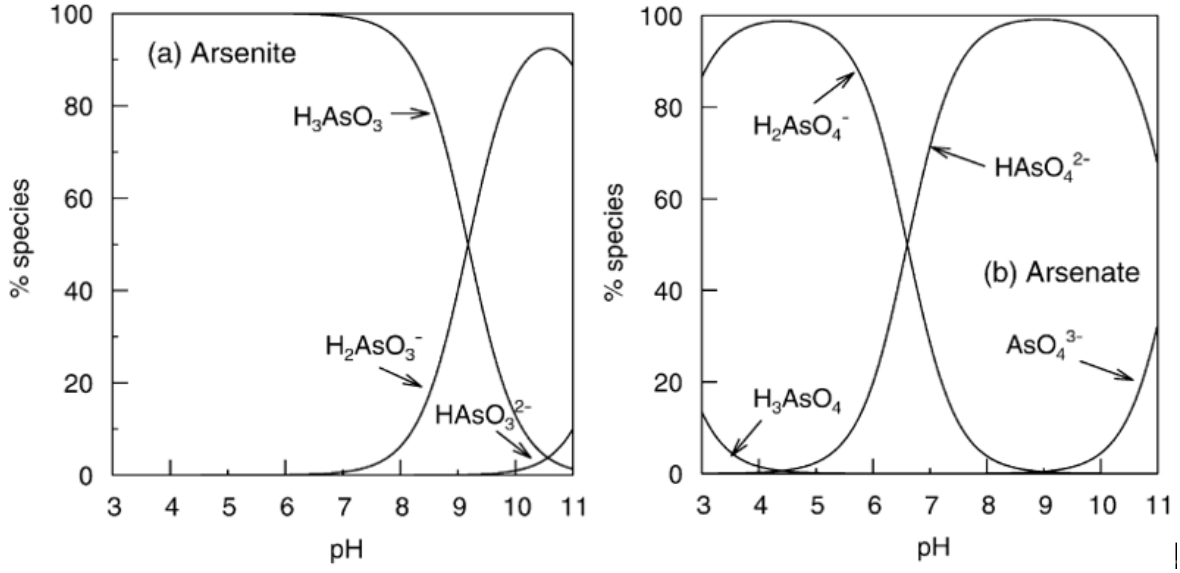

Fig 2-3 Effects of pH on the speciation of (a) arsenite and (b) arsenate (Smedley et al., 2001)

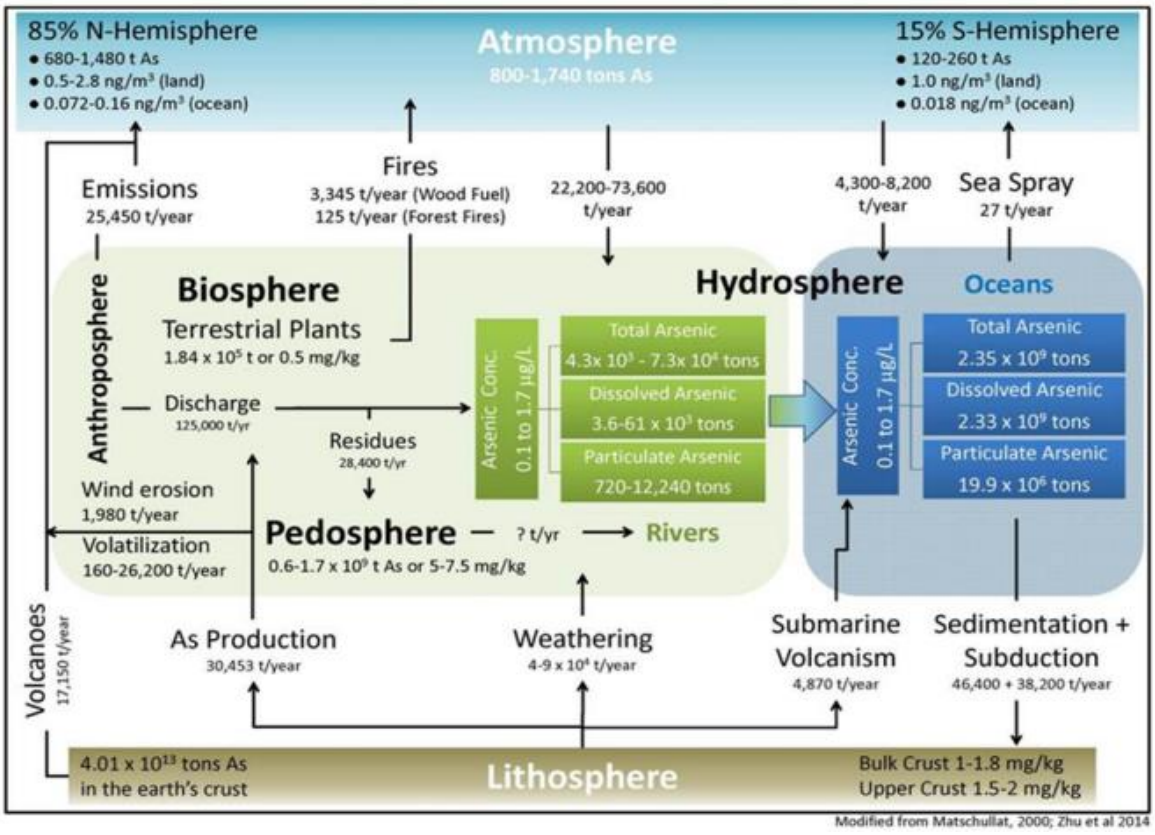

Fig 2-4 Main elements of the global arsenic cycle (Bowell et al., 2014)

Arsenic mobilization mechanisms are complex and include adsorption and desorption from mineral surfaces, dissolution of arsenic-bearing minerals, and microbial transformations. Organic matter and iron oxides play essential roles in arsenic sorption and retention in soil and sediment, influencing its mobility and availability to biota. Adsorption plays a crucial role in determining the mobility and bioavailability of arsenic. Various minerals, including phyllosilicates, silica, and hydrous oxides of iron (Fe) and aluminum (Al), have been studied for their efficacy in arsenic adsorption (Korte et al., 1991). The adsorption behavior of arsenate and other anions is influenced by both the nature of the anion and the surface properties of the adsorbent. Arsenic adsorption is notably influenced by its oxidation state rather than pH within the range of 5.5-7.5 (Ferguson et al., 1974). Extensive studies have shown that arsenate exhibits faster rate of adsorption on amorphous iron oxides compared to arsenite.

The reactions involved in As release and mobility encompass transfers from solution to solid phases, conversions between different oxidation states, and ligand exchanges. These processes are

purely chemical or rely on exclusively microbial mediation, while others may involve either chemical or microbial pathways.

2.3. Landfill Gas Condensate

Landfills are pivotal facilities for the disposal of municipal solid waste (MSW). In the United States, they must adhere to stringent environmental regulations. Municipal Solid Waste Landfills (MSWLFs) serve as primary repositories for nonhazardous household waste (Pinel-Raffaitin et al., 2006).

The composition of MSW comprises both inorganic and organic materials. The latter class of materials include food scraps, wood debris, paper, and lawn clippings, and other components of household waste (EPA, 2023). The microbial degradation of organic matter within MSW results in the release of gasses, notably carbon dioxide and methane, with landfill environments' anaerobic conditions being conducive to methanogenesis. The operational framework of landfilling involves the organization of waste into cells, subsequent compaction, and covering with soil layers. When oxygen becomes depleted due to microbial activity, these cells transition to anaerobic states, facilitating the production of methane gas. Upon reaching capacity, landfill cells are sealed utilizing impermeable cover materials, thereby containing emitted gasses and forming LFG.

Within the active zone of MSWLFs, landfill gas (LFG) emerges as a fundamentally important end product, constituting approximately 50% of methane, with carbon dioxide comprising 45%, nitrogen 5% and a small amount of non-methane organic compounds such as volatile organic compounds (VOCs) and hazardous air pollutants (HAPs). MSWLF-associated emissions contribute significantly to anthropogenic methane levels, accounting for approximately 15% of such emissions as of 2019, according to data provided by the Environmental Protection Agency (EPA).

Treatment of LFG, which is an obligatory for further uses of this product, involves collection, extraction, and purification. LFG collection systems include vertical and/or horizontal gas extraction wells to capture LFG emitted from the landfill. Once collected, the gas is transported to treatment facilities where it undergoes purification to remove moisture, VOCs, siloxanes and other contaminants. Purified LFG can then be utilized as a renewable energy source for electricity

generation, heating, or as a vehicle fuel, thereby reducing greenhouse gas emissions and dependency on non-renewable fossil fuels. Advanced treatment technologies enable the conversion of LFG into high-purity biomethane, suitable for injection into natural gas pipelines or use as a transportation fuel. Landfill gas treatment plays a crucial role in reducing environmental pollution, minimizing odor emissions, and harnessing the sustainable energy potential of waste resources.

Landfill gas condensate is a liquid with highly variable composition that is influenced by waste composition, landfill age, climate, and leachate recirculation practices. Common constituents of LFG condensate include organic substances, various sulfur-containing species, dissolved gasses and traces of heavy metals. Volatile organic compounds (VOCs), chlorinated compounds, and other hazardous substances are also present at varying levels thus further complicating its composition.

Fig 2-5 provides a schematic depiction of the formation of various As species, both organic and inorganic, in three landfilled waste, leachate, and biogas. This illustration offers a concise summary of the potential sources and main processes that affect arsenic mobility and speciation in landfill environments.

WASTE		LEACHATE		BIOGAS	
Potential sources	**Species**	**Processes**	**Species**	**Processes**	**Species**
Soil, glass, metallic components, agricultural products	$AsO(OH)_3 \leftrightarrow As(OH)_3$	Leaching , Reduction Oxidation	$AsO(OH)_3 \leftrightarrow As(OH)_3$		
Agricultural products	$AsO(OH)_2CH_3$	Leaching, Methylation	$AsO(OH)_2CH_3 \leftrightarrow As(OH)_2CH_3$	Ethylation	$As(CH_3)_x(C_2H_5)_{3-x}$
Agricultural products	$AsO(OH)(CH_3)_2$	Leaching, Methylation	$AsO(OH)(CH_3)_2 \leftrightarrow AsOH(CH_3)_2$	Hydridation	$As(CH_3)_2H$
		Methylation	$As^+OH(CH_3)_3$	Volatilisation Methylation	$As(CH_3)_3$
Marine waste	$As^+(CH_3)_3CH_2COOH$	Leaching, Alkylation cycle	$As^+(CH_3)_3CH_2COOH$		

Fig 2-5 Sources and processes associated with arsenic occurrence and speciation in waste, leachate, and biogas. (Pinel-Raffaitin et al., 2007)

Previously, As was regarded as being stable in its inorganic forms upon disposal, earning it the classification of "inert, immobile, relatively nontoxic" within landfill environments (Parris et al., 1976). This view on As stability in landfills has changed due to the recognition of effects of multiple biochemical processes that strongly affect As mobility, notably increasing it via the formation of methylated As species. Biomethylation of As and other metalloids, including Sb, is attributed to complex biochemical processes driven by bacteria, fungi, yeast, and algae. Research indicates that under strongly reducing conditions, particularly in the presence of reduced sulfur compounds, biomethylation and volatilization of arsenic compounds, notably the formation of arsines, are facilitated (Zhao et al., 2013). Organo-arsines can then be released into the environment alongside the primary constituents of LFG: methane and carbon dioxide. Although inorganic forms of arsine and stibine (SbH_3) may undergo rapid oxidation upon release into the air, methylated forms exhibit greater resistance to oxidation under atmospheric conditions (Wang et al., 2014).

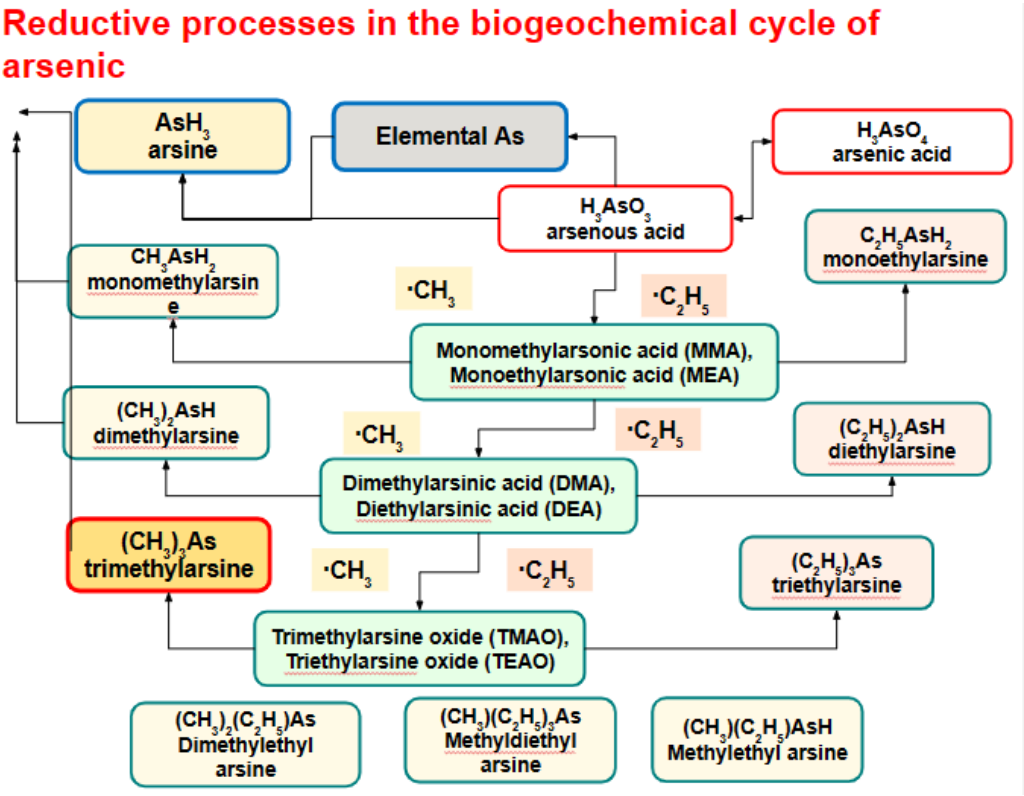

Fig 2-6 Sequence of reductive and methylation/ethylation processes in the biogeochemical cycle of arsenic (Gregory Korshin, lecture slides)

Fig 2-6 presents a detailed sequence of the reductive and methylation/ethylation processes that are critical for the biogeochemical cycle of arsenic. These processes entail the conversion of arsenic from higher to lower oxidation states, often facilitated by microbial activity within anaerobic environments. For instance, under reducing conditions prevalent in sediments, soils, and groundwater, arsenate [As(V)] undergoes reduction to arsenite As(III), which exhibits increased mobility and toxicity. As(III) is quite reactive in microbially mediated transformations that yield methylated solutes and volatile organic-arsenic compounds like arsines, contributing to arsenic's atmospheric transport.

2.4. Conventional Arsenic Removal Methods

In recent years, there has been significant research devoted to studying arsenic removal techniques aimed at reducing arsenic levels in the environment. This research has primarily focused on the removal of inorganic As solutes. Currently employed methods include adsorption, ion exchange, phytoremediation, chemical precipitation, electrokinetic methods, membrane process and electrocoagulation (Hao et al., 2018, Hu et al., 2018). These techniques are being investigated for their effectiveness in mitigating arsenic contamination and are crucial for advancing environmental remediation efforts.

- **Adsorption:** The effectiveness of arsenic removal through absorption is governed by several mechanisms, including physical adsorption, surface complexation, and ion exchange. Physical adsorption involves the non-specific binding of arsenic molecules to the surface of adsorbent materials, driven by Van der Waals forces and electrostatic interactions (Maitlo et al., 2019). Surface complexation, prevalent in hydrous metal oxides and activated alumina, entails the formation of inner-sphere or outer-sphere complexes between arsenic species and functional groups on the adsorbent surface (Shih et al., 2005).

  Various conventional adsorbents such as activated carbon (AC), hydrous metal oxides like activated alumina, and ion exchange resins have been utilized for arsenic removal (Dhaliwal et, al; 2020). Additionally, new adsorbents such as Ce(IV)-doped iron oxide, kaolinite-humic acid complexes, and ferruginous manganese ore are being developed and evaluated for their efficacy in arsenic removal (Karakurt et al., 2019).

Activated carbon is widely utilized for the removal of various compounds (Mohan et al., 2019). Activated carbon is available in granular (GAC) and powdered (PAC) forms, with PAC exhibiting a larger active surface area, albeit being more challenging to separate from treated waters. Enhancement of removal efficiency can be achieved by functionalizing the PAC surface.

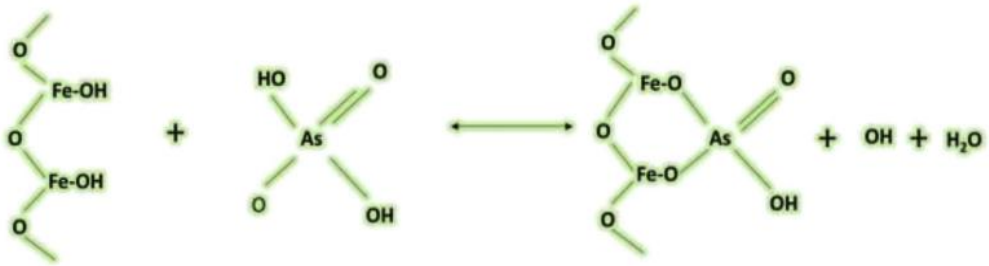

Fig. 1. Arsenic adsorption cycle system by MNPs 37–39. Modified from (Monárrez-Cordero et al., 2016).

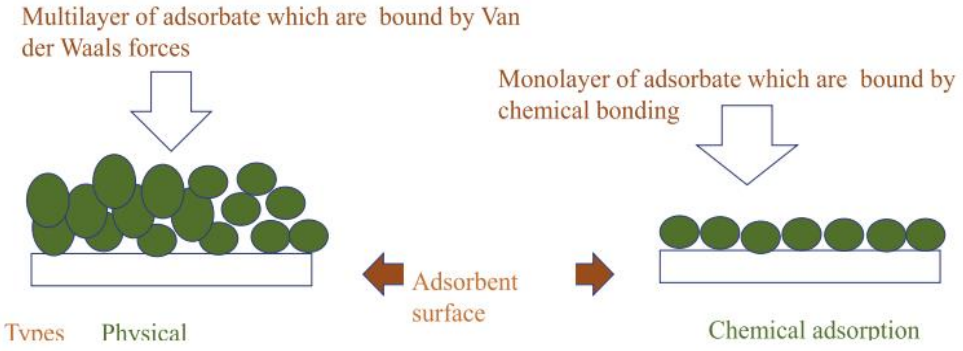

Fig 2-7 Outline of the general principles of adsorption processes (Sarkar et al.,2016)

Different adsorbents exhibit varying optimum removal efficiencies within specific pH ranges. Adsorbent pretreatment techniques, such as activation by heating or acid treatment, have shown to enhance arsenic removal efficiency significantly. However, sorbents necessitate replacement once the adsorption bed becomes saturated and exhausted, ultimately losing its separation capacity entirely. The presence of other anionic components such as sulfate, chloride, or natural organic matter can also competitively decrease arsenic removal efficiency. Additionally, they are best suited for wastewater treatment with low arsenic concentrations (Laatikainen et al., 2016).

- **Ion Exchange:**

Ion exchange resins can be highly efficient tools for the selective extraction of ions from contaminated water sources. Functioning on the principle of solid-phase ions being exchanged with their counterparts in the aqueous phase, these resins facilitate the comprehensive removal and recovery of metal contaminants. An ion exchanger can be tailored for a particular arsenic species, thereby escalating expenses and limiting versatility (Huang et al., 2015).

- **Chemical Precipitation**

The use of chemical precipitation to remove arsenic involves exploiting the solubility differences between arsenic compounds under varying pH and chemical conditions. Chemical precipitation involves adding a precipitating agent to the water containing arsenic ions, leading to the formation of insoluble arsenic-containing compounds that can be separated from the water through sedimentation or filtration (Shih et al., 2005).

In the case of arsenite As(III), it can be oxidized to arsenate As(V) using readily available oxidizing agents such as chlorine or permanganate. Arsenate can then be precipitated by ferric chloride or aluminum sulfate, which may form insoluble arsenic compounds, primarily ferric arsenate or aluminum arsenate, respectively (Long et al., 2019), or As(V) can adsorb Fe or Al flocs formed in this process. The addition of lime (calcium hydroxide) or sodium hydroxide can also raise the pH of the solution, facilitating the precipitation of arsenic as calcium arsenate or magnesium ammonium arsenate, which are less soluble at higher pH levels. The efficiency of chemical precipitation for arsenic removal depends on factors such as the initial concentration of arsenic, pH, temperature, and the presence of other competing ions in the water.

- **Membrane separation technology:**

Membranes function as selective barriers, enabling the controlled passage of molecules through them, facilitated by a driving force. This typically involves the use of reverse osmosis (RO) or nanofiltration (NF) membranes, which retain arsenic species and other solution components yet allow water molecules to pass through. While RO and NF membrane processes generate significant volumes of retentate, their efficiency tends to be high. However, their implementation is associated with high costs and a tendency for

fouling in many situations (Ungureanu et al., 2015). Use of membranes to treat LFG condensate has been only cursorily studied (Zhao et al. 2013) yet it is possible to anticipate that most membrane materials may be easily fouled or damaged due to the presence of VOCs and other foulants in the condensate. Thus, membrane treatment of LFG condensate must involve its extensive pretreatment.

2.5. Removal of Arsenic using Zero Valent Iron and Microelectrolysis

In recent years, water treatment methods based on zerovalent iron (ZVI) have emerged as a highly promising technology for remediating and treating groundwater and wastewater contaminated with a diverse array of organic and inorganic pollutants. Research studies exploring applications of ZVI in water treatment have consistently highlighted its remarkable properties, both in reduction and adsorption, particularly for a wide range of toxic metals (Gillham et al., 1994).

ZVI is characterized by its environmentally friendly properties, commercial availability, relative cost-effectiveness, and effectiveness in the removal of many pollutants. For instance, its low standard redox potential (-0.45 V) makes it effective in reducing oxidized contaminants like Cr(VI). The removal mechanism involves electron transfer from ZVI to contaminants, thus converting them into less harmful or non-toxic species. Additionally, in the presence of dissolved oxygen (DO), ZVI form reactive oxygen species by producing H_2O_2 through electron transfer to O_2. These species are capable of degrading and oxidizing various organic compounds.

The standard reduction potential E_0 (V) of the iron half-reaction is -0.409 V (Yokogawa, 2014), where the negative sign indicates the reductive nature of the reaction. Therefore, ZVI tends to be easily oxidized in environmental conditions, primarily through aqueous corrosion reactions in Fe^0/H_2O systems. The oxidation of Fe^0 follows an electrochemical mechanism, with Fe^0 dissolution as the anodic process and hydrogen gas at low pH or oxygen reduction in oxic conditions as the cathodic process. The oxidation of Fe^0 by H^+/O_2 leads to the formation of Fe^{2+} species, which may undergo hydrolysis to form Fe^{2+} hydroxocomplexes and solids such as $Fe(OH)_2$. However, Fe^{2+} and especially its hydroxo complexes can react with molecular oxygen (O_2). This process accelerates with increasing pH, leading to the formation of Fe^{3+} and precipitation Fe^{3+}-dominated solids such as $Fe(OH)_3$ and other (hydr)oxides. The oxidation of ZVI may

eventually result in the formation of surface layers of maghemite or lepidocrocite that block the surface and diminish the reactivity of ZVI over time.

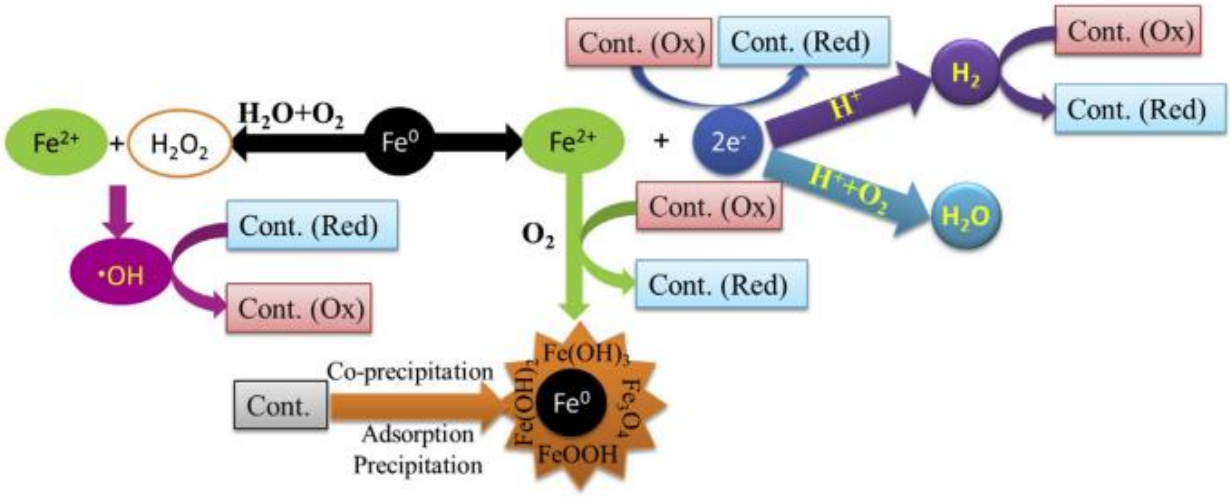

Fig 2-8 Scheme of the main reactions in the Fe^0 /H_2O system and typical mechanisms of contaminants removal in ZVI processes (Guan et al., 2015)

The precise mechanism governing As removal during microelectrolysis (ME) remains subject to ongoing investigation. It is currently hypothesized that it involves electrochemical reactions occurring at the interface between ZVI and activated carbon (AC), in either PAC or GAC form, which serve as the active media for the treatment process. Due to its ability to remove a diverse range of dissolved constituents, AC is widely favored for various treatment applications (Nowicki, 2016). AC is believed to facilitate the electrochemical oxidation (corrosion) of ZVI, giving rise to the formation of numerous micro-galvanic cells. Concomitantly, reduction reactions take place on the surfaces of both iron and activated carbon particles, leading to the generation of Fe(II) and Fe(III) ions. These ions play a pivotal role in enabling significant electron transport to suitable electron acceptors (Liu, Korshin et al., 2022).

While ZVI is commonly employed for treating inorganic arsenic, the removal of organic arsenic represents an unexplored area of research. Prior research has shown that ZVI, especially in combination with activated carbon, can be effective in removing methylated arsenic species such as DMA (Liu, Korshin et al. 2022). ZVI has several benefits, including its reductive power, which may facilitate the transformation of various contaminants, including arsenic, into less harmful forms although the nature of species formed via the reduction of organo-As species remains to be

elucidated. The widespread availability and low cost of ZVI make it an attractive option for remediation projects while ZVI's low toxicity ensures minimal environmental impact, aligning with sustainable remediation goals. The coupling of ZVI with activated facilitates the removal of a broad spectrum of pollutants including those found in LFG condensate. Thus, the ME approach can address the specific challenge of arsenic removal from LFG condensate and landfill leachates.

2.6. Prior research on the development of microelectrolysis to remove arsenic for LFG condensate

Since 2019, the University of Washington (UW) group has been carrying research aimed at identifying and developing an effective treatment technology to remediate As-contaminated landfill leachate and LFG condensate. In this context, Dr. Korshin's team has evaluated the performance of conventional treatment methods and found them ineffective for As removal from these matrices.

Further analysis of potential treatment processes for organo-As removal showed that microelectrolysis (ME) treatment represents the most viable solution. This innovative method is capable of effective removal of organic arsenic from LFG condensate via a combination of reduction, complexation, adsorption and volatilization thus bringing arsenic concentrations in the treated water to a level suitable for discharge without exceeding the predetermined maximum daily load. While arsenic is the primary target contaminant, the developed ME technology holds promise for addressing other emerging contaminants as well.

ME treatment used a combination of ZVI and GAC, collectively referred to as "active media," interacting in an acidic and oxygen-free environment. ZVI serves as the reducing agent in this process, facilitating electrochemical corrosion and creating a dynamic reducing environment conducive to organo-As removal. Through galvanic cells, ME treatment effectively removes arsenic and other compounds from contaminated LFG Condensate, depositing them onto the surface of solids and resulting in reasonably high levels (80% ~ 95%) of arsenic removal. (Malik, 2020; Rifkin, 2021; Walters, 2022; Pinochet-Troncoso, 2023; Schlepp, 2024).

Since the completion of the prior analysis and initial development of ME treatment, the UW team has continued to refine the technology by optimizing the treatment process for specific operational

variables. Experimental ME treatment of LFG condensate has been conducted within fixed bed and fluidized column reactors. Performance optimization of the fluidized column reactor involved adjusting variables such as pH, media recycling, treatment time, anaerobic conditions, carrier gas, reactor headspace, process activation mode, and media agitation (Walters, 2022; Pinochet-Troncoso, 2023). A significant advancement in the ME process was achieved via the transition from fine (PAC) to coarse active media (GAC) for easier reuse and cleanup. Supplementary doses of active media were found to extend the media's useful life, enabling multiple rounds of LFG condensate batch treatment (Pinochet-Troncoso, 2023).

Operational pH, when varied in a 3.0 to 4.5 range, was also found to have a relatively low impact on ME treatment efficacy. Oxidation reduction potential (ORP) measurements during the ME process provided insights into treatment monitoring, with correlations between ORP and arsenic removal investigated for potential real-time operational monitoring (Pinochet-Troncoso, 2023; Schlepp, 2024).

Larger-scale ME reactors that initially utilized carrier gasses like CO_2 or N_2 for arsenic removal, transitioned to mechanical mixing for efficient agitation of active media. Mass balance studies revealed that GAC retains the majority of removed arsenic, indicating the need for further investigation into the extent of arsenic volatilization in ME reactors. This result was obtained by magnetically separating the ZVI/GAC phases and performing separate digestions for them (Panico, 2023).

Fig 2-9 Mini Column Reactor set up and probes placement

Due to a number of reasons whose discussion goes beyond the scope of this thesis, only the condensate sample that was taken in June 2023 was available for most of the experiments reported in this thesis. Due to the limited amount of that sample (referred to henceforth as SR19), we had to use a smaller ME reactor size. That reactor referred henceforth as MC1 (Mini Column 1) has a volume of 250 mL of sample at a time. In recent developments, the research team has embarked on pioneering the implementation of magnetic drive mixing, a novel approach utilizing two pieces of magnets, as opposed to conventional mechanical mixing techniques. Concurrently, the team has introduced innovative types of Fe-GAC absorbents as well as a comprehensive gas-tight absorption tube system tailored specifically for capturing arsine volatilization, representing a significant advancement in mass balance calculations.

In conclusion, the University of Washington research team's systematic approach and ongoing optimization efforts have advanced the understanding and application of ME treatment for arsenic removal from LFG condensate. Their findings hold promise for the development of scalable and efficient treatment solutions for contaminated water systems. Despite these advancements, challenges remain in achieving complete arsenic and antimony recovery during mass balance

calculations. Ongoing efforts are aimed at improving recovery rates to ensure accurate treatment efficacy assessments (Cheney-Irgens, 2022; Panico, 2023).

2.7. Goals of this study

Although extensive research has been conducted on the treatment of inorganic arsenic, previous studies on the removal of organo-arsenic compounds from aqueous matrices, particularly from LFG condensate, are limited. This thesis presents results of experiments that are part of the continuing ongoing efforts of the UW group to optimize the ME treatment process for arsenic removal from LFG condensate, and implement it practically. The following key areas were the focus of this research:

- To establish correlations between iron release and arsenic (and antimony) removal rates under different ME treatment operational conditions, aiming to ascertain the feasibility of using concentrations of Fe solutes found in ME reactors as a predictor for ME treatment efficiency.
- To determine the applicability of field-deployable methods of iron analyses to quantify iron release in ME treatment and correlate it with As removal in ME treatment. This task includes testing the stability of Fe standards and confirming the accuracy of Fe concentration measurements in conditions pertinent to field deployment of ME treatment.
- To explore effects of post-treatment conditions on the stability of iron solutes released during ME treatment and determine possible effects of their transformations on the overall sequence of LFG condensate treatment using ME technology.

3. Materials and Methods

3.1. Methods for Microelectrolysis treatment

Table 3-1 Summary of the sample collection dates and arsenic concentration

Sample Round	Date	As, mg/L	Sb, mg/L	Fe, mg/L	pH
SR 18	May 12, 2023	15.4	2.4	301	--
SR 19	June 13, 2023	13.1 ± 0.3	2.3 ± 0.4	39 ± 28	5.3
SR 20	Nov 1, 2023	12.1 ± 0.6	6.9 ± 0.5	13.8 ±0.9	7.4
SR 21	Apr 26, 2024	13.6 ± 1	7.6 ± 0.3	1 ± 0.5	8.2

The sample collection procedure entailed a visit to the landfill utility, where sample containers were filled without leaving headspace from the condensate collection tank. Subsequently, the collected samples were stored in a cold room at a temperature of 4 °C.

Prior work of the UW group showed that LFG condensate samples exhibited a range of colors, from orange to relatively clear. Additionally, the levels of organic compounds varied, contributing to differences in sample opacity. Visually discernible layers of grease and oil were present on the surface of some of the samples. These hydrocarbons are attributed to lubricants used in LFG processing equipment.

Due to factors beyond the scope of this thesis, LFG condensate generated at the collocated LGF/biomethane production site was unavailable from June 2023. The UW group obtained a very limited amount (2L) of LFG condensate sample (referred to as SR20) in November 2023. That LFG condensate had been stored in an anoxic sump located at the research site from June 2023. A larger volume of the same LFG condensate was obtained in the late April 2024. The latter sample is referred to henceforth as SR21. SR20 and SR21 samples, characterized by turbidity and abundant black particulates, were not extensively utilized for experiments either due to their limited volume or due to their availability only very late in this study. Therefore, Therefore, most of the experiments are done with SR19, and only limited information on the results of experiments conducted with SR20 and SR21 is included in this thesis.

3.1.1. ME treatment: methods and procedures

This section describes methods and procedures used in the ME experiments reported in this thesis. Because this material may be used as guidance for further experimentation, this material in some cases is presented using a style typically employed to write standard operating procedures (SOPs).

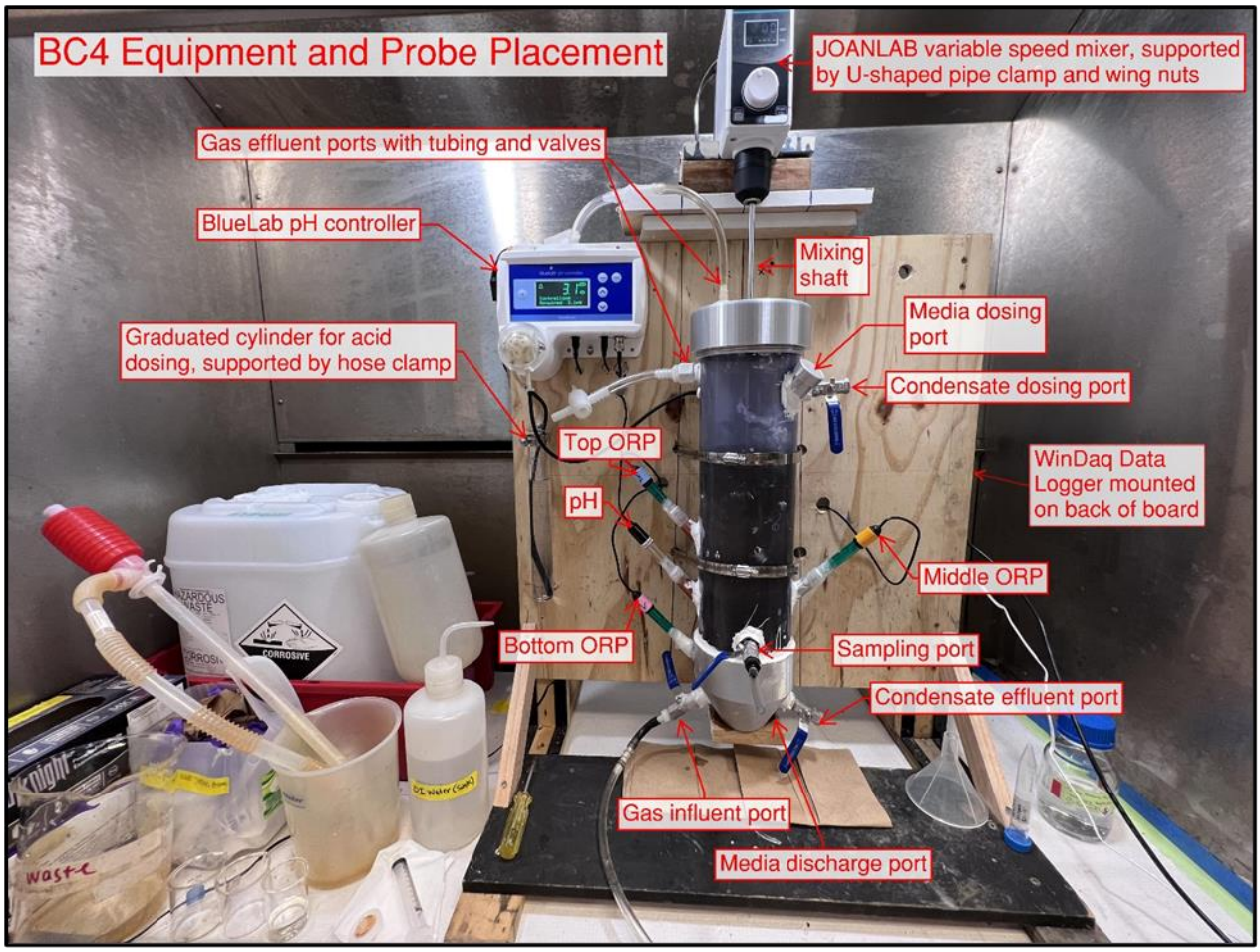

Fig 3-1 Visual of ME treatment experimental operations set up with BC4 (Schlepp, 2024)

3.1.2. General outline of ME treatment experiments:

The objective of this type of experiment is to evaluate the effectiveness of ME treatment that employs a combination of ZVI and GAC for the removal of contaminants such as arsenic from the LFG condensate and as needed from other matrixes.

1) **Design and Fabrication of Custom ME Reactor Components:** The ME reactor components, including the reactor cap, ORP/pH probe ports, mixing impellers, and conical reactor bottom, were designed using Autodesk software (Pinochet-Troncoso,

2023). The reactor cap design was further refined by Yak Yerbich-Louman, integrating elements from previous iterations and optimizing 3D printing parameters. The components were 3D printed using PLA filament on Creality Ender 3 and Flashforge Adventurer 4 3D printers. The assembly involved securing all pieces to the column using waterproof silicone, marine adhesive sealant, and self-leveling "lap" sealant. PVC tubing was cut to size using a bandsaw, and port holes were drilled using a Dremel tool. Impellers, softened with a heat gun, were affixed to a stainless-steel shaft and secured in place with heat shrink tubing.

2) **Experimental Setup and Pre-Experiment Preparation**: All relevant variables were recorded in the shared Google Drive's Matrix of ME Batch Experiments. Additionally, experimental details were meticulously documented in ORP data file names, ICP-MS sample names, and presentations. Key parameters, such as experiment date, condensate sample details, reactor specifications, treatment specifics, media dosing, and pH control, were carefully recorded. A sampling plan was developed, outlining protocols for sample collection and spent media retention.
3) **Sample Tubes and Sampling Equipment Preparation:** Aliquots for analyses for As and other elements were taken using 10 mL Falcon tubes that were labeled with experiment date, descriptive title, cycle number (if applicable), and sampling time. Tubes, along with a small beaker, a 10 mL syringe, and 0.45 μm Nylon filters, were meticulously arranged for sampling.
4) **Active Media Preparation:** Active media preparation involved calculating the required mass based on predetermined experimental doses. Using a precise analytical balance, the calculated mass(es) of media were weighed into a designated beaker with a spatula. For experiments involving cycling, any GAC and ZVI increments (top-offs) added in the reactor were pre-weighed and stored in individual containers.
5) **Condensate Preparation:** Condensate handling took place in a fume hood to ensure safety. Stored condensate was retrieved from the cold room and placed under the fume hood. The desired volume of condensate was transferred from the storage container into a secondary container using a manual hand pump.
6) **Reactor and Mixer Setup:** The reactor and mixer were set up according to standardized procedures (Pinochet-Troncoso, 2023 and Schlepp, 2024). Figure 3.1.1

shows the ME reactor set-up, specific to BC2/3 or MC2/3, was referenced for guidance. The mixing shaft was inserted into the reactor, positioned through the reactor cap's orifice, and secured. If utilizing a support stand, the mixer was secured to the support stand rod with an adjustable holder.

7) **pH Controlling System Setup:** The pH controlling system was set up to maintain optimal pH levels throughout the experiment. The 0.5 M sulfuric acid intake tubing was placed into a vessel of acid, and if acid consumption needed to be tracked, acid was poured into a graduated cylinder. The acid feed line was attached to the reactor's acid dosing port. For the experiments, the pH probe was removed from storage, rinsed with deionized water, and calibrated with pH 7 and 4 buffers to ensure accuracy.
8) **ORP Probes and Data Acquisition System Setup:** When ORP measurements were carried out, ORP probes and a data acquisition system were set up for data collection. ORP probes were removed from storage, rinsed with deionized water, and calibrated with a 256 mV ORP buffer solution. Probes were secured in place with Parafilm or caps to ensure an airtight seal and accurate readings.
9) **Gas Flow:** If a gas flow was required for the experiment, the gas setup was meticulously arranged. The gas regulator was initially closed, then gradually opened to control the gas flow rate to the reactor. Gas flow was regulated using a gas flow meter to ensure precise control and consistency throughout the experiment.
10) **Other aspects of ME experiments: Preparations for Start-Up:** Headspace flushing was conducted if applicable, with the appropriate gas effluent port opened for flushing gas. Gas delivery hose was connected to the gas influent port, and the reactor was flushed with the desired flow rate to remove atmospheric oxygen. Condensate was dosed into the reactor, ensuring all reactor ports were closed, and probes were secured with Parafilm or caps. Initial pH adjustment was performed using the pH controller's manual dosing function, with adjustments made incrementally to allow for equilibration.
11) **Sample collection:** Each tube was meticulously labeled with essential information, including the experiment date, descriptive title, cycle number (if applicable), and sampling time, to maintain traceability. Samples were collected at regular intervals,

typically every 10 minutes, and filtered using 0.45 μm Nylon filters to remove any particulate matter that may interfere with subsequent analyses.

12) **Draining Reactor (Cycling):** In cases where cycling was implemented, the reactor's effluent was drained as required for further experimentation. The effluent discharge valve was opened to discharge treated effluent while ensuring the retention of settled media within the reactor. Optionally, tubing was connected to the effluent discharge valve to facilitate draining into a waste container, and the effluent was disposed of in combined hazardous waste carboys as per established protocols.
13) **Draining Reactor (No Cycling or Final Cycle):** If no further cycles of treatment were required or if it was the final cycle, the reactor was drained via the media discharge port to remove the slurry of media and effluent. To facilitate the removal of media from the reactor, the mixer was optionally turned-on during drainage, ensuring thorough evacuation of the reactor's contents.
14) **Clean-Up:** The clean-up process was meticulously executed to maintain the integrity of equipment and ensure the safety of laboratory personnel. The reactor and probes were thoroughly rinsed using treated effluent in a squeeze bottle to flush out any residual media inside the reactor. Probes were carefully removed from the reactor, either by unscrewing caps or cutting Parafilm, and rinsed meticulously with DI water to remove any adhered contaminants. For particularly dirty probes, a specialized cleaning protocol detailed in the Supplementary Information was followed. A final rinse of the reactor was performed using water, paying close attention to probe and sample ports, as well as valves where liquid had passed through. Subsequently, a paper towel attached to the end of a brush was used to dry the inside of the reactor, wiping away any residual GAC particulates on the reactor sides.
15) **Gas Shut Off:** Finally, the gas shut-off procedure was executed to safely disconnect the gas supply and ensure laboratory safety. The gas delivery tubing outlet was placed in the fume hood to exhaust any residual gas, minimizing exposure to potentially hazardous substances. The regulator valve was gradually opened to allow residual gas to flow through the system, followed by the closure of the cylinder valve to stop gas flow. Once pressure readings indicated no back pressure in the system, the regulator

valve was closed, and the gas hose was safely removed from the hood, minimizing trip hazards.

3.1.3. Supplementary Information:

a) ME treatment utilizes a combination of two active media types: ZVI and GAC. The dosing of these media is based on a mass ratio. Typically, ZVI and GAC are dosed in a ratio of two-to-one mass ratio (2:1), where the total mass of the media is divided accordingly. For instance, in a treatment scenario with a volume (V) of 2 liters, the dosing rate (d) would be 50 grams per liter for both ZVI and GAC, following the 2:1 dosing ratio by mass.

An example of calculations for active media dosing is given below:

Treatment volume (*V*): 2 L

Dose (*d*): 50 g/L ZVI and GAC, 2:1 dosing ratio (by mass, respectively)

Total mass media (M)=V×d
M=2 L × 50 g/L=100 g
Total mass ZVI (Z)=M/3×2
Z=(100 g)/3×2=66.7 g
Total mass GAC (G)=M/3×1
G=(100 g)/3=33.3 g

Top off Dose (TD): 2g/L dosage added before each cycle (not including cycle 1), ZVI and GAC, 2:1 dosing ratio (by mass, respectively)

3.2. Sequential filtration and weight measurements

3.2.1. Goals

The objective of this experiment was to determine the concentration of suspended iron-dominated solids and the concentration of soluble As and Sb in the pH-adjusted ME treated effluent. Assess contribution of varying particle size using a sequential filtration approach to bring some insights into membrane size for pilot-scale design.

3.2.2. Method

A 50 mL aliquot of ME treated effluent was taken and its pH was adjusted to 7 using a 1 N NaOH solution. The sample was aerated to induce the oxidation of the green precipitate that formed in the ME treated sample prior to its oxidation. Air exposure resulted in the development of an orange hue of the solids, undoubtedly due to the oxidation of Fe(II) species to Fe(III) species. The oxidized solution was sequentially filtered using syringe filters with pore sizes ranging from 5 um to 0.2 um. The detailed information of the filters is listed as follows.

Table 3-2 Information of Syringe Filters

Filtration Order	**Size(um)**	**Brand**	**Material**
1	5	Allpure	Nylon
2	1	Whatman	PES
3	0.45	Adamas-Beta	PTFE
4	0.2	VWR	PTFE

The filtered solutions were acidified and stored in falcon tubes as distinct samples. They were subsequently diluted. Iron concentration in the diluted samples were determined using an ICP-MS instruments, as described below.

3.3. Absorbance spectra measurements

3.3.1. Experimental Goal

Absorbance spectra were measured either to track the formation of precipitates in pH-adjusted ME-treated solutions, or to record the absorbance of solutions containing varying amounts of iron in the presence of 1,10-phenanthroline which form colored complexes with Fe^{2+} ions. Since most of the Fe released during the ME treatment is in the form of ferrous ions, the 1,10-Phen method, which is the standard for ferrous ion determination, was selected for this purpose.

3.3.2. Method

In the experiments, the UV-Vis spectrophotometer (Shimazu UV-2007) was initially warmed up for at least 20 minutes is observed. The baseline correction was performed by scanning milliQ water from 200 nm to 800 nm. Following this step, a sample was placed into a suitable cuvette (1 cm optical pathlength in this study).

To prevent contamination for future measurements, the cuvette and any other sample handling equipment are meticulously cleaned with deionized (DI) water. This ensures the reliability and accuracy of subsequent measurements.

Data from the instrument's acquisition software were copied and saved in Excel for further analysis.

3.4. Inductively coupled plasma mass spectroscopic (ICP-MS) measurements

Inductively coupled plasma mass spectrometry (ICP-MS) stands as an established analytical technique within the industry. ICP-MS analytical methods use inductively coupled plasma (ICP) to atomize and ionize sample components with the precision and sensitivity of mass spectrometry (MS) to detect and quantify elements at trace levels (PerkinElmer, n.d.). In ICP-MS, the sample is introduced into a high-temperature plasma where it is vaporized, atomized, and ionized. The resulting ions are then separated based on their mass-to-charge ratio and detected, allowing for the simultaneous measurement of multiple elements (Elemental Analysis Core, n.d. and EPA, 2024). The ICP-MS analysis for this research, based on the EPA's Method 6020B, utilizes a PerkinElmer Nexion 2000B instrument for determining As, Sb, and Fe. This instrument is housed in the Nanoengineering and Sciences Building's Research Training Testbeds (RTT) facility at the University of Washington.

3.4.1. Preparation of ICP-MS calibration standards

Stock Agilent ICP-MS standards for each element targeted were in the analyses. The product codes for the Agilent standards for the elements of interest for this study are listed below:

- Arsenic (As): ICP-033

- Copper (Cu): ICP-029
- Iron (Fe): ICP-026
- Antimony (Sb): ICP-151
- Yttrium (Y): IMS-115

A set of calibration standards was prepared using the primary standards. The range of ICP-MS calibration standards was determined by the dilution factor of the initial samples and other requirements. A typical range of calibration standards is as follows: As and Sb: 1, 10, 50, 100, and 500 ppb; Fe 1000, 2000, 5000, 10000, and 50000 ppb.

These calibration standards were prepared for As and Sb present together, while Fe standards were prepared separately. Each calibration standard for the As, Sb and Fe analytes had an internal standard, yttrium, at a constant concentration of 1 ppb. The provided calibration ranges and dilution factors served as a baseline and were modified according to the requirements of a specific sample set. The sample dilution factors for iron analysis were from 200 to 500. All samples prepared for ICP-MS analysis had a 5% nitric acid concentration (by volume). 10 mL Falcon tubes were used for both experimental samples and calibration standards. Additional information regarding other ICP-MS standards and operational procedures can be referenced in Pinochet-Troncoso (2023) and Schlepp (2024).

To confirm the accuracy of UW ICP-MS analysis, selected sets of the samples generated in ME experiments were submitted to the King County Environmental Laboratory (KCEL) for the determination of other analytes of interest. The KCEL laboratory holds accreditation from the Washington State Department of Ecology (WDOE) (King County, 2024). These samples mainly consisted of untreated LFG condensate, ME treatment effluent and calibration standards. Because KCEL is a third-party institution, complete details of KCEL analytical procedures will not be provided in this thesis.

3.5. 1,10-phenanthroline spectrophotometric method of determination of iron

The goal of employing the standard 1,10-phenanthroline (1,1-Phen) method is to quantitatively determine the concentration of ferrous (Fe^{2+}) ions in ME-treated effluents and other samples (APHA, 1997). In this method, 1,1-Phen acts as a chelating agent that forms a strong complex with ferrous ions. This complex has an intense orange color. Spectrophotometric measurements of the absorbance of this complex allow correlating it with the concentration of ferrous ions. The intensity of the absorbance (which is visually perceived as the orange color) of the 1,1-Phen/Fe^{2+} complex is directly proportional to the concentration of ferrous ions in the solution. The experiment involves creating a calibration curve using known concentrations of ferrous ion. Once the correlation between the absorbance of the 1,1-Phen/Fe^{2+} complex is established, the unknown Fe^{2+} concentration in a sample can be determined by comparing the sample's absorbance to that found in the calibration curve. But the limit of detection needs to be tested in the future.

3.5.1. Reagents:

1) Hydrochloric acid, HCl, concentrated, containing less than 0.00005% iron.
2) Hydroxylamine solution: Dissolve 10 g $NH_2OH{\cdot}HCl$ in 100 mL water.
3) Ammonium acetate buffer solution: Dissolve 25g ammonium acetate NH_4CH_3COO in 15 mL water. Add 70 mL conc (glacial) acetic acid. Because even a good grade of NH_4CH_3COO may contain a significant amount of iron, prepare new reference standards with each buffer preparation.
4) 1,10-phenanthroline solution: Dissolve 100 mg 1,10-phenanthroline monohydrate, $C_2H_8N_2H_2O$, in 100 mL water and add 2 drops concentrated HCl. (Note: One milliliter of this reagent is sufficient for no more than 100 μg Fe.)
5) Stock iron solution: If ferrous ammonium sulfate is preferred, Dissolve 1.404 g $Fe(NH_4)_2(SO_4)_2{\cdot}6H_2O$ in 100 mL water. Dilute to 1000 mL with water and mix; 1.00mL =200μg Fe.
6) Standard iron solutions: Prepare daily for use. (Usually, prepare a set of five standards with concentrations of 0 ppm, 0.1 ppm, 0.25 ppm, 0.5 ppm, 1 ppm, 1.5 ppm, and 2 ppm. However, adjustments to this standard set can be made based on specific experimental requirements or circumstances.

3.5.2. Experimental procedures

Standards Preparation: Iron standard solutions are made by pipetting 50 μL of the ferrous stock solution into a volumetric flask to achieve a desired Fe^{2+} concentration. In this thesis, calibration solutions had concentrations 0.1 ppm, 0.5 ppm, 1 ppm, 1.5 ppm, and 2 ppm. 5 mL $NH_4C_2H_3O_2$ buffer solution, 2 mL hydroxylamine solution, and 4 mL phenanthroline solution were added to each 100 mL volumetric flask containing the calibration solution Following this, the mixtures are diluted to the mark with milliQ water and thoroughly mixed before allowing 10 to 15 minutes for optimal color development.

Absorbance/color measurements: A set of standards ranging from 1 to 100 μg Fe in a final 100-mL volume is created for visual comparison. The UV instrument is then switched on, and a 20-minute warm-up period is allowed. A baseline measurement is taken using DI Water across the wavelength range of 200 nm to 700 nm. The absorbance of each standard and sample is measured across the same wavelength range using the same measuring cell. Subsequently, the data from the UV Probe software is transferred to Excel for analysis. A calibration curve is generated using the peak points of each standard, and the sample data is compared to this curve to calculate the iron concentration of samples.

A second set of samples may need to be prepared without adding phenanthroline if they are colored or turbid. Prepared blanks are used instead of distilled water to set the photometer to zero absorbance. Each developed sample with phenanthroline is then read against the corresponding blank without phenanthroline. The observed photometer readings are translated into iron values using the calibration curve. It is important to note that this procedure does not compensate for interfering ions. All steps are conducted with strict adherence to safety protocols and waste disposal procedures to ensure accurate and reliable results.

3.5.3. Supplementary information concerning the standard 1,10-Phen method

- Three molecules of phenanthroline chelate each atom of ferrous iron to form an orange-red complex. The equation for the reduction of the iron(III) ion to the iron(II) ion is:

$$4Fe^{3+} + 2NH_3O \rightarrow 2N_2O + 4Fe^{2+} + 6H^+$$

- Interfering substances in the analysis include strong oxidizing agents, cyanide, nitrite, and phosphates (particularly polyphosphates over orthophosphate), chromium, zinc concentrations exceeding 10 times that of iron, cobalt and copper concentrations exceeding 5 mg/L, and nickel concentrations exceeding 2 mg/L. Bismuth, cadmium, mercury,

molybdate, and silver precipitate phenanthroline. Initially boiling with acid converts polyphosphates to orthophosphate and removes cyanide and nitrite, which could otherwise interfere. The addition of excess hydroxylamine helps mitigate errors caused by high concentrations of strong oxidizing reagents. In the presence of interfering metal ions, a larger excess of phenanthroline may be required to replace that complexed by the interfering metals. In cases of excessive concentrations of interfering metal ions, the acid extraction method may be employed. If noticeable color or organic matter is present, it may be necessary to evaporate the sample, gently ash the residue, and redissolve in acid. Ashing can be performed in silica, porcelain, or platinum crucibles boiled for several hours in 6 N HCl. Excessive amounts of organic matter may require digestion before utilizing the extraction procedure.

- Nitrite presents a risk of yielding false negative outcomes during soluble and ferrous analysis. Additionally, it serves as a notable positive interference in total analysis. Samples containing nitrite exhibit color changes to yellow, orange, or red upon the introduction of thioglycolic acid solution (A-6000).
- The stability of the orange-red complex is high, with no observed fading for up to six months. This suggests that the standards can be stored for a minimum of six months without any significant degradation.
- Hydroxylamine is added to the solution with the purpose of converting any ferric ions (Fe^{3+}) back to ferrous ions (Fe^{2+}). This enables the detection of the total iron content in the solution.
- Ammonia acetate buffer helps maintain a stable pH level in the solution and control the effects of interfering ions on the accuracy of the analysis. By maintaining a specific pH around 3.2-3.3, the buffer can minimize the interference of ions that might otherwise affect the formation of complexes or reactions involving the metal ions of interest.
- Dispose of all solutions and leftover reagents from this experiment appropriately by transferring them into the designated Hazardous Waste Bottle. This encompasses the blank, unknown, and standard solutions, as well as any remaining stock iron standard solution, residual concentrated sulfuric acid, hydroxylamine hydrochloride, and ortho-phenanthroline solutions. Additionally, include any solid ferrous ammonium sulfate remnants from the experiment. If uncertain about the correct container, please seek clarification.

3.5.4. Stability of the Standards

The stability of standards in the 1,10-Phen method is highly important for its practical use, notably in field conditions. In principle, factors such as exposure to light, air, and contaminants can all affect the stability of the standards over time. To test the stability the 1,10-Phen standard prepared the reagents and conditions used in the study, an initial set of calibration standards spanning Fe concentrations of 0 ppm, 0.1 ppm, 0.3 ppm, 0.5 ppm, 1 ppm and 1.5 ppm (Set A) was prepared on November 23, 2023. The resulting absorbance spectra are show presented below.

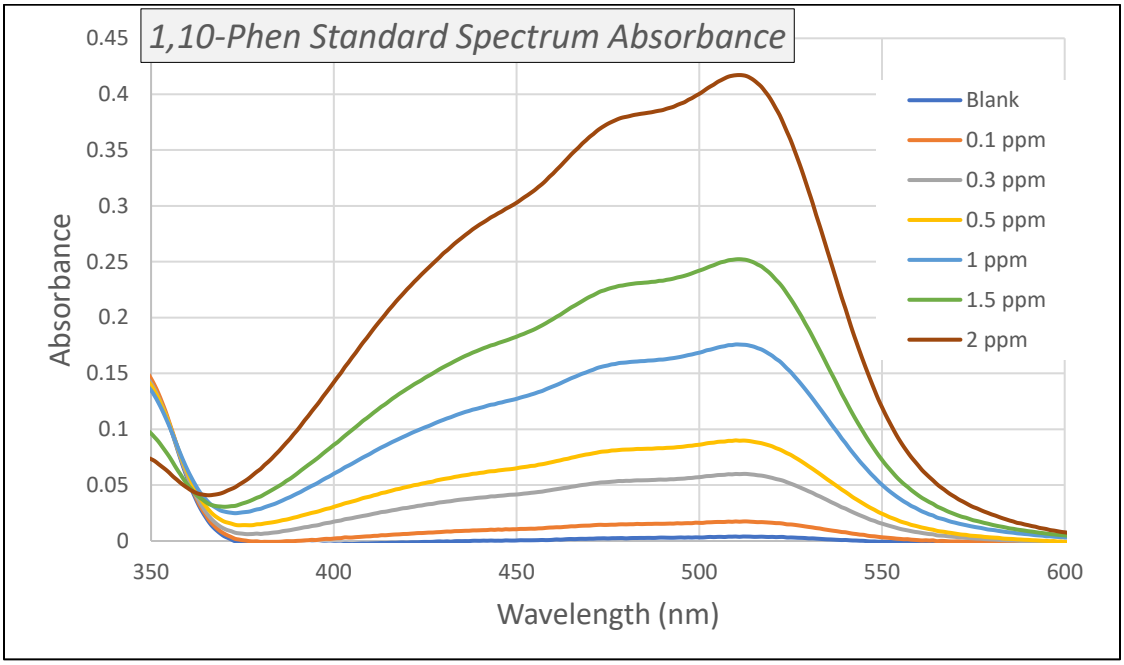

Fig 3-2 Absorbance spectra of Set A calibration standards and 1000X diluted SR18 and SR19 samples (prepared on 2023-11-21).

To examine the quality and repeatability of the standards, absorbance spectra measurements were repeated on December 2nd, 2023 and December 12th, 2023. Fig 3-3 indicates consistent absorbance values compared to the initial measurement on November 21st, 2023. All three sets of calibration measurements exhibited an R^2 value of 0.99 although some deviation from the slope was observed the third repetition.

These measurements however had to be repeated since later in December 2023 it was realized that hydroxylamine may not have been added to the previously prepared calibration standards, potentially leading to lower stability of the standards and underestimation of total iron content. A

new series of calibration standards (Set B) was prepared by adding, as required by the standard method, two 2mL aliquots of hydroxylamine solution. Additionally, a 2 ppm Fe calibration standard was introduced to expand the measurement range. The absorbance spectra and a calibration curve obtained in these measurements are presented in Figures 3-2 and 3-3, respectively. The data resulted in a an R^2 value of 0.99, affirming the excellent correlation and the accuracy of the calibration standards. On January 11th, repeated calibration measurements using the same standards were carried out. The measurements shown in Fig 3-3 yielded consistent practically identical results.

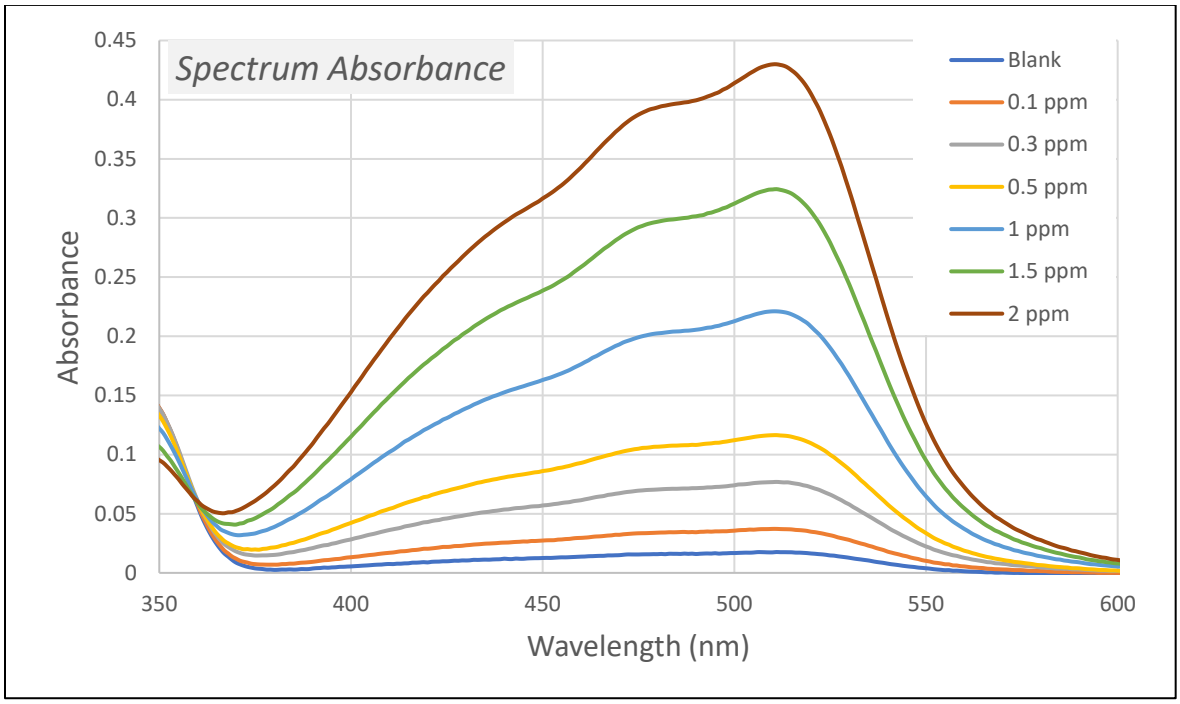

Fig 3-3 Absorbance spectra of Set A calibration standards (prepared on 2023-11-21 and remeasurement on 2024-01-11)

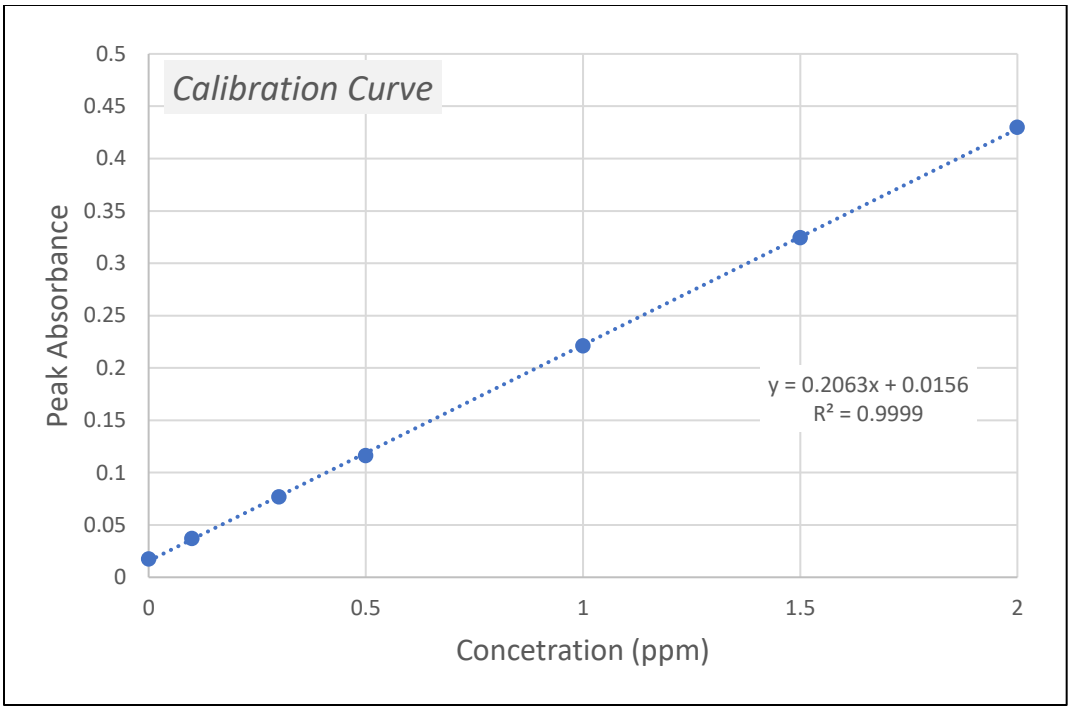

Fig 3-4 2023-12-15 Absorbances of the calibration standards measured at 514 nm (prepared by Fisher Chemical)

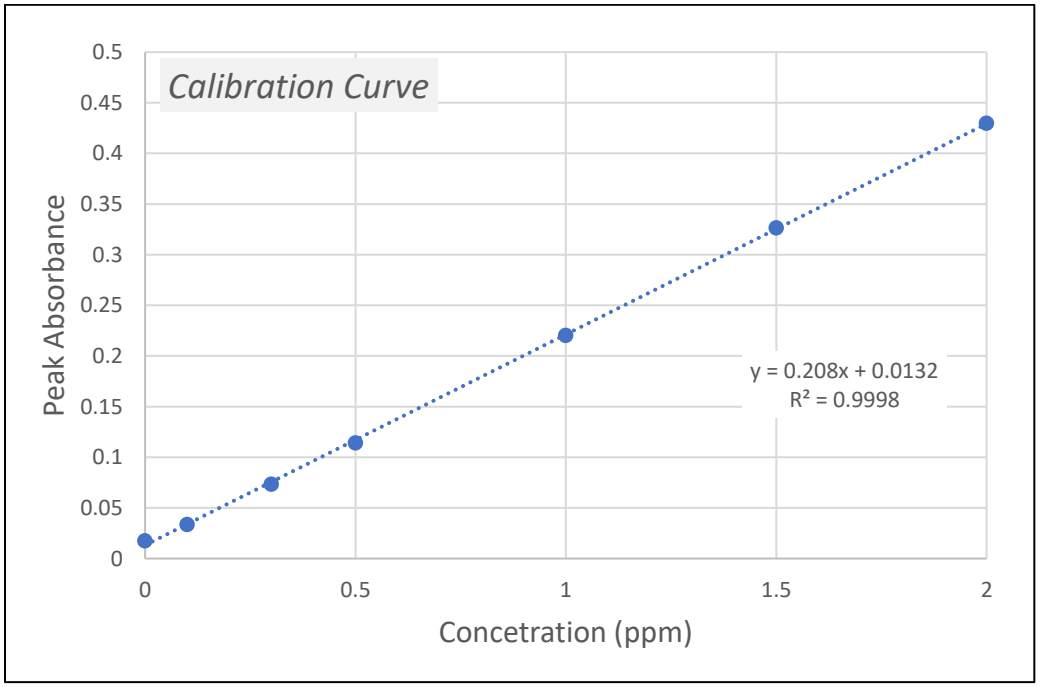

Fig 3-5 2024-01-11 Absorbances of the calibration standards measured at 514 nm (prepared by Hi Media)

Due to the depletion of the batch of ammonium acetate that was used in the experiments described above (Fisher Chemical™, Batch No: MFCD00013066), a different brand of ammonium acetate (Hi Media, Batch No: GRM3882-500G) was purchased from Amazon. As this alternative option came at a significantly lower cost, its quality and efficacy need to be validated. A new set of standards were prepared using the new reagent (Set C). Remarkably, there was practically no difference between the two sets of calibration standards, with both exhibiting an R^2 value of 0.999 and the slope, as shown in Fig 3-6.

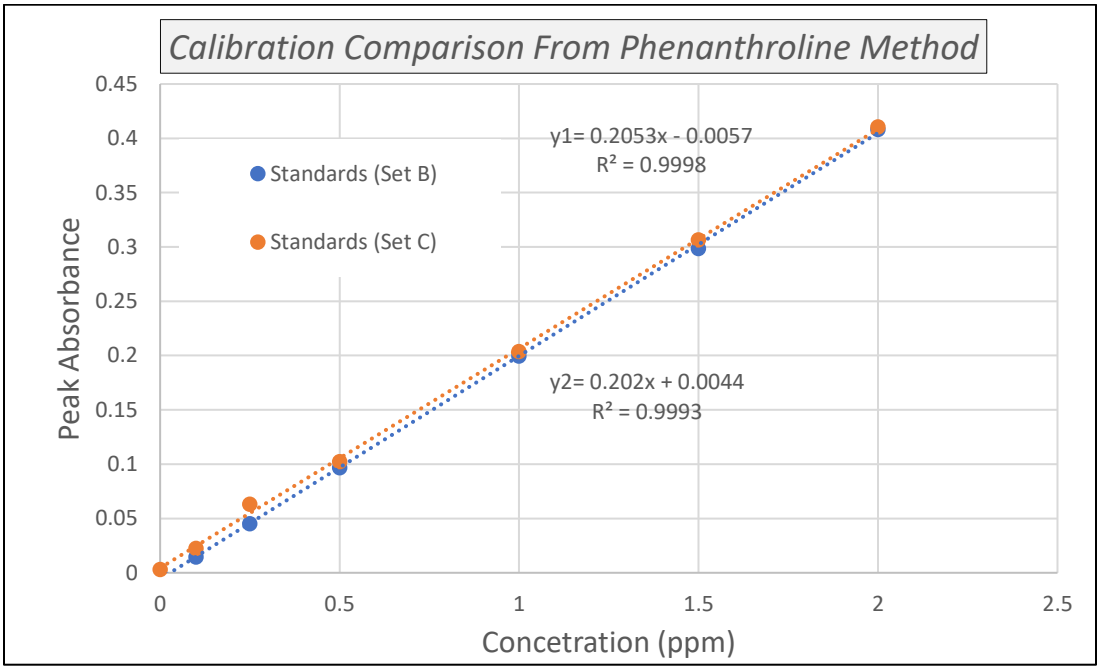

Fig 3-6 1,10-Phen Standards Calibration Curve Comparison (Set B was prepared on 2023-12-23 and Set C was prepared on 2024-02-05)

Table 3-3 Information of sets of 1,10-Phen method standards

Name	Prepared Date	Brand of ammonium acetate	Measurement Range	Additional Information
Set A	2023-11-21	Fisher Chemical™	0 - 1.5ppm	Without Hydroxylamine
Set B	2023-12-15	Fisher Chemical™	0 - 2ppm	With Hydroxylamine
Set C	2024-02-05	Hi Media	0 - 2ppm	With Hydroxylamine

All the information of 3 sets of the 1,10-Phen method calibration standards is concluded in Table 3-3. These rounds of examination and testing of the 1,10-Phen calibration standards showed that the prepared standards can be reliably stored in the cold room for at least two months without no discernible alteration to the calibration curves obtained based on the absorbances. These results also showed that the use of various brands of ammonium acetate does not result in appreciable changes of the calibration data.

3.5.5. Comparison of 1,10-Phen and ICP-MS results

To check the precision of the Fe calibration standards prepared in the UW lab, Fe concentrations determined based on them, and, on the other hand, Fe concentrations determined by ICP-MS, we sent to KCEL our phenanthroline standards and ICP-MS calibration standards to KCEL, which is a certified analytical lab.

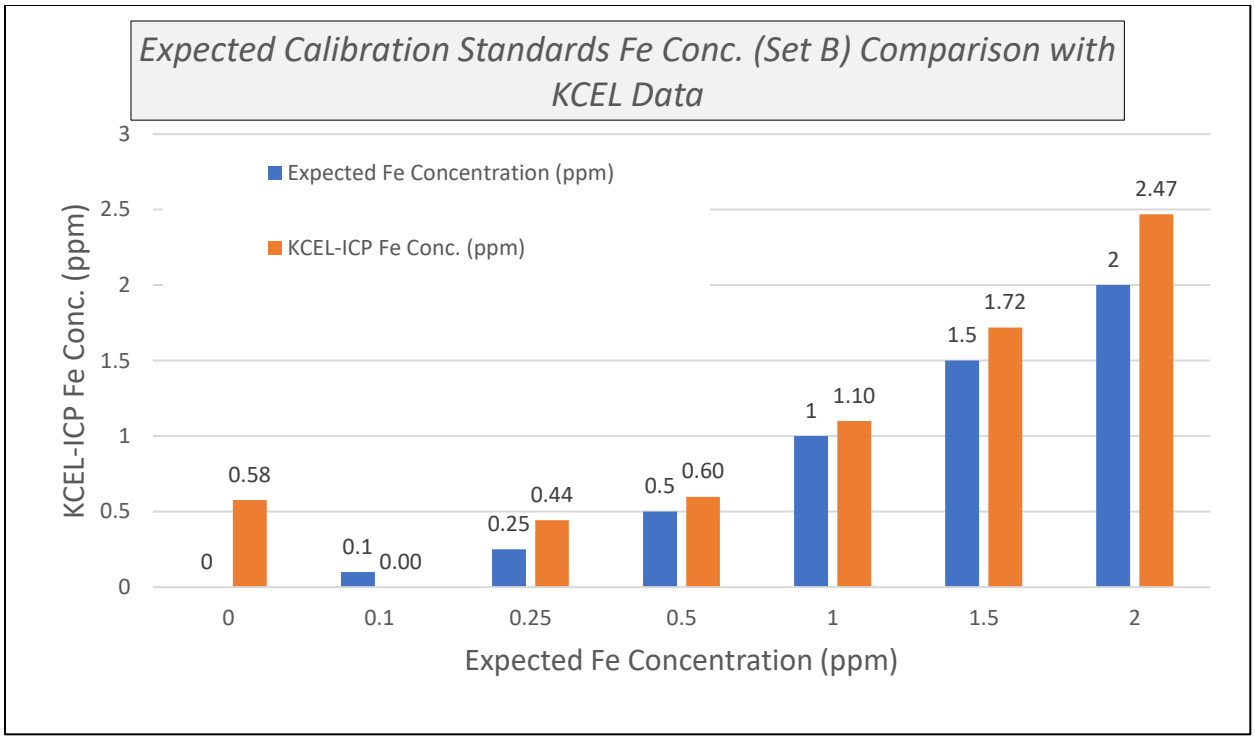

Fig 3-7 Expected Phenanthroline calibration standards (Set B) concentration (prepared on 2024-01-17) comparison with KCEL data

Fig 3-7 compares the anticipated and measured Fe concentrations found in the initial set of the 1,10-Phen standards. There was one notable difference between the Fe concentrations expected to be found in the 0.1 ppm samples. However, 0.58 ppm was found in the KCEL-analyzed sample, probably due to the more precision of KCEL's ICP. There was also a difference in Fe concentrations found in the 2 ppm sample but it did not affect the overall performance of the 1,10-Phen method. The Fe concentrations in the remaining standards align well with their expected values. The absolute Fe concentrations in the standards prepared for the 1,10-Phen analyses tend to be higher than their respective nominally expected values, but these differences were mitigated by subtracting the Fe concentration in the blank.

3.5.6. ICP-MS calibration standards comparison

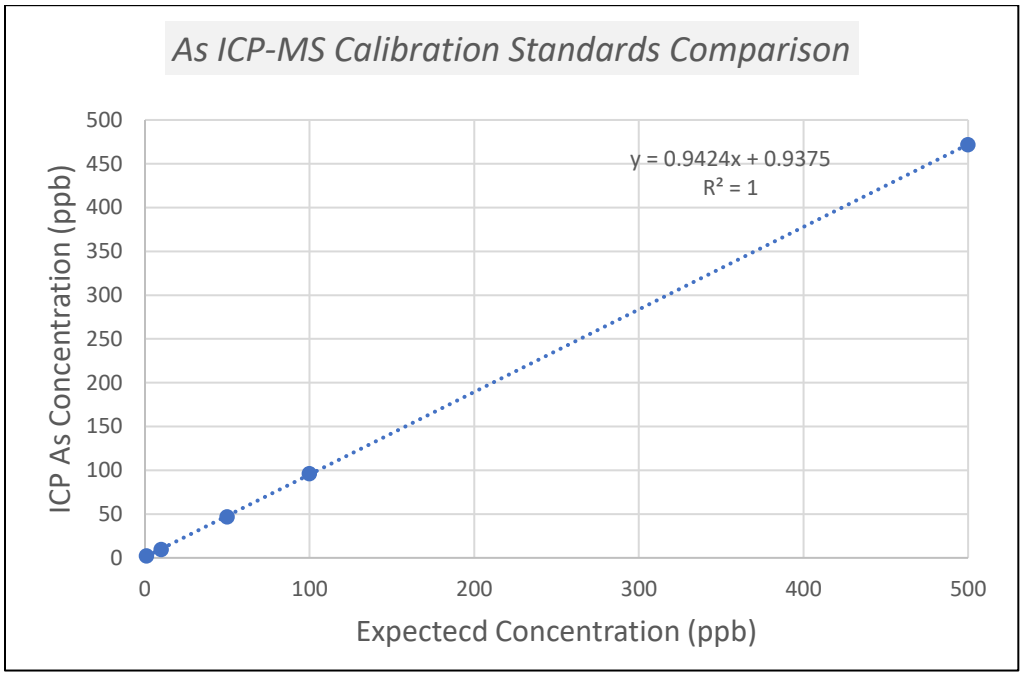

Fig 3-8 As Concentration ICP-MS Calibration Standards Comparison

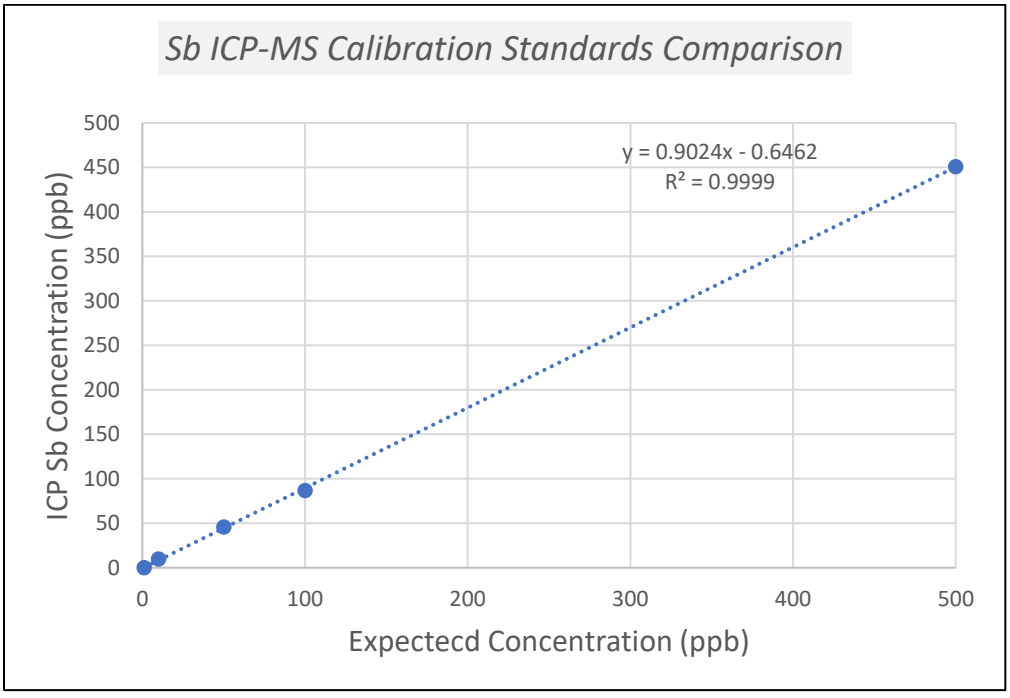

Fig 3-9 Sb Concentration ICP-MS Calibration Standards Comparison

Fig 3-8 and Fig 3-9 illustrate the correlations between the expected and measured concentrations of As and Sb in the standard used for ICP-MS analyses performed on the UW campus. Both correlations are nearly perfect, with R^2 values close to 1, affirming the accuracy of the standards prepared for the UW ICP-MS analysis.

Fig 3-10 presents further comparison between the measured concentrations of As and Sb and their expected values. The figure shows that the nominal concentrations of As and Sb expected for the UW standards were slightly lower, by 5% and 10% respectively, compared with the concentrations of these elements determined by KCEL. However, these differences are deemed acceptable for the purposed of this study.

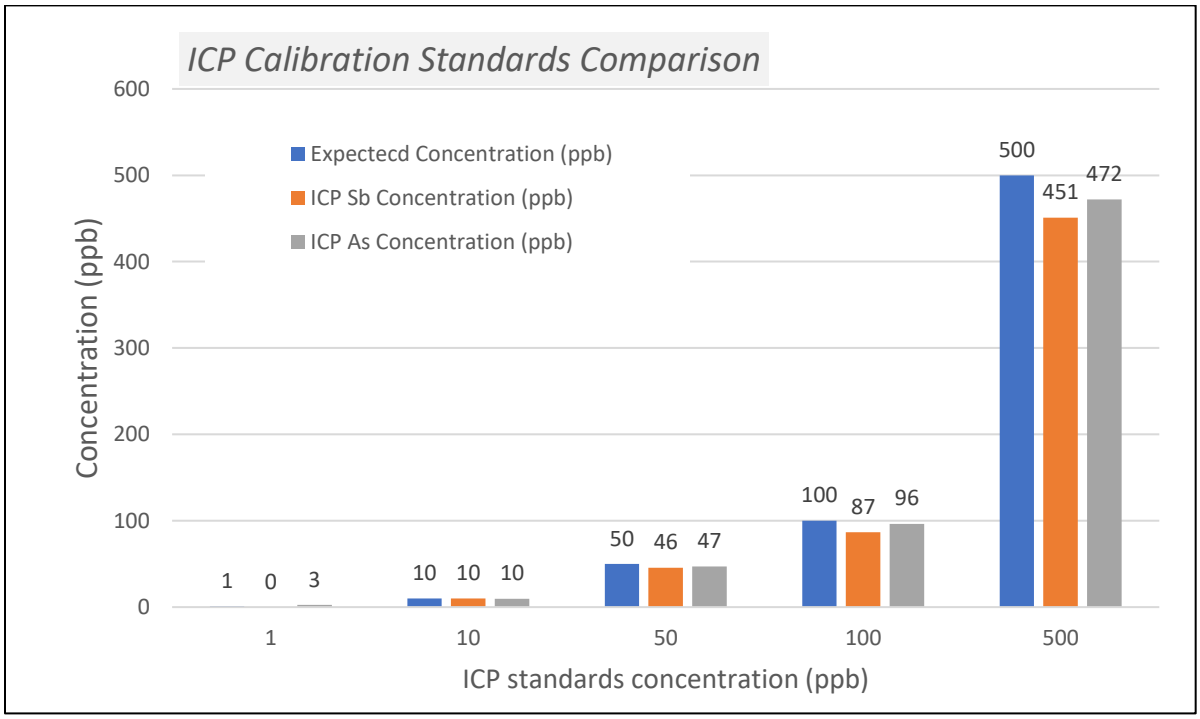

Fig 3-10 Expected concentration and ICP-MS As and Sb Calibration Standards Comparison

3.6. Hach Color Wheel Iron Method

3.6.1. Method

The Hach Iron Test Kit serves as a quick but rough estimation method for determining iron concentration, operating on a principle akin to standard phenanthroline methods. This involves the addition of 1,10-phenanthroline to the sample to produce an orange color whose intensity is

compared with the reading of a standard color wheel. This approach is deemed to be useful for rapid measurements of Fe concentrations, for instance in field conditions while the standard spectrophotometric method of absorbance measurements offers higher precision. An outline of procedures needed for color-wheel Fe measurements is given below.

- **Preparation:** Place the color disc on the center pin of the color comparator box, ensuring that the numbers are facing the front. Use the indoor light color disc when the light source is fluorescent light, and the outdoor light color disc when the light source is sunlight. Before conducting the test, rinse the tubes with the sample. After the test, rinse the tubes with deionized water.
- **Color Comparison:** If the color match falls between two segments, use the value that is in the middle of the two segments. If the color disc becomes internally wet, separate the flat plastic sides to open the color disc. Remove the thin inner disc and dry all parts with a soft cloth before reassembling. Undissolved reagent does not affect the test accuracy. To verify the test accuracy, use a standard solution as the sample. If the sample contains rust or precipitated iron, thoroughly mix the sample and then fill the tubes. Wait 2–5 minutes after adding the reagent. Dissolved iron develops color immediately. For samples containing more than 4 mg/L iron, which goes over the testing range, consider diluting the sample as follows: Use a 3-mL syringe to add 2.5 mL of sample to each tube. Dilute the sample to the 5-mL mark with deionized water. Use the diluted sample in the test procedure and multiply the result by 2.

3.6.2. Comparison of 1,10-Phen results determined spectrophotometrically and using the color wheel approach

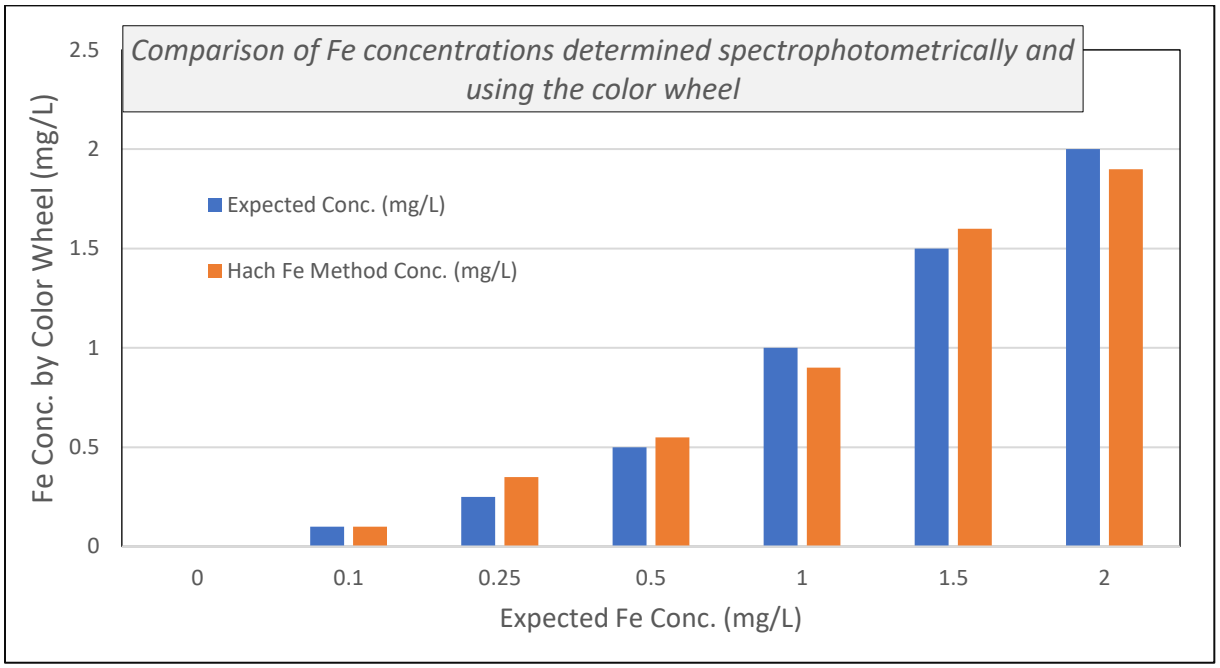

Fig 3-11 Comparison of Fe concentrations determined based on spectrophotometric measurements and those determined the color wheel approach.

Given that the color wheel approach is most suitable for ME operation in field conditions, we compared results of 1,10-Phen measurements carried out using the high precision spectrophotometer and, on the other hand, the color wheel provided by Hach. Figure 3-11 compares Fe concentrations determined based on the absorbance measurements and those determined visually using the Hach color wheel. Figure 3-11 demonstrates that the results of these two methods are very close, with only minor differences between the spectrophotometric data and those determined based on the visual color matching. These data demonstrate that the color wheel method provides sufficiently precise results and can serve as a convenient and reliable on-site measurement technique to determine Fe concentrations in ME-treated LFG condensate samples.

3.7. Iron Release Data Comparison

Iron concentrations in practically all samples generated in the ME experiments were determined using the 1,10-Phen spectrophotometric method and UW ICP-MS equipment. Some of the samples

were also sent to KCEL. As a result, Fe concentrations were determined in these samples using three different analyses of which the results obtained in KCEL are deemed to be most precise.

3.7.1. Comparison of Fe concentrations determined using three methods

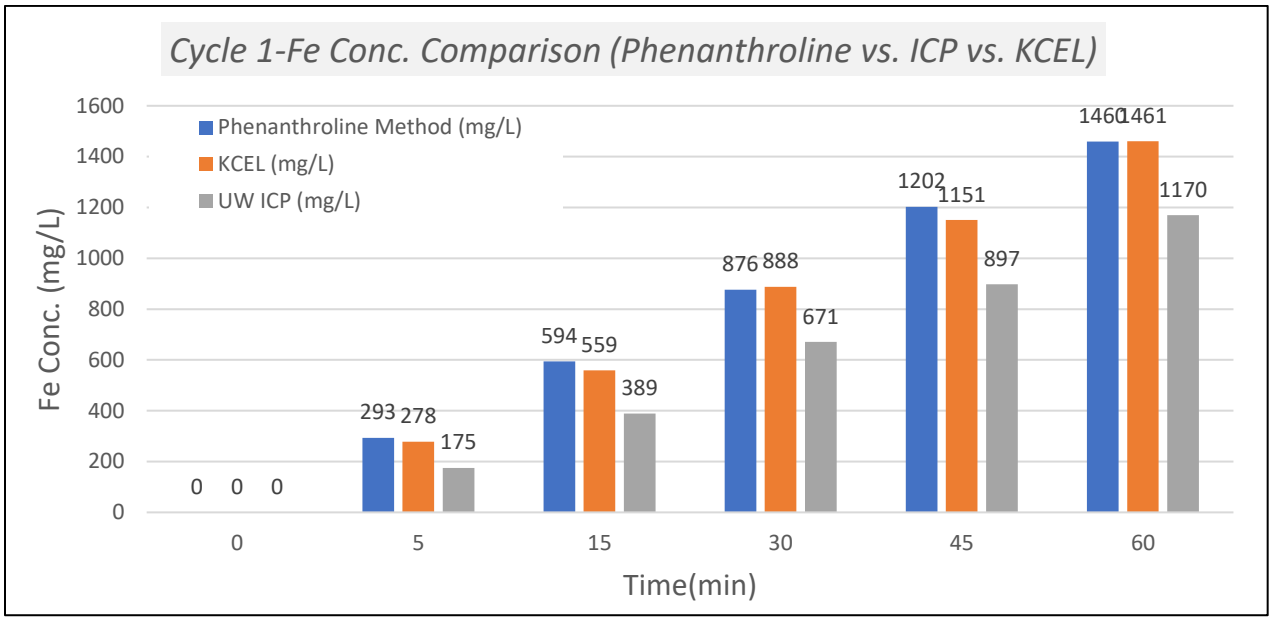

Fig 3-12 Comparison of Fe concentrations determined using the 1,10-Phen method and ICP-MS measurements in UW and KCEL Experimental conditions: First cycle of ME treatment, SR19 condensate sample, MC1 0.25L ME reactor, pH 3, ZVI/GAC weight ratio 2, ZVI/GAC dose 50 g/L, combined ZVI/GAC 2 g/L pH 3, 1000 rpm mixing. ME treatment experiment was performed on 12/21/23.

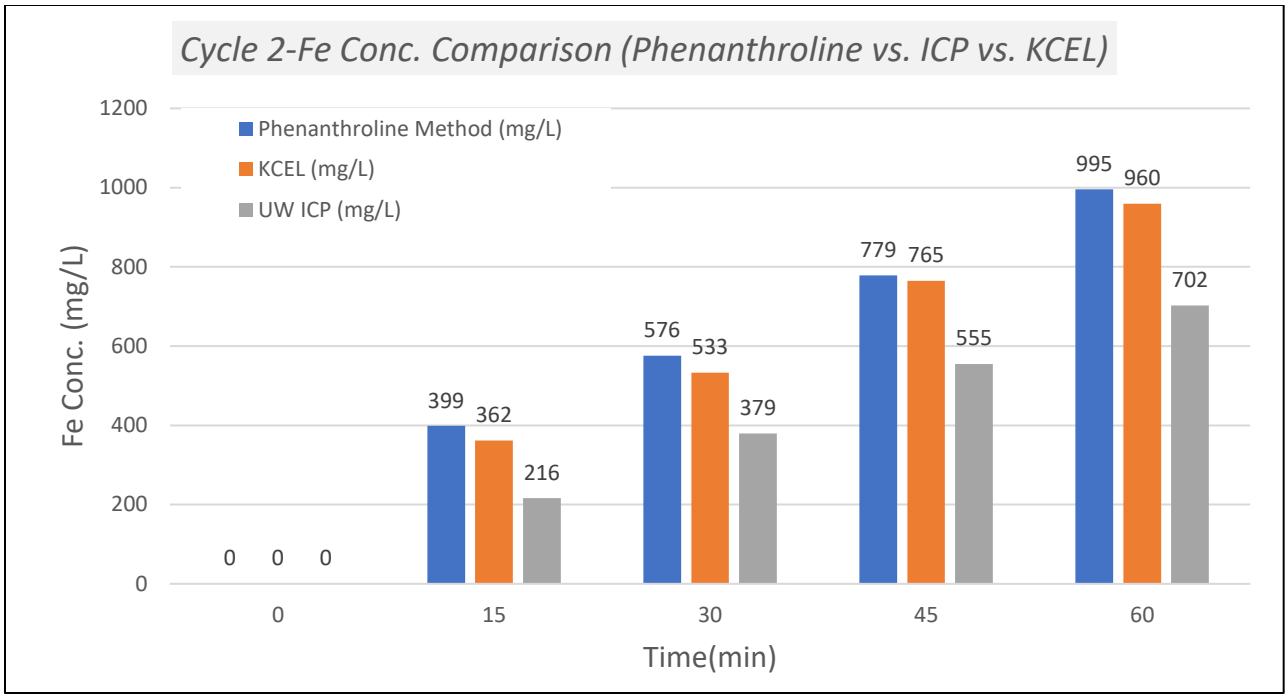

Fig 3-13 Comparison of Fe concentrations determined using the 1,10-Phen method and ICP-MS measurements in UW and KCEL Experimental conditions: Second cycle of ME treatment, SR19 condensate sample, MC1 0.25L ME reactor, pH 3, ZVI/GAC weight ratio 2, ZVI/GAC dose 50 g/L, combined ZVI/GAC 2 g/L pH 3, 1000 RPM mixing. ME treatment experiment was performed on 12/21/23.

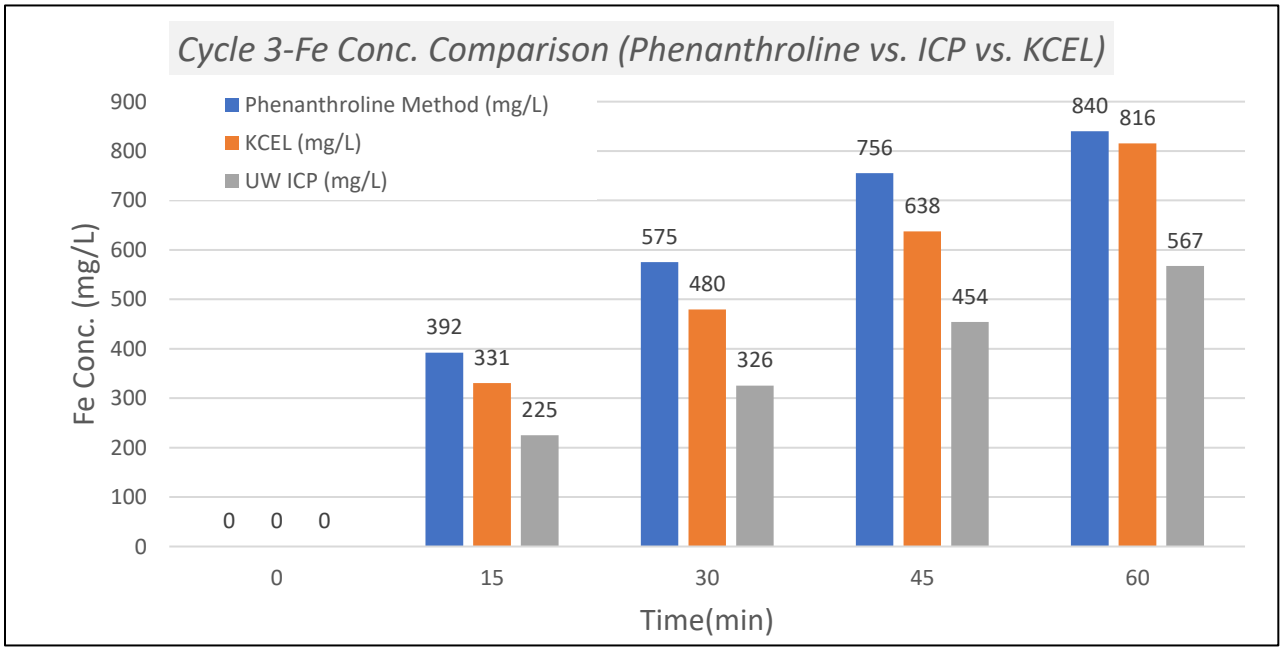

Fig 3-14 Comparison of Fe concentrations determined using the 1,10-Phen method and ICP-MS measurements in UW and KCEL Experimental conditions: Third cycle of ME treatment, SR19 condensate sample, MC1 0.25L ME reactor, pH 3, ZVI/GAC weight ratio 2, ZVI/GAC dose 50 g/L, combined ZVI/GAC 2 g/L pH 3, 1000 rpm mixing. ME treatment experiment was performed on 12/21/23

Fig 3-12, Fig 3-13 and Fig 3-14 show the iron release data for three consecutive 1 hour-cycles of the typical SR19 ME experiment which was conducted in December 2023. The data show that the 1,10-Phen method yields Fe concentrations that are approximately 5% higher than those obtained in KCEL analyses. The UW-ICP data show Fe concentrations approximately 10% lower than those determined in the KCEL measurements. This difference reflecting a consistent difference between Fe concentrations determined using UW-ICP equipment and those reported by KCEL. These results also show the close similarity between the Fe analytical data obtained using the 1,10-Phen method and highly precise KCEL ICP-MS data.

Table 3-4 Interference element concentration range from KCEL

Interference element	Concentration range (ug/L)
Nickel (Ni)	157±150
Manganese (Mn)	9000±700
Chromium (Cr)	26±12

The standard 1,10-Phen method (section 3.5.3) states that elevated Fe concentrations detected using this spectrophotometric method may be attributed to interferences of Ni, Mn and Cr. Table 3-4 shows that the concentration of Ni detected in our samples ranged from 6 to 300 µg/L, which is below the maximum acceptable concentration of 2 mg/L for Ni as an interference. However, Ni is released more slowly from ZVI compared to Fe (Anderson et al., 1989) and may begin to accumulate in the ME-treated solutions during the second, third, and subsequent treatment cycles, thus potentially increasing its interference in 1,10-Phen analyses for iron. However, given the relatively low Ni concentrations observed in ME-treated solutions, Ni was not likely to interfere in the 1,10-Phen analyses carried out in this study.

Manganese (Mn) can also potentially affect results of 1,10-Phen measurements. Our samples exhibited high concentrations of Mn, ranging from 8300 to 9700 ug/L. These Mn concentrations are high enough to result in significant interferences in 1,10-Phen analyses for Fe. On the other hand, chromium can be considered an interference only if its concentration exceeds ten times that of iron. Given the considerably higher concentrations of Fe in our samples, Cr was not considered an interference for 1,10-Phen measurements carried out in this study.

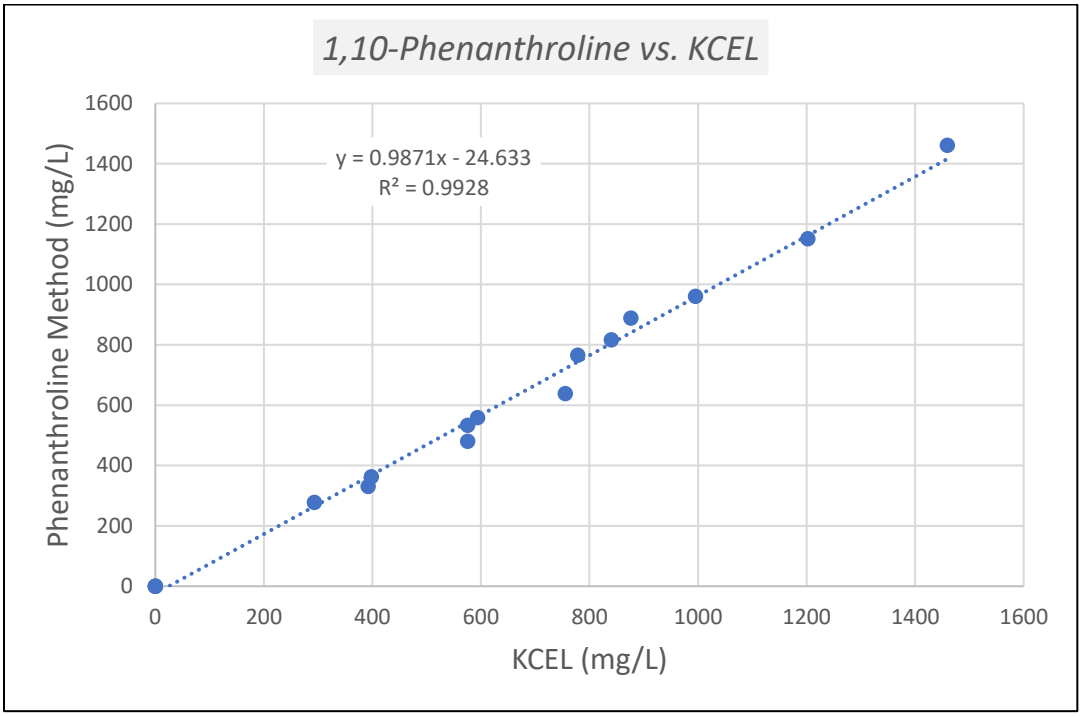

Fig 3-15 Correlation between Fe concentrations determined using the 1,10-Phen method and KCEL ICP-MS method for SR19 condensate sample, MC1 0.25L ME reactor, pH 3, ZVI/GAC weight ratio 2, ZVI/GAC dose 50 g/L, combined ZVI/GAC 2 g/L pH 3, 1000 rpm mixing.

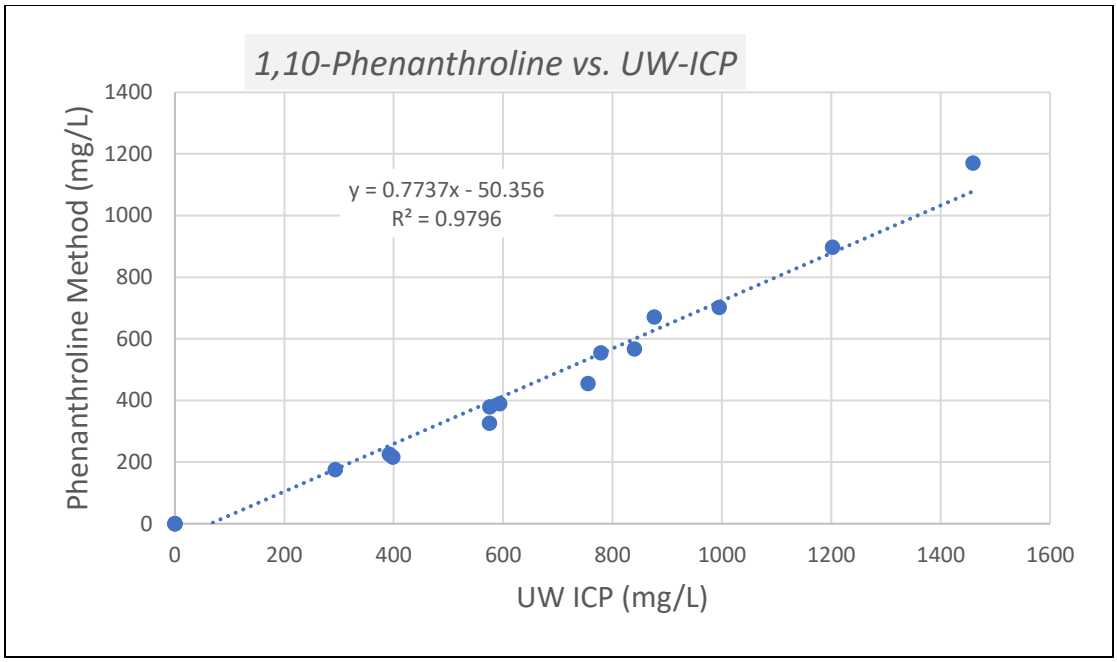

Fig 3-16 Correlation between Fe concentrations determined using the 1,10-Phen method and UW ICP-MS method for SR19 condensate sample, MC1 0.25L ME reactor, pH 3, ZVI/GAC weight ratio 2, ZVI/GAC dose 50 g/L, combined ZVI/GAC 2 g/L pH 3, 1000 rpm mixing.

Fig 3-15 and Fig 3-16 show the correlations between Fe concentrations determined using the spectrophotometric 1,10-Phen method, and KCEL or UW ICP-MS data. Despite the presence of Mn and species possibly interfering in 1,10-Phen analyses for iron, both figures show the presence of very linear correlation between 1,10-Phen and, on the other hand, ICP-MS KCEL and UW data, with R^2 values of 0.99 and 0.98, respectively. As mentioned above, the correlation is especially strong and has a nearly one slope for the correlation between the 1,10-Phen and KCEL data.

The concentration of interfering species that may affect the results of the 1,10-Phen method is likely to vary dramatically between different batches and commercially available types of ZVI. Additionally, the model we established in this study quantifies a typical trend for a relationship between As and Sb removal and Fe release during ME treatment. This model will have to be elaborated in the future using data of further lab-scale experiments that use varying doses and types of ZVI as well as experimental results to be obtained in the planned pilot- and full-scale implementation of ME treatment.

We conclude that despite the higher susceptibility of the 1,10-Phen method to the presence of potentially interfering compounds, its data correlate very well with the data of a certified analytical laboratory (KCEL) that used a highly sensitive ICP-MS instrument and a full complement of QA/QC procedures. The results thus demonstrate conclusively that the 1,10-Phen method is highly reliable, sensitive and reproducible and, as such, it can be used for Fe concentration determinations in ME-treated solutions generated in laboratory conditions and, upon completion of further tests, in pilot-scale ME treatment. Further experiments concerned with the quantitation of the interferences typical for ME treated solutions will be conducted in the future but such experiments go beyond the scope of this thesis.

4. Experimental results

4.1. Iron release during microelectrolysis treatment of LFG condensate and effects of different system conditions

Determination of the kinetics of Fe release is crucial for ME treatment because, as discussed in the sections that follows, Fe concentrations can serve both as an indicator of the extent of ME treatment and as a predictor of As removal efficiency. Several variables can influence Fe release, including operational pH, top-offs dosage, mixing regime, and etc.

1,10-Phen method was the main method employed to determine aqueous Fe concentrations in these experiments due to its convenience, stability and reasonably accurate analytical capabilities, despite the presence of potentially interfering elements such as Ni and Mn. To accommodate the 1,10-Phen method for analysis of ME-treated effluents that tend to have high Fe concentrations, all samples were diluted by a factor of 1000 to ensure that the Fe concentration remained within the calibration standard range of 0 ppm to 2 ppm. Similar corrections were also necessary in the ICP-MS analyses when this technique was used which involved adjusting the sample dilution factors from 200x to 500x.

4.1.1. Fe release in the baseline conditions of ME treatment

The standard operating conditions for typical ME treatment involve the following parameters: a pH of 3 controlled by 0.5 M H_2SO_4, continuous mixing at 1000 rpmrpm, a ZVI-GAC media dosage ratio of 50 g/L at 2:1, pre-treatment with CO_2 gas flush, and the addition of 2 g/L of combined ZVI and GAC top-offs in each cycle except for the initial cycle. Samples were taken every 10 min for determining Fe concentrations, mostly for the 1,10-Phen method, and for As and Sb concentration determination using ICP-MS.

The data presented in

Fig 4-1 and Fig 4-2 show that both in the case of ME treatment of SR19 and SR21 LFG condensates, Fe release is most rapid during the first cycle and then decreases in subsequent ME treatment cycles. This observation is in accord with prior measurements of Fe release carried in the context of exploration of ME treatment. It is notable that ME treatment of SR19 resulted in higher Fe concentrations compared with those for SR21. However, the properties of these samples are different in the sense that SR21 had been stored in the gas blower sump under anoxic conditions

for nine months (from June 2023 to April 2024) prior to being sampled and used in our experimental work, while SR19 was sampled while the biomethane plant was operating and then used for tests soon after its delivery in the lab. The significance of differences between the properties of stored and freshly generated LFG condensates and their influence on As/Sb removal and Fe release in ME treatment will be explored in the future.

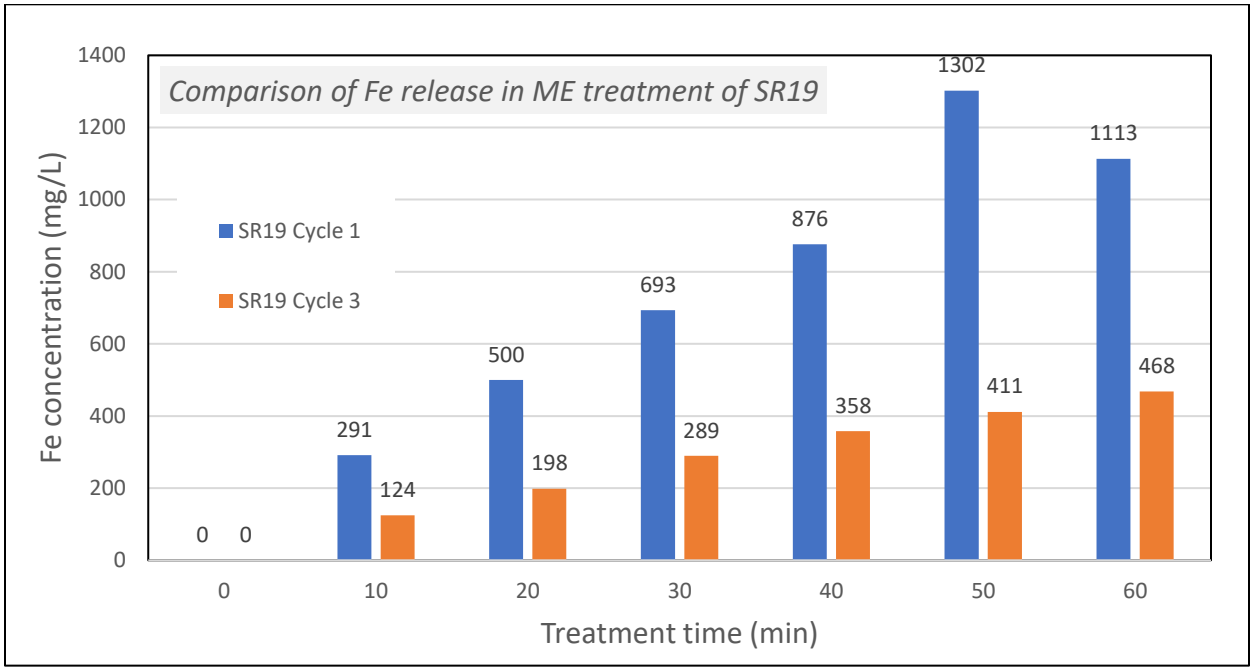

Fig 4-1 Comparison of Fe release during the first and third cycles of ME treatment of SR19 condensate, baseline conditions. 0.25 L MC1 reactor, 50 g/L active media dose, 2:1 ZVI/GAC weight ratio, 2 g/L ZVI/GAC top offs, pre and post treatment CO_2 flush, 1000 rpm mixing.

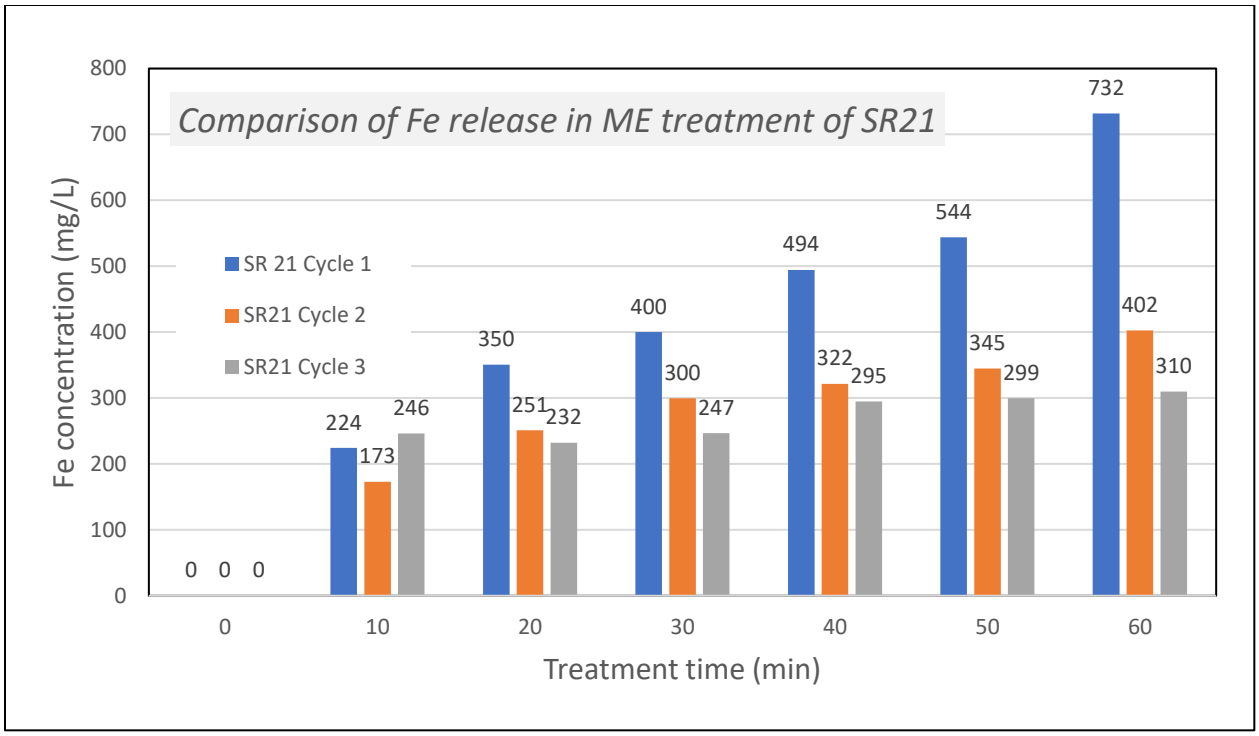

Fig 4-2 Comparison of Fe release during the first, second and third cycles of ME treatment of SR21 condensate, baseline conditions. 0.25 L MC1 reactor, 50 g/L active media dose, 2:1 ZVI/GAC weight ratio, 2 g/L ZVI/GAC top offs, pre and post treatment CO_2 flush, 1000 rpm mixing.

4.1.2. Effects of variable compositions of active media top-off on Fe release and As removal

Three sets of SR19 ME treatment experiments were conducted using different compositions of the active media top-off compositions. These measurements were done for multiple cycles of ME treatment. Effects of combined ZVI/GAC top-offs were compared with those observed for GAC or ZVI additions only. The combined top-off dose was raised from 1 to 2 g/L to examine the impact of an elevated top-off dose on enhancing the performance of ME treatment media across multiple treatment cycles.

Fig 4-3 shows that Fe concentrations release with GAC additions only increase with time but consistently decreases with each ME treatment cycle. Fig 4-4 presents the results of Fe release measurements with ZVI top-offs only. Surprisingly, there was almost no discernible difference between the Fe release results obtained for GAC only and ZVI only top-offs.

Fig 4-5 shows that the use of combined ZVI/GAC top-offs resulted in higher release of Fe compared to that observed for GAC alone or ZVI alone top-offs. This phenomenon is likely attributable to the stronger action of the galvanic coupling between the GAC and ZVI phases in the case of additions of combined ZVI/GAC media.

Fig 4-6 compares As removal rates determined for multiple ME treatment cycles that used different top-offs. This figure confirms that the use of combined ZVI/GAC top-offs in the consecutive ME treatment cycles tended to result in a somewhat higher efficacy compared to that the ZVI-only top-off option albeit the difference between the As removal results for these two options was minimal. The use of GAC-only top-offs resulted in a lower treatment efficacy. This indicates that the passivation of ZVI surfaces that was partially compensated in the case of ZVI/GAC and ZVI-only top-offs was not compensated in the case of GAC-only top-off since in that case no fresh Fe(0) surface was added to the reactor.

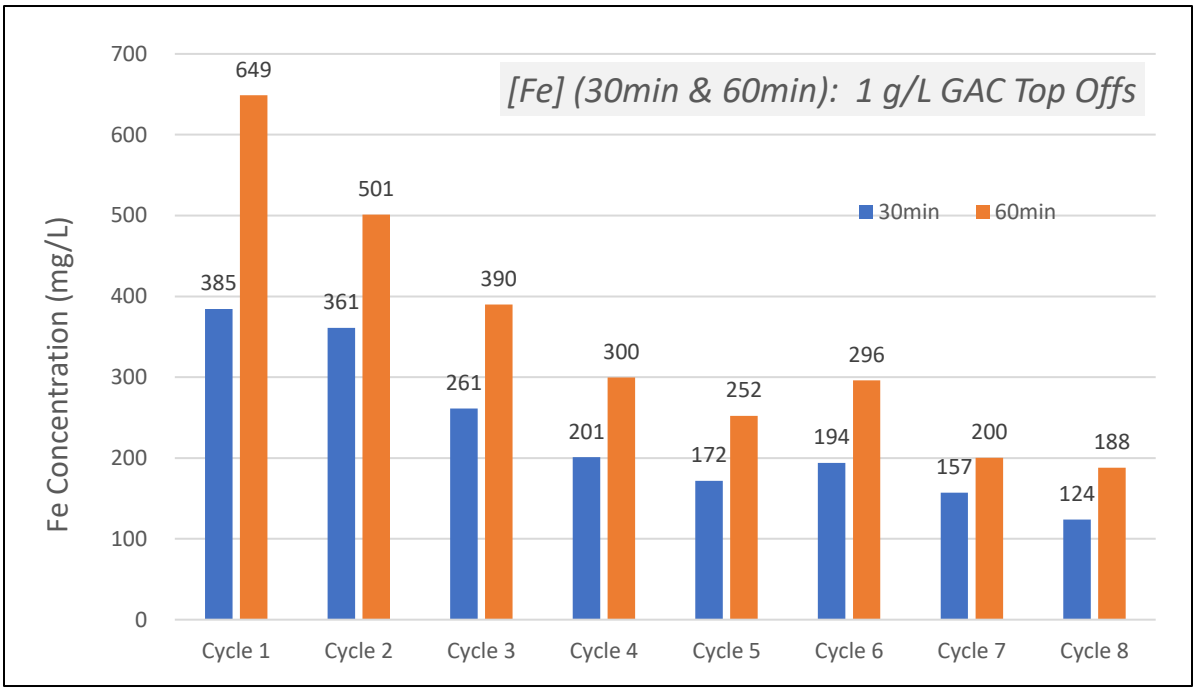

Fig 4-3 Fe release in multi-cycle ME treatment of SR19 condensate after 1 g/L GAC top offs at the beginning of each cycle. 0.25 L MC1 reactor, 50 g/L initial active media dose, 2:1 ZVI/GAC weight ratio, pre and post treatment CO_2 flush, 1000 rpm mixing.

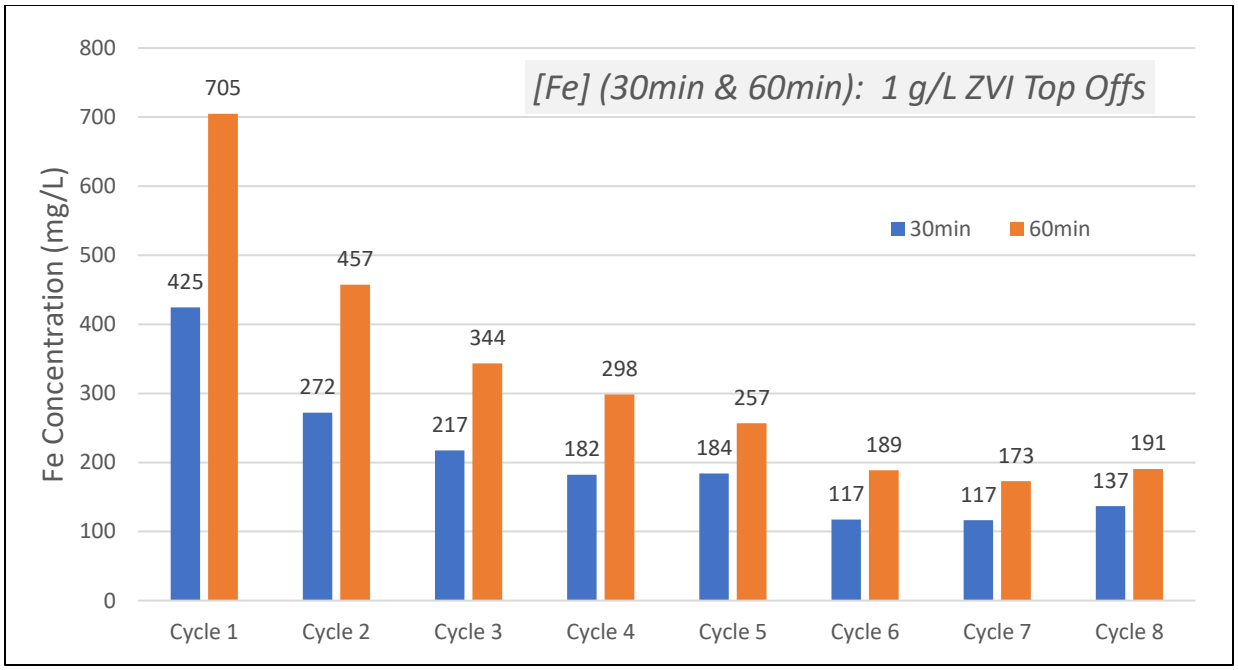

Fig 4-4 Fe release in multi-cycle ME treatment of SR19 condensate after 1 g/L ZVI top offs at the beginning of each cycle. 0.25 L MC1 reactor, 50 g/L initial active media dose, 2:1 ZVI/GAC weight ratio, pre and post treatment CO_2 flush, 1000 rpm mixing.

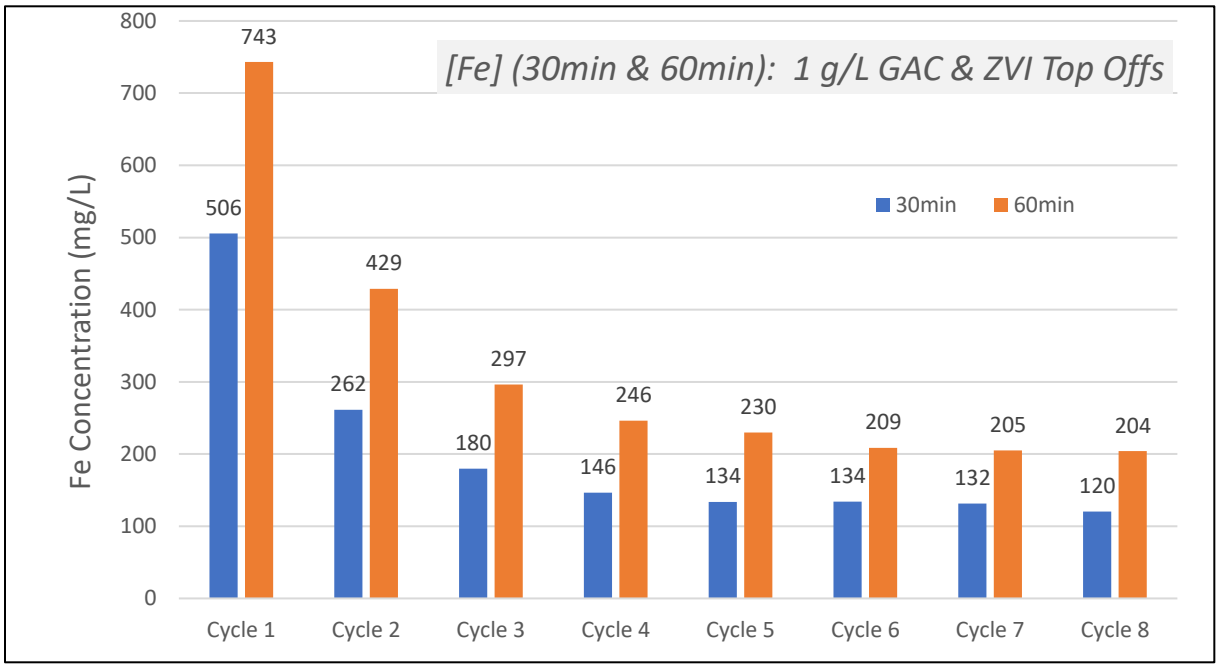

Fig 4-5 Fe release in multi-cycle ME treatment of SR19 condensate, 1 g/L ZVI/GAC top offs at the beginning of each cycle. 0.25 L MC1 reactor, 50 g/L initial active media dose, 2:1 ZVI/GAC

weight ratio, pre and post treatment CO_2 flush, 1000 rpm mixing.

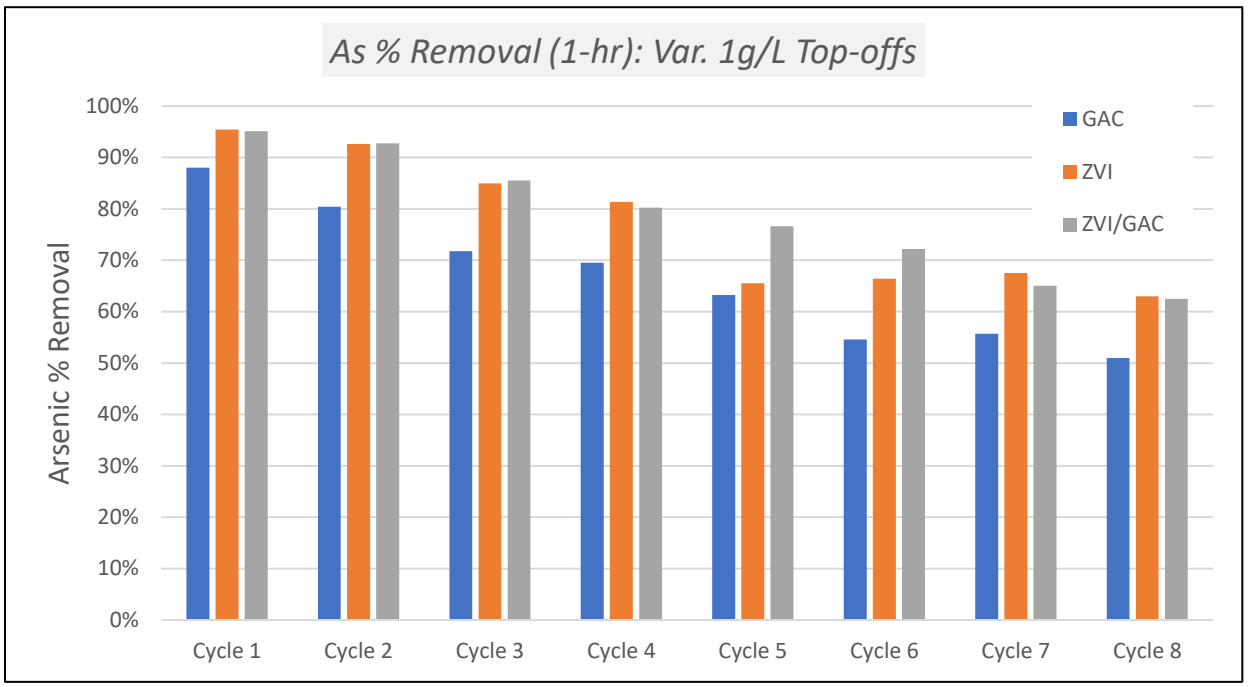

Fig 4-6 Comparison of As removal in multi-cycle ME treatment of SR19 condensate that used different top-offs at the beginning of each cycle. 0.25 L MC1 reactor, 50 g/L initial active media dose, 2:1 ZVI/GAC weight ratio, pre and post treatment CO_2 flush, 1000 rpm mixing.

4.1.3. Effects of pH variations on Fe release and As removal in ME treatment

Previous studies have consistently highlighted the significance of pH optimization in ME treatment due to its influence on the kinetics of the process within the liquid matrix. Operating at pH 3.0 has been repeatedly demonstrated to yield the most efficient removal kinetics for As and Sb (Pinochet-Troncoso, 2023; Schlepp, 2024).

To corroborate the prior findings regarding the impact of pH on Fe release and As removal in ME treatment, ME treatment cycles were conducted in this study at four different pH values. In these experiments, it was hypothesized that the extent of Fe dissolution was influenced by the operational pH, prompting a particular interest in exploring pH values greater than 3.0 to ascertain whether such acidic conditions were necessary for cyclical ME treatment and to investigate the potential for reducing the need for post-treatment pH adjustments. ZVI/GAC top-off doses in these experiments were increased to 2 g/L, in agreement with the findings from the prior experiments of our group.

Fig 4-7 shows that ME treatment at lower pH levels results, as expected in higher levels of Fe dissolution. Approximately 10% more Fe was detected for pH 3 across all cycles comparing to pH 3.5 and pH 4. Fe release results obtained for pH 3.5 and pH 4 were similar for a one-hour treatment duration for all ME treatment cycles.

Carrying out ME treatment at pH 2 or pH 2.5 was not considered in these experiments due to the excessive aggressivity expected for highly acidic solutions in contact with the ZVI/GAC media. We expected that lowering pH below 3 could result in approximately ten times more Fe release that would pose more challenges for post-treatment, notably pH adjustment, ME-treated solutions that contain very high Fe levels.

An additional consideration was that the reductive generation of volatile As compounds, which requires sufficiently high proton concentrations, may be considerably enhanced in ME treatment utilizing pH <3 (Pantsar-Kallio et al., 2000). However, such ME treatment in such conditions may provide fundamentally important data on As volatilization, and such experiments may be carried out in the future studies of the fundamental aspects of As volatilization and overall As balance ME operations.

Fig 4-8 shows As removal results for ME treatment at four different operational pH values. The data indicate that pH effects are relatively modest. Consistent As removal rates exceeding 80% were achieved pH values from 3.5 and 4.5. Surprisingly, As removal at pH 3 was not optimal in these series of experiments, in contrast with the data of other ME treatment experiments carried out at pH 3. We believe that these experiments may need to be repeated to establish the reproducibility of measurements for ME treatment at varying pHs. However, the The overall conclusion that stems from the observations is that pH variations in the range 3.0 to 4.5 do not appear to result in significant changes of As removal by ME treatment carried out for six consecutive ME cycles. This finding may have significant implications for the pilot- and full-scale implementation of ME treatment, particularly concerning the stringency of pH controls, quantity of acid utilized in the process and post-ME treatment pH adjustment.

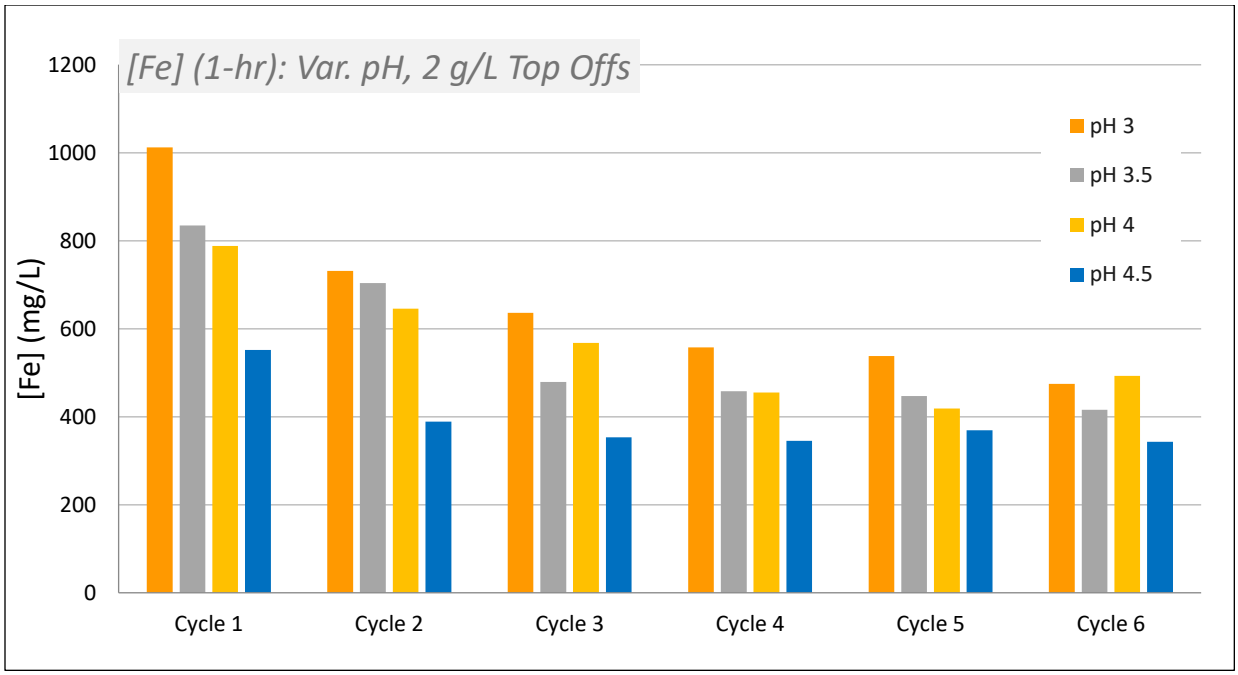

Fig 4-7 Fe release in multi-cycle ME treatment of SR19 condensate at varying pHs. 2 g/L ZVI/GAC top offs at the beginning of each cycle. 0.25 L MC1 reactor, 50 g/L initial active media dose, 2:1 ZVI/GAC weight ratio, pre and post treatment CO_2 flush, 1000 rpm mixing.

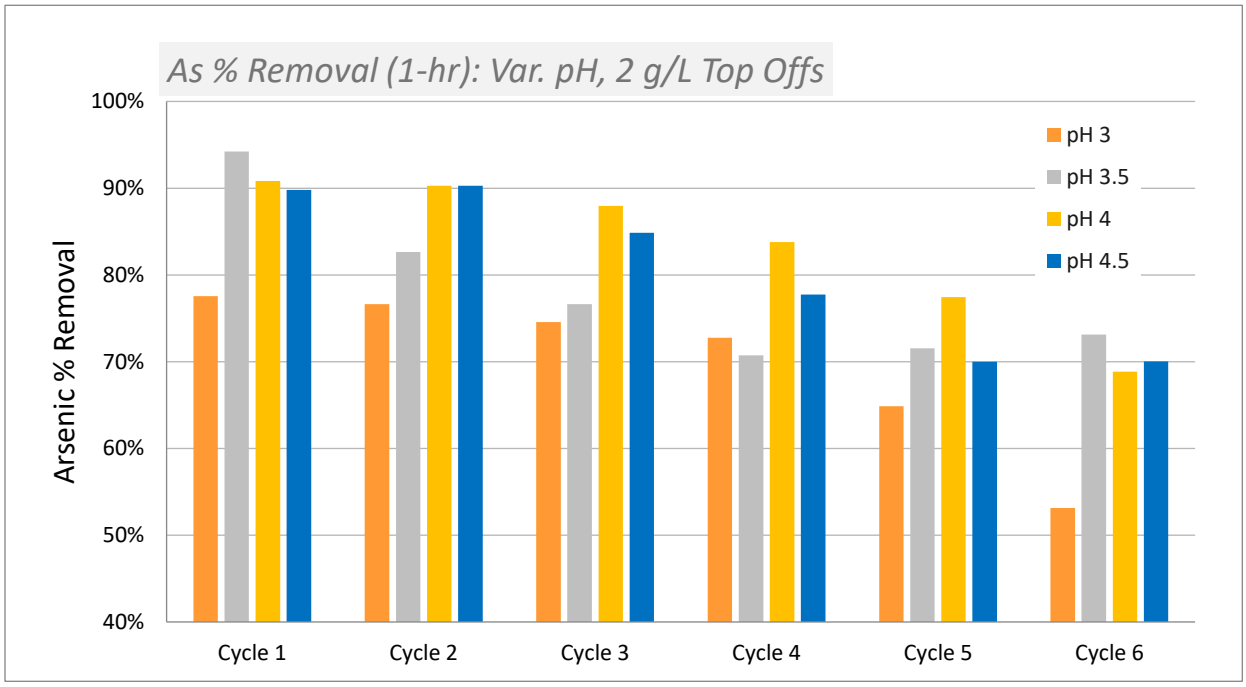

Fig 4-8 Comparison of As removal in multi-cycle ME treatment of SR19 condensate at varying pHs. 2 g/L ZVI/GAC top offs at the beginning of each cycle. 0.25 L MC1 reactor, 50 g/L initial active media dose, 2:1 ZVI/GAC weight ratio, pre and post treatment CO_2 flush, 1000 rpm mixing.

4.1.4. Effects of variable mixing speed of Fe release and As removal

To expand the data set concerning effects of ME treatment conditions on Fe release and As removal, additional experiments were conducted using four different mixing speeds that ranged from 250 rpm to 1000 rpm. These experiments utilized the magnetic coupling system that ensures better control of redox conditions in ME reactors and also better controls of the rotation of the impellers. In these experiments it was hypothesized that Fe release and As removal would increase with the impeller rotation mixing speed because this is likely to enhance the rate of formation of micro-galvanic cell which catalyze both Fe release and As removal in ME treatment.

Fig 4-9 shows effects of increasing impeller rotation rates on Fe release. The data clearly demonstrate that Fe release increases with the mixing intensity. For instance, measurements of Fe concentrations show that at 250 rpm they were approximately 40% lower compared with those at 500 rpm or 750 rpm, and a significant increments of Fe release was observed to a 1000 rpm mixing rate at all ME treatment times. This was accompanied by the similar trend in As removal although the increment in As removal when the rotation rate was increased from 250 to 1000 rpm was less pronounced than that in the case of Fe release. The data indicate that increased mixing intensity results in a more efficient formation of ZVI/GAC micro-galvanic cells that catalyze both Fe release and As removal. However, these trends need to be explored further for various ME reactor geometries and flow pattern. This is a matter of future research, both experimental and modeling-based, by our group.

The presented data indicate that further optimization of ME treatment is necessary. Key targets include ensuring sufficient suspension of ZVI/GAC particles, optimizing conditions for their collisions to form micro-galvanic cells, and maintaining adequate contact between ZVI and GAC particles to ensure their catalytic action.

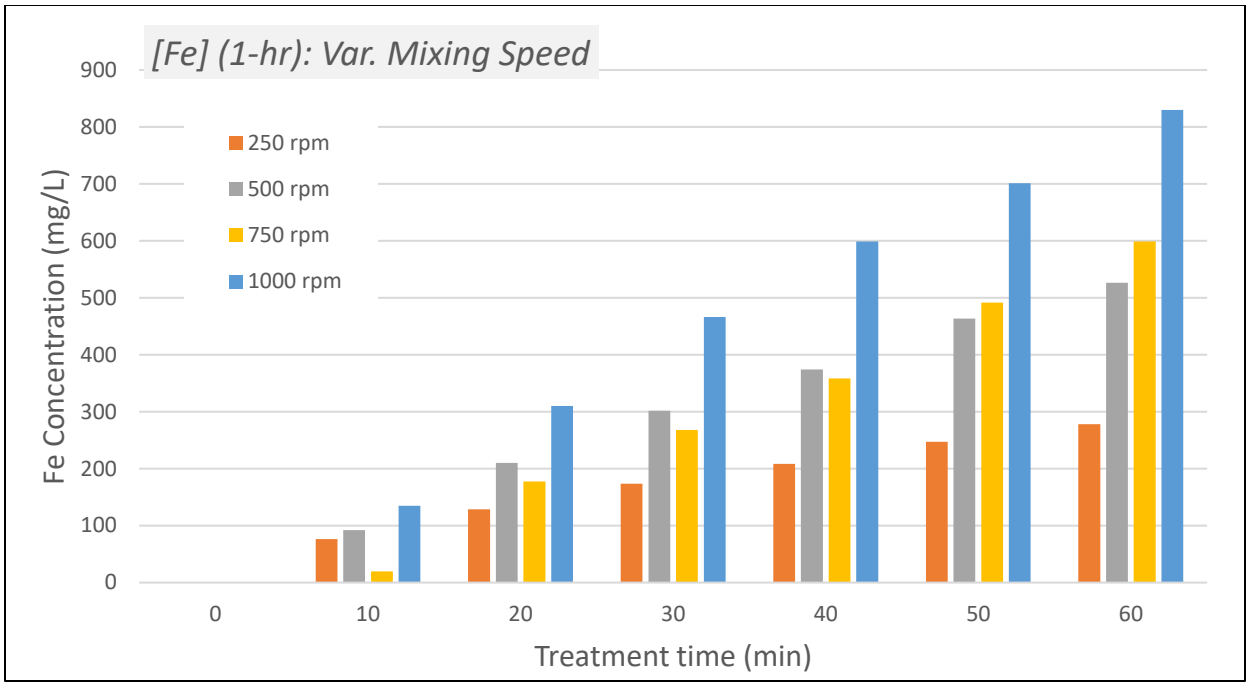

Fig 4-9 Effects of varying mixing conditions on Fe release during ME treatment of SR19 condensate. 0.25 L MC1 reactor, pH 3.0, 50 g/L active media dose, 2:1 ZVI/GAC weight ratio, 2 g/L ZVI/GAC top offs, pre and post treatment CO_2 flush.

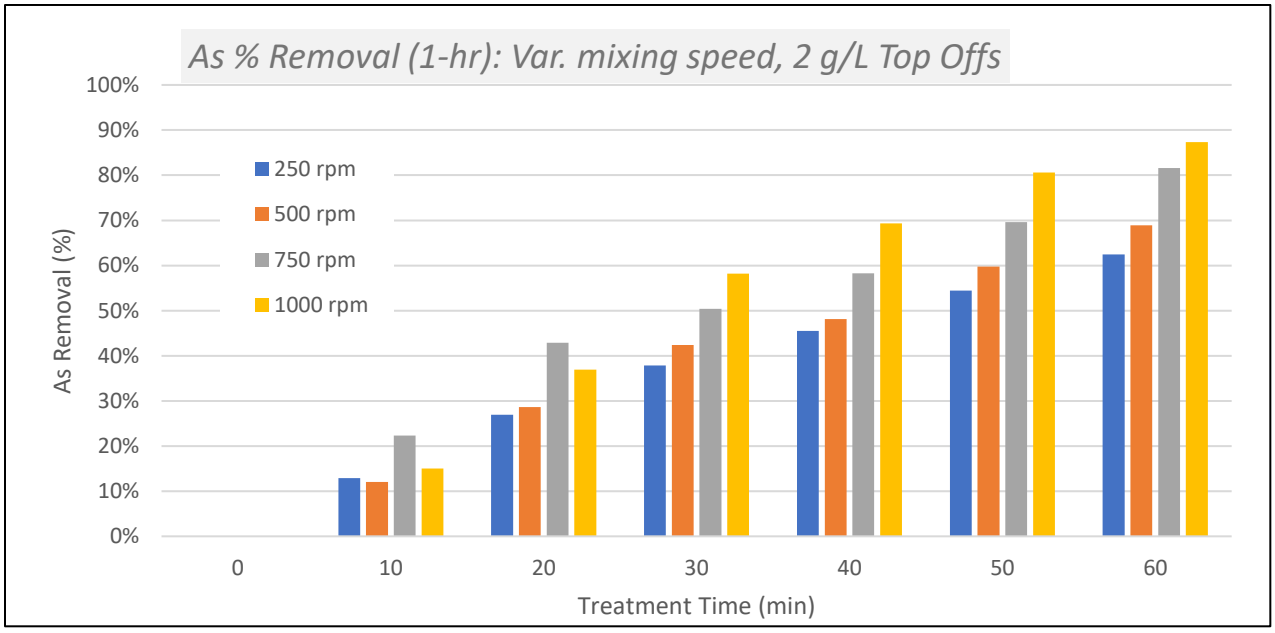

Fig 4-10 Effects of varying mixing conditions on As removal during ME treatment of SR19 condensate. 0.25 L MC1 reactor, pH 3.0, 50 g/L active media dose, 2:1 ZVI/GAC weight ratio, 2 g/L ZVI/GAC top offs, pre and post treatment CO_2 flush.

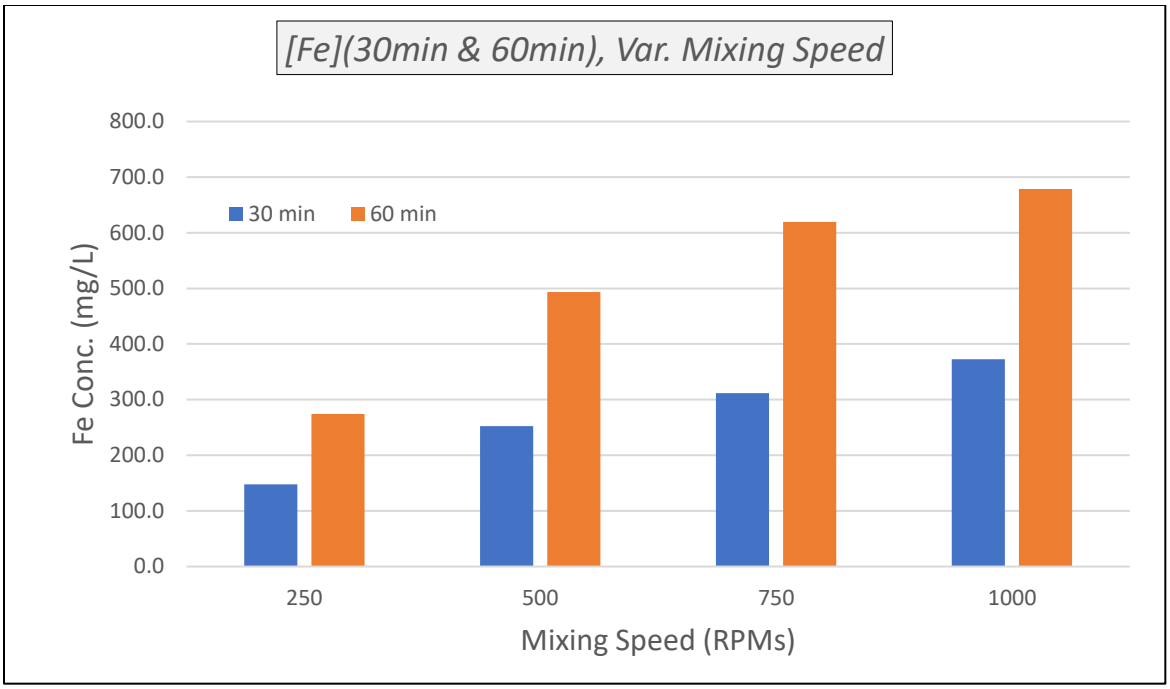

Fig 4-11 Effects of varying mixing conditions on Fe release at 30min and 60min during ME treatment of SR19 condensate. 0.25 L MC1 reactor, pH 3.0, 50 g/L active media dose, 2:1 ZVI/GAC weight ratio, 2 g/L ZVI/GAC top offs, pre and post treatment CO2 flush.

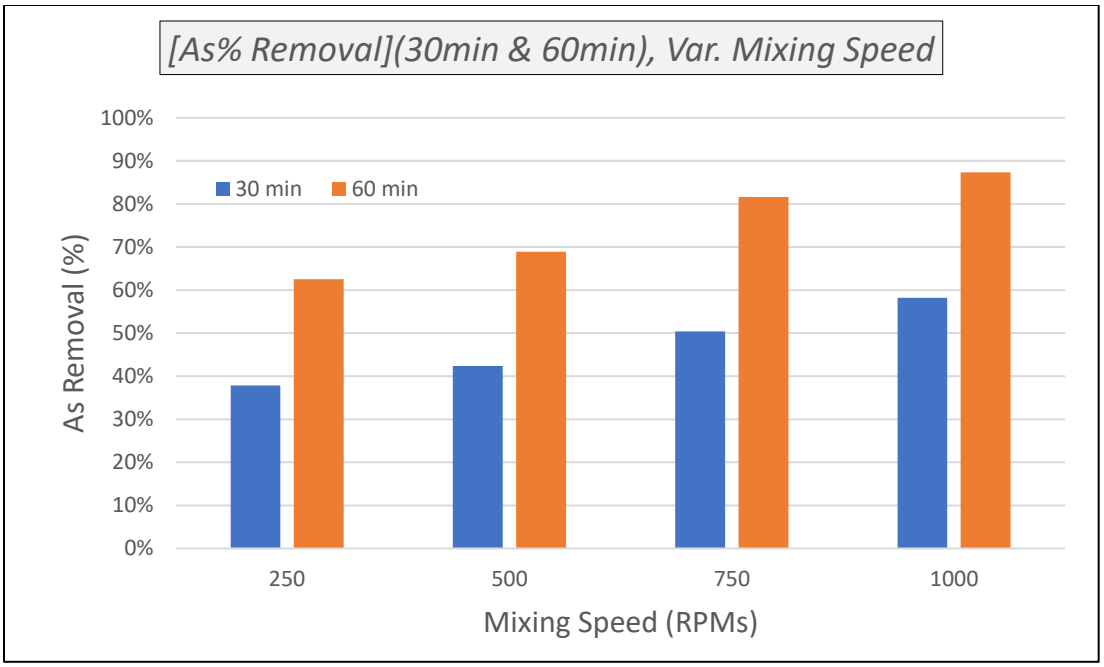

Fig 4-12 Effects of varying mixing conditions on As removal at 30min and 60min during ME treatment of SR19 condensate. 0.25 L MC1 reactor, pH 3.0, 50 g/L active media dose, 2:1 ZVI/GAC weight ratio, 2 g/L ZVI/GAC top offs, pre and post treatment CO2 flush.

4.2. Iron release as a surrogate of the efficiency of microelectrolysis treatment

In the prior research carried out by the UW group, measurements of changes of the oxidation-reduction potential (ORP) during ME treatment were used as a surrogate parameter that was deemed to be useful in evaluating the efficiency of arsenic removal. This choice stems from the opportunity to measure the redox potentials in situ and nearly instantaneously, whereas analyzing arsenic and antimony concentrations by ICP-MS requires a turnaround time from several hours to several weeks (Pinochet-Troncoso, 2023).

While ORP measurements can in principle provide a means of monitoring ME treatment progress by tracking the development of a reducing environment resulting from reactions induced by ZVI and GAC, actual measurements of ORP values showed that sufficiently precise ORP data were challenging to measure precisely due to interferences caused by the mixing process during which ZVI and GAC particles impinged on the ORP probe. Additionally, the frequency of sampling of ORP probes proved to be excessive (100 data points per second) although this issue was corrected

by post-processing. A more challenging complication was that a high degree of variability was observed to exist between the data obtained with different ORP probes. Ultimately, the reliability and stability of commercially available ORP electrodes used in our experiments proved to be inconsistent and insufficient. Despite attempts to enhance calibration consistency and utilize higher-quality probes, calibration drift persisted throughout ME treatment, casting doubt on their accuracy. ORP calibration solutions are typically intended for calibrating to +256 mV. However, these standard calibration solutions correspond to highly oxidative conditions, which do not represent the predominantly reductive conditions in ME treatment. Given these challenges, there arose a need to develop a more dependable surrogate parameter to track ME treatment efficiency (Schlepp, 2024).

The reason for selecting Fe release as a surrogate parameter are as follows. Throughout the course of ME treatment, ZVI continually interacts with solution components, notably protons, resulting in the oxidation of Fe(0) to Fe(II) and the release of Fe solutes. Fe(II) are deemed to dominate Fe solutes released in ME treatment due to the anoxic conditions that are required for the success of ME treatment.

Due to the intrinsic nature of ME processes that cause ZVI to be oxidized and Fe solutes to be released, measurement of Fe concentrations released in the reactor is likely to serve as a reliable indicator of the extent of ZVI phase reactions, which play a pivotal role in the removal of As from the solution. Analytical data, both gained in the preceding research (Schlepp 2024) and reported in this thesis, indicate a discernible relationship between the quantity of dissolved Fe released during ME treatment and the subsequent As removal. Consequently, the investigation reported herein addresses quantitation of Fe release and correlating it to As removal, as necessary to monitor the progress of ME treatment.

4.3. Correlation of As Removal Rate and Fe release

The examination of the Fe/As correlations involved comparing changes of the Fe concentrations throughout ME treatment with the removal rate of As. This approach focused on quantifying the changes of Fe concentrations from the initiation of any cycles of ME treatment rather than relying on absolute Fe concentrations. Furthermore, it was noted that trends in Fe/As correlations were somewhat different for a specific treatment cycle number. These differences however did not

compromise the applicability of the Fe/As correlations to estimating the extent of As removal, as presented in more detail below. Table 4-1 presents the experimental details of all typical ME treatment involved in the correlation between Fe release and As removal.

Table 4-1 Experimental Details of typical ME treatment for As/Fe correlation

Date	Sample	Vol. (L)	Reactor	Cycle No.	Media Dose (g/L)	TO Dose (g/L)	TO Type	pH	Mixing Speed (rpm)	Mixing Regine	Gas
230725	SR19	2	BC2	8	50	1	GAC	3	1000	Upflow	CO_2
230726	SR19	2	BC2	8	50	1	ZVI	3	1000	Upflow	CO_2
230727	SR19	2	BC2	8	50	1	GAC& ZVI	3	1000	Upflow	CO_2
230827	SR19	2	BC3	3	50	2	GAC& ZVI	3	1000	Upflow	CO_2
230827	SR19	2	BC3	3	50	2	GAC& ZVI	3	1000	Downflow	CO_2
230822	SR19	2	BC3	6	50	2	GAC& ZVI	3	1000	Upflow	CO_2
230822	SR19	2	BC3	6	50	2	GAC& ZVI	3	1000	Upflow	CO_2
230828	SR19	2	BC3	6	50	2	GAC& ZVI	3.5	1000	Upflow	CO_2
230829	SR19	2	BC3	6	50	2	GAC& ZVI	4	1000	Upflow	CO_2
230830	SR19	2	BC3	6	50	2	GAC& ZVI	4.5	1000	Upflow	CO_2
230922	SR19	2	BC3	3	50	2	GAC& ZVI	3	1000	Upflow	CO_2
231019	SR19	2	BC4	3	50	2	GAC& ZVI	3	1000	Upflow	CO_2

231221	SR19	0.25	MC1	3	50	2	GAC& ZVI	3	1000	Upflow	CO_2
240110	SR19	0.25	MC2	3	50	2	GAC& ZVI	3	1000	Upflow	CO_2

Fig 4-13 show the correlations between As percentage removal and Fe release across ten "typical" ME treatment conditions. These experiments were conducted mostly with the MC reactor described in the preceding sections of the thesis, and an initial active media dose of 50 g/L for CR ZVI and IPW GAC, continuous mixing at 1000 rpm, a pH level of 3.0 which was adjusted with H_2SO_4, and pre- and post-treatment CO_2 flush. LFG condensate samples SR19 and, in a limited extent, SR20 were employed. Typically, three cycles of ME treatment using the same initial ZVI/GAC batch were carried out with small increments (top-offs) of ZVI/GAC added for each consecutive cycle.

While some differences were observed for the consecutive treatment cycles, the experimental results confirm the concept's validity of assessing ME treatment efficiency through Fe release quantification. In general, cycles of ME treatment after the first cycle show diminishing Fe concentrations and also somewhat lower As removal rates, yet the overall correlation between As removal and Fe release remains consistent.

To interpret the observed Fe/As correlation based on a numerical model, it was suggested that the experimental results can be fitted using an analytical expression similar to a Langmuir isotherm which has been widely used in the studies of adsorption processes (Yan et al., 2017, Al-Ghouti et al., 2020). The applicability of the Langmuir-type expression in the case of ME treatment for arsenic can be tied to the potentially critically important effects of As adsorption on the ZVI/GAC media which also involves the oxidation of ZVI and attendant release of Fe solutes.

The Langmuir-type expression that used the experimental data is presented below:

$$R_{As} = \frac{R_{max} \times [Fe] \times K_{Fe\_As}}{1 + [Fe] \times K_{Fe\_As}}$$

In the above expression, R_{As} – is the removal of arsenic expressed as the fraction of its initial concentration, [Fe] is the increment of the concentration of iron (mg/L) released at any point of

ME treatment and corrected for the Fe concentrations prior to the initiation of the ME treatment, and K_{Fe_As} is the apparent binding constant which can be adjusted to achieve the best fit between the model and experimental data. Within this model, the inverse values of K_{Fe_As} represents the Fe concentration corresponding to a 50% As removal. The inverse value of K_{Fe_As} was adjusted to 167 mg/L to obtain the best fitting between the experimental and model data.

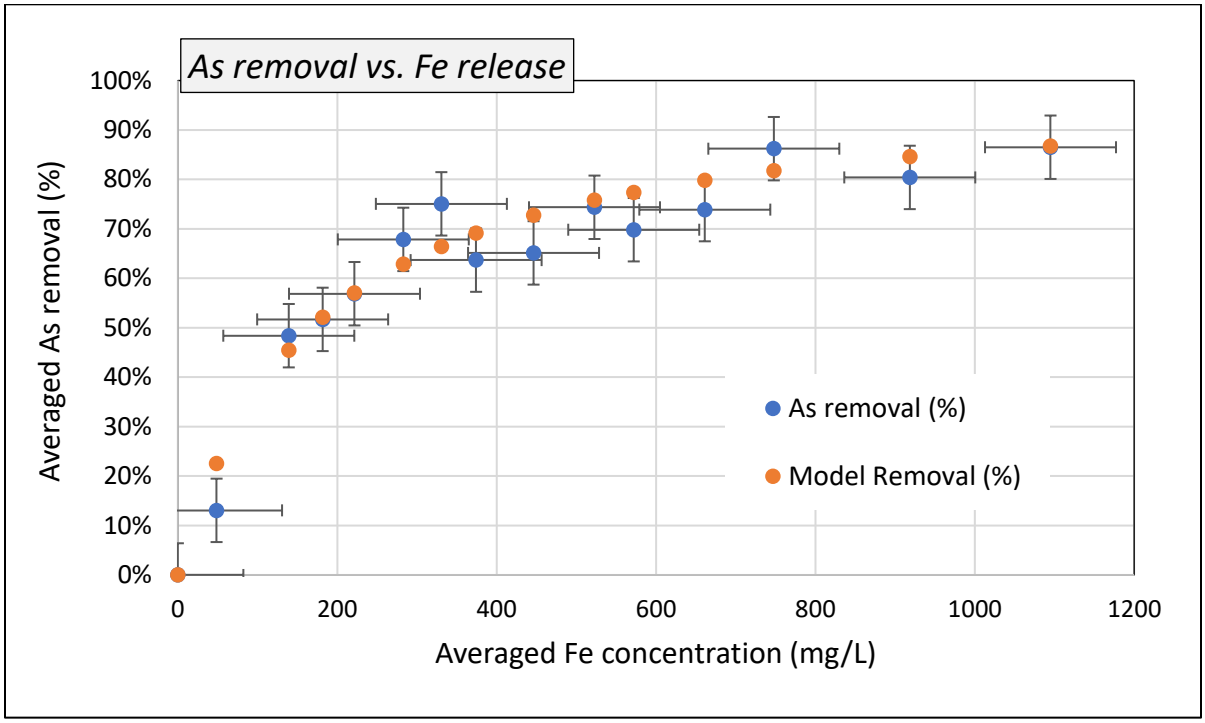

Fig 4-13 Correlation of As removal rate and Fe release for typical ME treatment with model comparison, typical ME cycles (66 cycles)

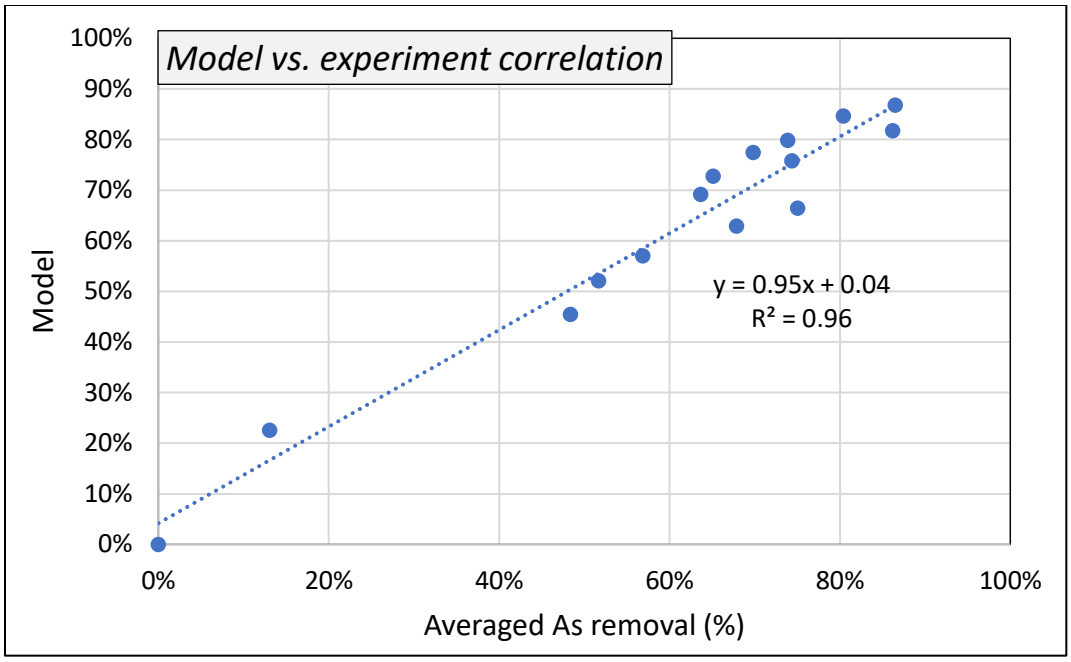

Fig 4-14 Model vs. ME treatment averaged As removal rate correlation (66 cycles)

Fig 4-13 and Fig 4-14 show the close convergence between the experimental relationship between the averaged Fe concentrations and As removal rates and, on the other hand, their fitting using the model described above. An R^2 value of 0.96 and a 0.95 slow of the correlation between the model and experimental data proves the applicability of the model. This also proves the relevance of correlating As removal with Fe release, particularly concerning the identification of specific thresholds for specific levels of As removal, for instance 50% or 90%, in relation to predetermined ranges of Fe release, for instance 0 to 200 mg/L, 200 to 400 mg/L, etc.

Table 4-2 As removal (%) vs Fe release for typical ME treatment at pH3 and its standard deviation

Range of Fe release (mg/L)	**Fe Conc. (mg/L)**	**As removal (%)**	**Model Removal (%)**	**Standard Dev. Of Fe Conc. (mg/L)**	**Standard Dev. of Sb removal (%)**
	0	0%	0%	0	0%
0<Fe<50	49	13%	23%	3	13%
50<Fe<150	139	48%	45%	12	11%
150<Fe<200	182	52%	52%	14	15%

200<Fe<250	222	57%	57%	15	14%
250<Fe<300	283	68%	63%	15	13%
300<Fe<350	331	75%	66%	12	13%
350<Fe<400	374	64%	69%	14	10%
400<Fe<450	446	65%	73%	25	16%
450<Fe<550	523	74%	76%	15	11%
550<Fe<600	572	70%	77%	11	21%
600<Fe<700	661	74%	80%	24	11%
700<Fe<800	748	86%	82%	31	7%
800<Fe<1000	918	80%	85%	56	5%
1000<Fe<1200	1095	87%	87%	64	7%

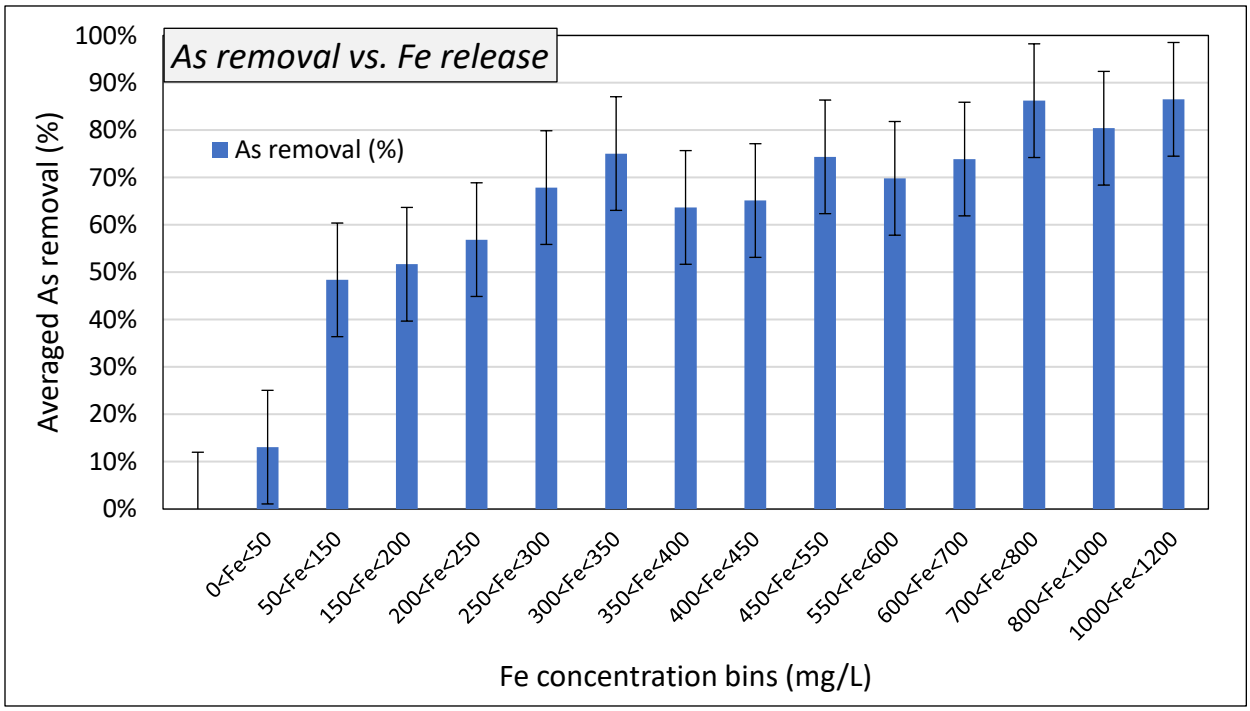

Fig 4-15 As removal vs. Fe release with standard deviation

Table 4-2 and Fig 4-15 demonstrate a clear trend of increasing As removal efficiency that follows the increases of Fe concentrations in ME treated LFG condensate solutions. Both experimental data and model predictions exhibit a strong correlation between Fe concentrations and As removal

percentages. Results shown in Table 4-2 and Fig 4-15 are also important in the context of establishing thresholds of Fe release that correspond to desired levels of As removal.

To illustrate the relationship between the As/Fe correlation and the treatment cycle number, all data pertaining to typical ME treatment experiments is presented below. The initial treatment cycle differs from subsequent cycles, exhibiting higher levels of Fe release that correspond to comparable levels of As release.

The variability observed in the As/Fe trends, particularly evident in Cycles 2 and 3, may partly ascribed to the changes of the reactivity (partial passivation) of ZVI surfaces during consecutive ME treatment cycles as well as to the presence of increasing concentrations metal ions such as Ni and Mn that affect the precision of 1,10-Phen determinations of Fe concentrations released during ME treatment.

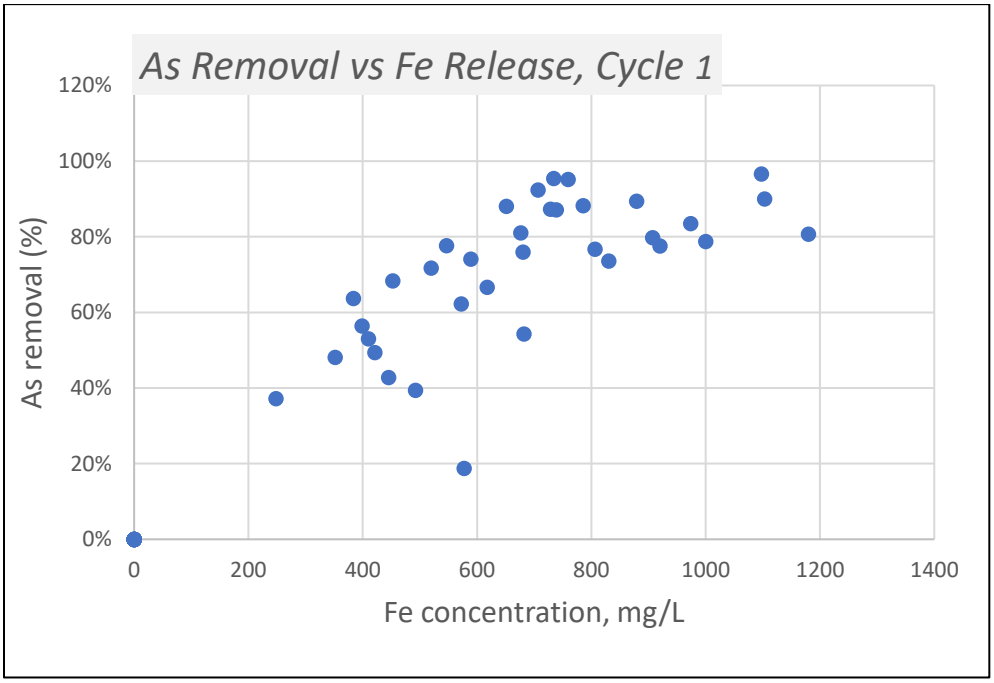

Fig 4-16 Correlation of As removal and Fe release for typical ME treatment (Cycle1)

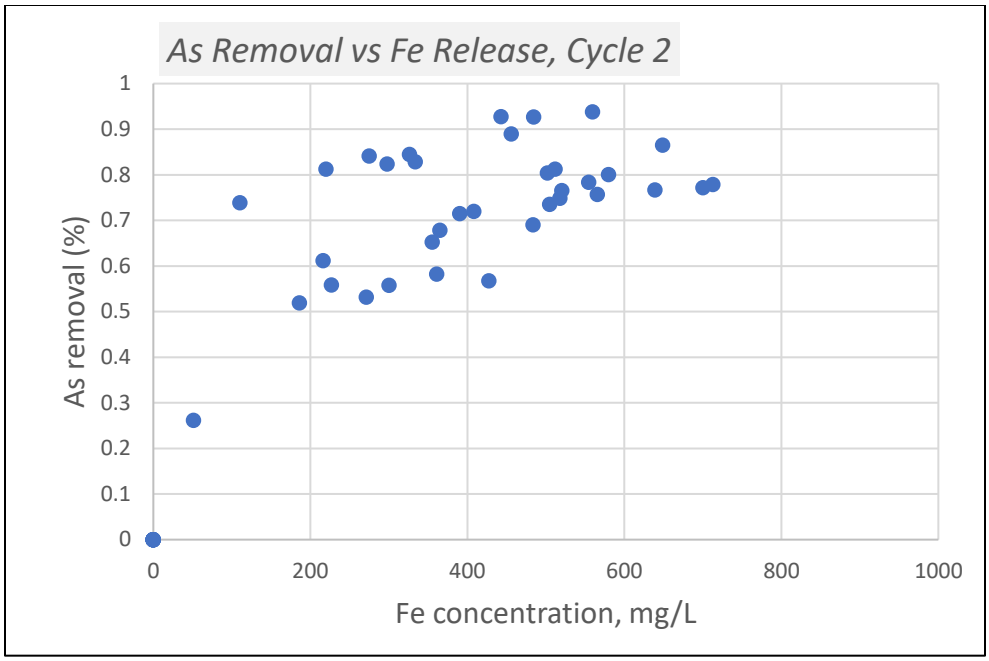

Fig 4-17 Correlation of As removal and Fe release for typical ME treatment (Cycle2)

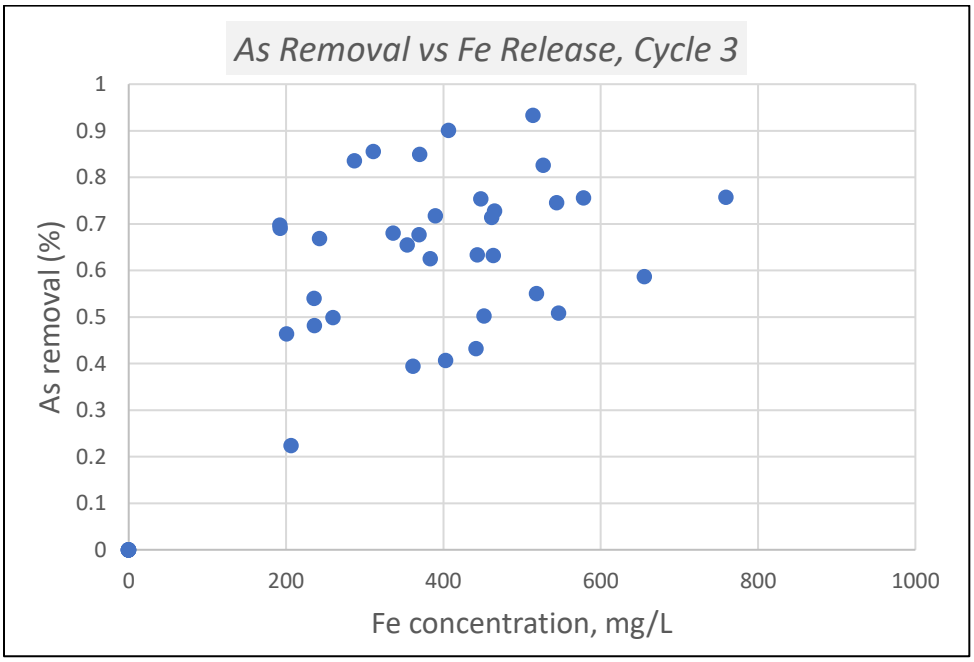

Fig 4-18 Correlation of As removal and Fe release for typical ME treatment (Cycle3)

These changes can be observed in Fig 4-16, Fig 4-17 and Fig 4-18 that show the separate data for 3 cycles from all typical ME experiments. The data demonstrate that the initial treatment cycle differs notably from subsequent cycles, in the sense that it is characterized by higher release of Fe

solutes when comparable levels of As removal are achieved. As mentioned above, this phenomenon is likely to stem from the initial activation and subsequent changes of ZVI surfaces during in ME treatment. During the activation phase that takes place during the first cycle of ME treatment, surface scales, or rusts, naturally formed on ZVI surfaces because of oxidation before introduction into the ME reactor, are dissolved. The removal of these preformed scales leads to higher Fe release during the initial cycle compared to subsequent phases of ME treatment. However, subsequent cycles, particularly Cycles 2 and 3, exhibit a similar trend and nearly reach the same treatment plateau as observed in Cycle 1.

These findings indicate that correlating As removal with Fe release observed during ME treatment provides a practical approach for predicting treatment efficiency. The concentrations of dissolved Fe can be accurately and promptly determined using established methods such as the 1,10-Phen method. This method is suitable for use in field conditions field conditions that are likely to take place during pilot- and full-scale implementation of ME treatment of LFG condensate. Further tests of this approach constitute one of the goals of current research activities of our group.

4.4. Correlation of Sb Removal and Fe release

Given the similarity of many aspects of the environmental chemistry of As and Sb, Sb can serve as an additional parameter with which to enhance the notion of using Fe release as a surrogate for As removal in ME treatment. In general, Sb is more readily removed from LFG condensate compared to As. Typically, as high as 80% of Sb is removed within the initial 15 minutes of ME treatment.

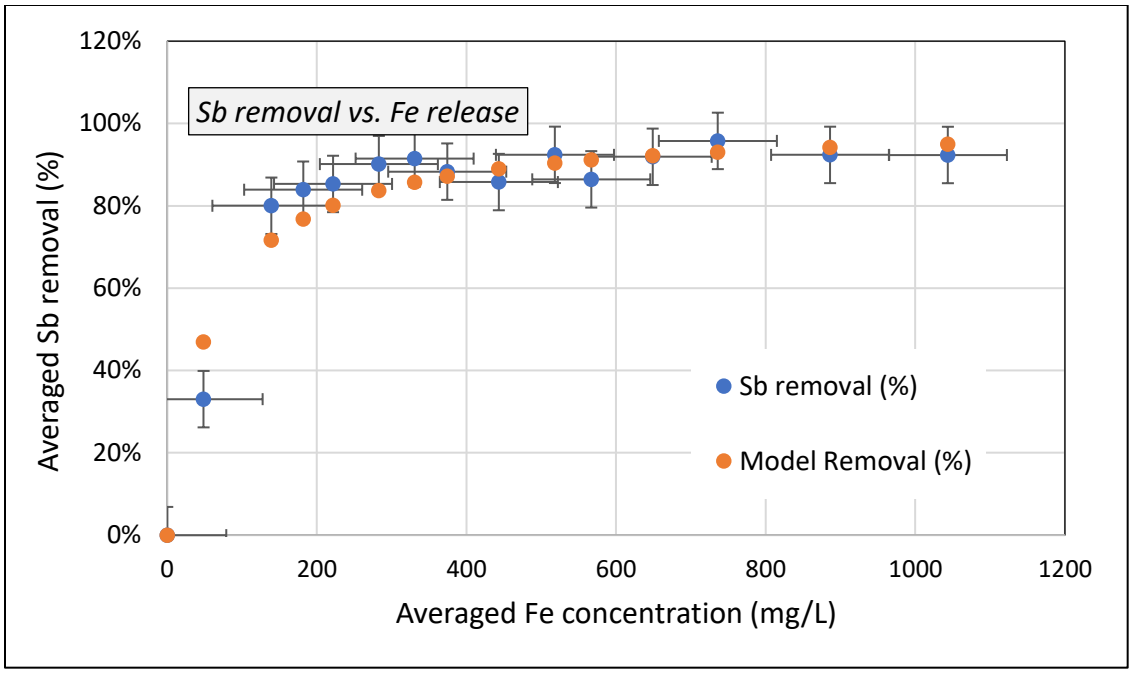

Fig 4-19 Correlation of Sb removal rate and Fe release for typical ME treatment with model comparison, all typical ME cycles

Fig 4-19 shows the correlation between Sb removal rate and Fe release for all typical ME treatment experiments, alongside with a comparison with the model data similar to that used to fit As removal results. The faster removal of Sb, compared to that of As, may be attributed to the potentially higher affinity of Sb species found in LFG condensate to the reactive sites on ZVI and GAC surfaces.

The Langmuir-type expression that used the Sb experimental data is presented below:

$$R_{Sb} = \frac{R_{max} \times [Fe] \times K_{Fe\_Sb}}{1 + [Fe] \times K_{Fe\_Sb}}$$

The correlation between the model and experimental data for Sb removal rate and Fe release yields an R^2 value of 0.85. This results shows that Fe release serves as a good surrogate parameter with which to predict both As and Sb removal in ME treatment. The inverse value of K_{Fe_Sb} that corresponds to the 50% removal of Sb by ME treatment is determined by fitting the experimental data to be at 55 mg/L. Its much lower value compared to that for As (167 mg/L) is indicative to the higher affinity of the reactive sites in the ZVI/GAC media to Sb species found in LFG condensate.

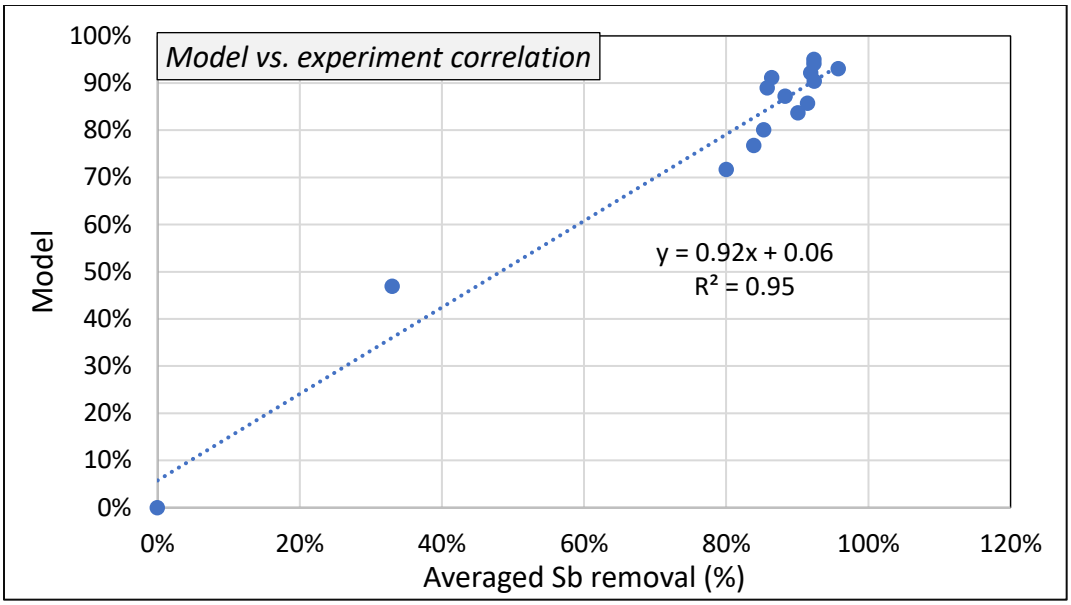

Fig 4-20 Model vs. ME treatment averaged Sb removal rate correlation

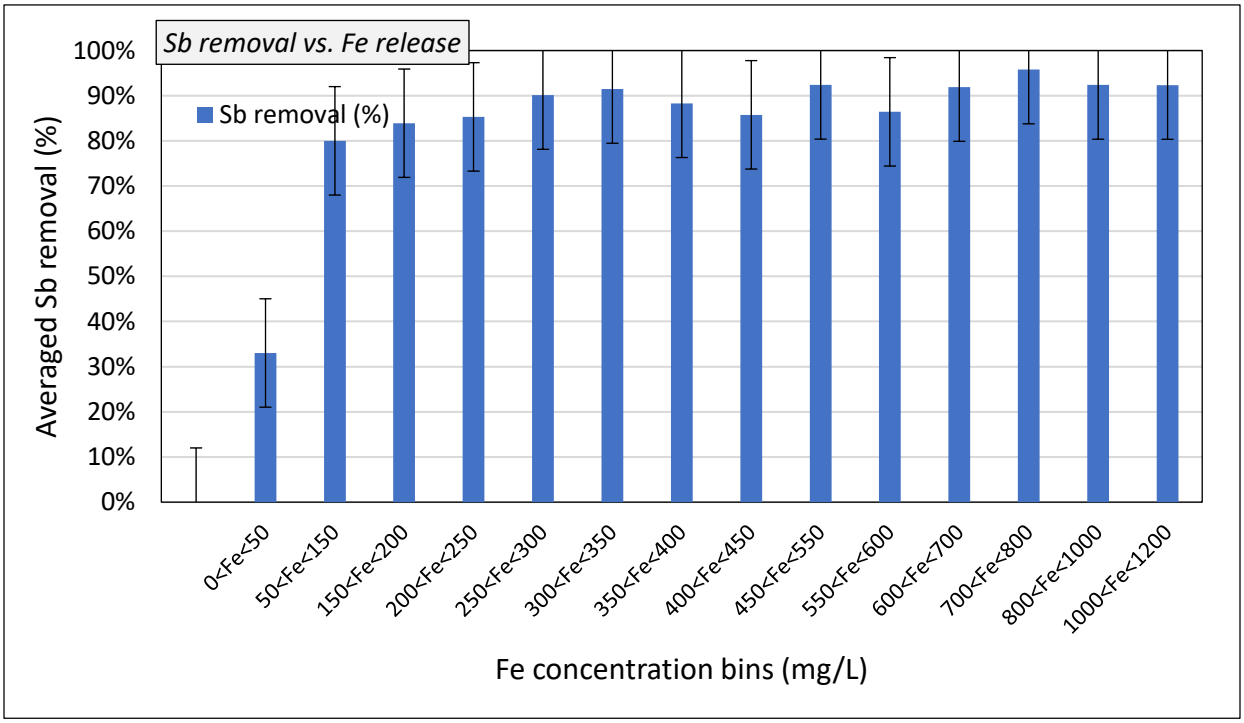

Fig 4-21 Sb removal vs. Fe release with standard deviation

Fig 4-20 highlights the correlation between Fe concentration, Sb removal and model comparison. Within the initial bin (0<Fe<50 mg/L), Sb removal exhibits a significant increase from 33% to 80% as Fe concentration rises to 139 mg/L. Sb removal remains relatively high, ranging from 84% to

96%, across higher Fe concentration bins. This emphasizes the potential predictive value of Fe release in determining Sb removal efficiency.

As demonstrated in more detail in Table 4-3, most of the standard deviation of each Fe release range is less than 0.11, indicating the difference between Sb% removal and the model curve is relatively small. This further proves the applicability of the established model to estimate Sb and As removal in ME treatment.

Fig 4-22, Fig 4-23 and Fig 4-24 demonstrate the correlations between Fe concentrations released during sequential ME treatment cycles and concomitant Sb removal rates. Similarly to the observations made in the case of As removal, the correlations between Fe release and Sb removal are stronger for ME treatment cycles cycle 1 and 2 but such correlations become weaker for further cycles. It can be therefore suggested that future work should focus on the development of separate correlations between Fe release and As/Sb removal of treatment cycle 1, cycle 2, cycle 3, and subsequent cycles.

Table 4-3 Sb removal (%) vs Fe release for typical ME treatment at pH3 and its standard deviation

Range of Fe release (mg/L)	**Fe Conc. (mg/L)**	**Sb removal (%)**	**Model Removal (%)**	**Standard Dev. Of Fe Conc. (mg/L)**	**Standard Dev. of Sb removal (%)**
	0	0%	0%	0	0%
0<Fe<50	49	33%	47%	3	33%
50<Fe<150	139	80%	72%	12	5%
150<Fe<200	182	84%	77%	14	7%
200<Fe<250	222	85%	80%	15	12%
250<Fe<300	283	90%	84%	15	7%
300<Fe<350	331	91%	86%	12	6%
350<Fe<400	374	88%	87%	14	11%
400<Fe<450	443	86%	89%	23	11%

450<Fe<550	518	92%	90%	15	6%
550<Fe<600	567	86%	91%	11	10%
600<Fe<700	649	92%	92%	29	4%
700<Fe<800	736	96%	93%	26	2%
800<Fe<1000	886	92%	94%	56	2%
1000<Fe<1200	1044	92%	95%	57	4%

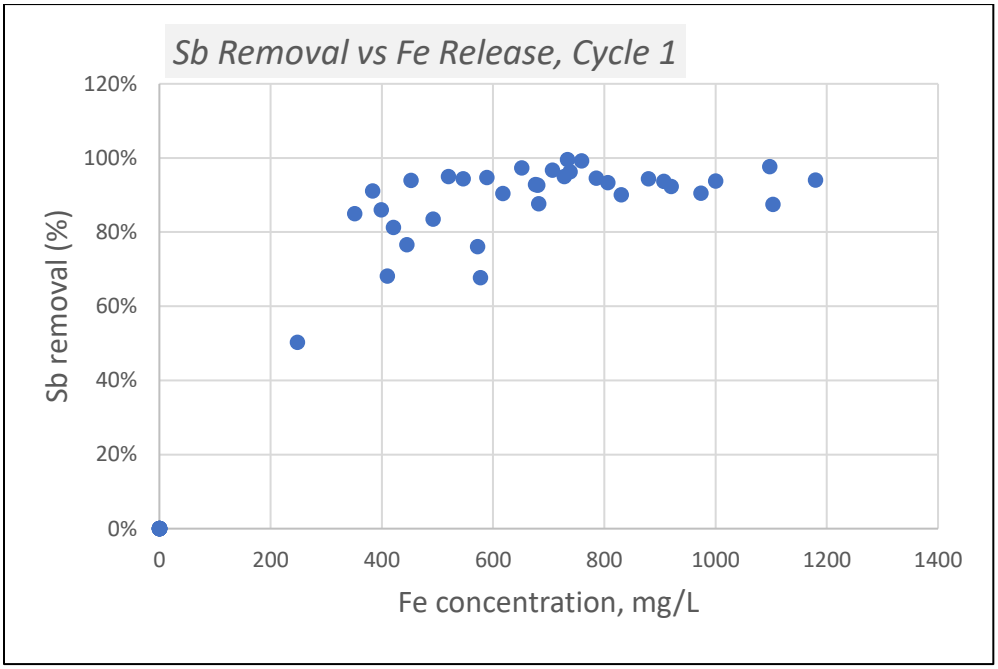

Fig 4-22 Correlation of Sb removal and Fe release for typical ME treatment(Cycle1)

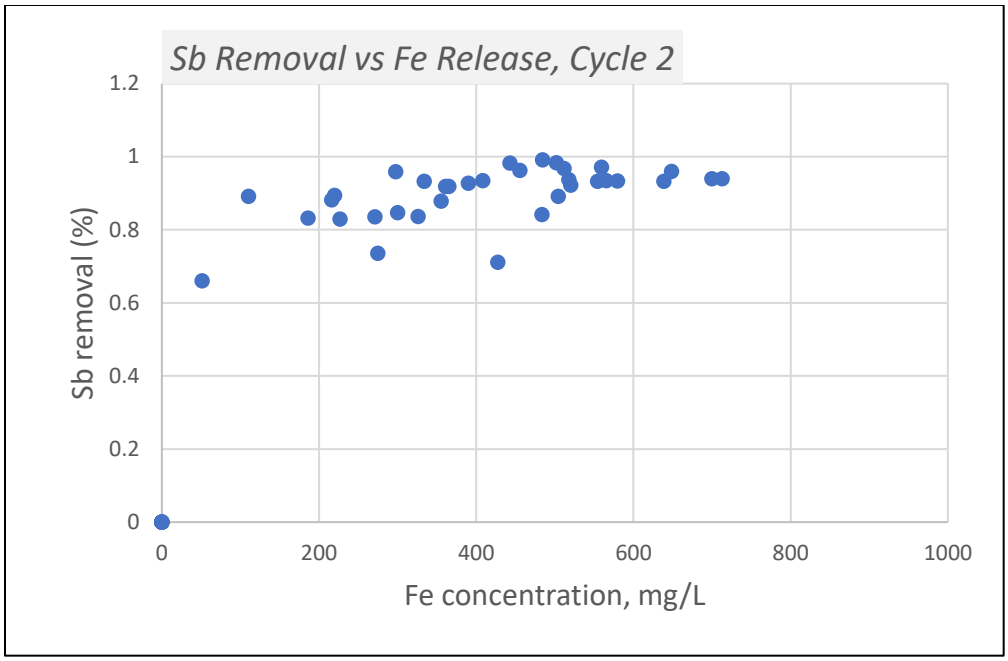

Fig 4-23 Correlation of Sb removal and Fe release for typical ME treatment (Cycle2)

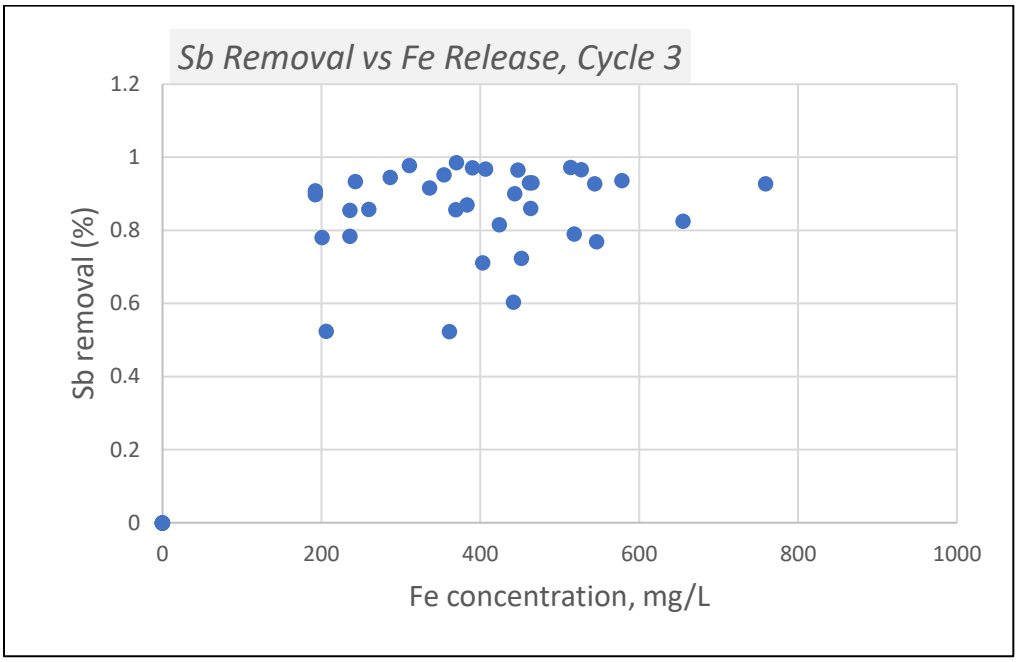

Fig 4-24 Correlation of Sb removal and Fe release for typical ME treatment (Cycle3)

4.5. Effects of post-treatment pH adjustment on the formation of solids in ME-treated LFG condensate

4.5.1. Fe weight estimation

The adjustment of pH of ME-treated effluents from pH 3, as required during the ME treatment, to ca. 7 or above, as needed for discharge, was observed to be accompanied by the immediate formation of voluminous, green-colored suspended solids. The observed green color is known to be characteristic for ferrous iron species. Subsequent exposure of the green-colored suspension to air caused the green particulates to change their color from green to orange, indicating the occurrence of oxidation of ferrous to ferric iron.

Given that the amount of iron precipitates formed in ME treatment is necessary to ascertain to estimate requirements for post-ME treatment handling of both the ME-treated effluent and its byproducts that may need to be disposed of, a series of experiments was carried out to determine the weight of the solids formed in ME-treated SR19 solutions. To quantify their air-dried weight, a 40 mL aliquot was taken from the treated solution and its pH was adjusted to 7.0 using a titrator that gradually added 1 N NaOH base. The particulates that are readily formed in the pH-adjusted solutions were filtered out using two layers of 0.45 um filter paper. The filter paper with the solids retained by it was then dried at 105 ℃ for 24 hours, following which the weight of the filter paper containing the precipitate was measured and corrected by the blank (the filter paper without any deposited solids). The above procedure was performed four consecutive cycles of ME treatment, Cycle 1 Cycle 3, Cycle 5, and Cycle 7.

Table 4-4 Experimental details of Solid Weight Estimation

Experiment details:		
	Value	Unit
Ave weight of filter paper before drying:	1.3	g
Ave weight of filter paper after drying:	1.258	g
Pieces of filter paper used	2	
Oven temperature	105	℃
Time for drying	24	hr

Titrator	NaOH	
Volume sample	40	mL
Titrator conc.	1	N
pH	3~7	
Experiment date:	2023/7/25	
Measurement date:	2023/7/26	

The results obtained from these measurements are shown in Fig 4-25. They demonstrate that the concentration of air-dried solids separated from Cycle 1 ME-treatment effluent after its pH-adjustment is ca. 3.1 g/L, with little difference between the masses of solid separated from the unfiltered and pre-filtered effluents. Subsequent ME-treatment cycles result in lower yields of Fe-based solids, with their mass concentration varying from ca. 2.1 to 2.6 g/L for both the unfiltered and prefiltered ME-treatment effluents.

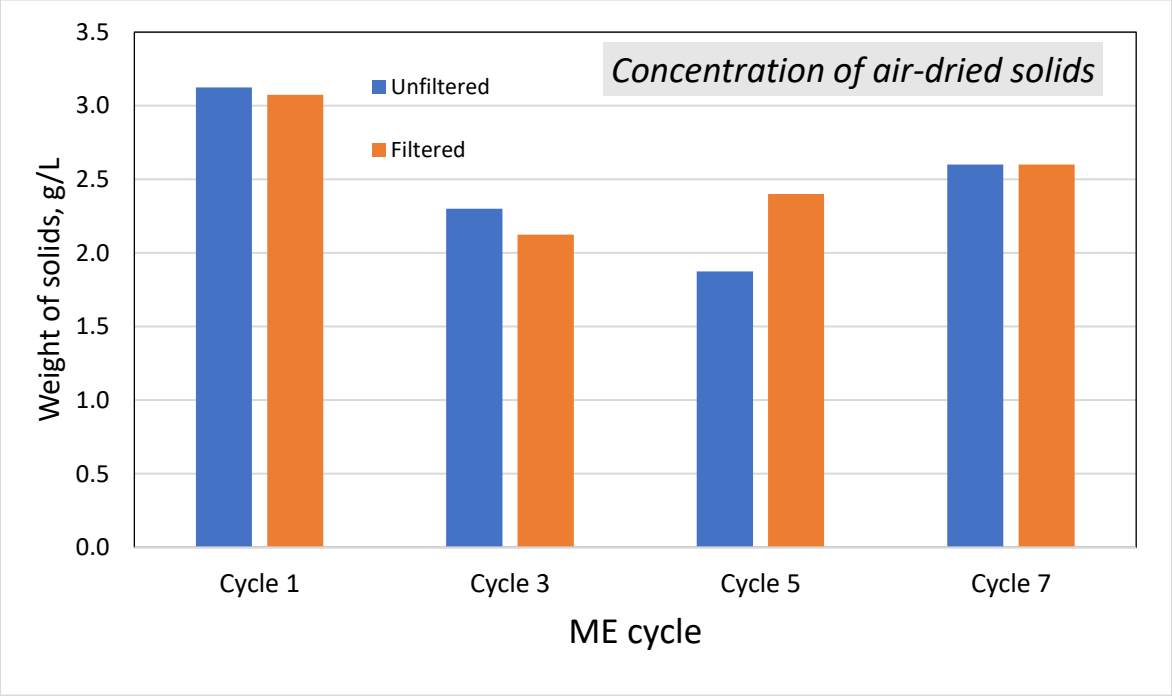

Fig 4-25 Mass concentration of air-dried solid formed in SR19 filtered effluent 8 Cycles-C1,3,5,7, GAC top only- 50 g/L GACcoco + ZVI CR + (1 to 2), pH 3, cont. mixing 25%, CO_2 1LPM at beginning, 07/25/2023

4.5.2. Sequential filtration

To further quantify the presence and properties of iron-containing particulates in ME treated LFG condensate, measurements of Fe concentrations and those of arsenic and antimony were determined using sequential filtration experiment. In this procedure, a 50 mL aliquot of ME-treated effluent was taken, and its pH was adjusted to 7.0. The sample was aerated for ca. 30 minutes during which the color of the suspended particles changed from green to orange, indicating the oxidation of ferrous to ferric iron. The sample was then filtered using syringe filters with different nominal pore sizes. The filtered samples were diluted using a 500x dilution factor and the concentration of Fe, As and Sb were determined using the UW ICP-MS instrument. During these measurements, the use of the 1 μm PES syringe filters was observed to need applying considerable pressure to drive the solution through the filter. Because applying excessive pressure during membrane treatment may result in mechanical distortion of the filter, results of filtration through the 1 μm PES filter may be less accurate compared with those for the other filters (See section 3.2).

The sequential filtration measurements showed that the concentration of Fe prior to filtration was ca. 990 mg/L (Fig 4-26). As the filter size decreased from 5 um to 0.2 μm, the Fe concentration decreased to 645 mg/L. However, Fe concentrations in the filtrate samples passing filter sizes less than 1.0 μm were largely and as high as ca. 600 mg/L. This indicates that the air oxidation of the ME treated effluent may not have resulted in a complete conversion of ferric to ferrous iron whose solubility is expected to be very low. Alternatively, the filtrate passing a 0.2 mm filter may still contain nano-size suspended particles whose size distributions and other properties remain to be ascertained.

In contrast with the decrease of Fe concentration in the sequentially filtered ME-treated samples, As and Sb concentrations marginally affected by filtration (Fig 4-27 and Fig 4-28). Prior to filtration, the As concentration is 2.95 mg/L. There was a slight increase in As concentration after the filtration through a 5 μm filter but this was likely an artifact associated with a limited precision of the ICP-MS measurements. Further filtration caused little change of As concentrations which remained almost the same (2.84 mg/L) as that prior to filtration. The same pattern was observed for Sb concentrations. These results show that As and Sb species remaining in ME-treated LFG condensate are mostly solutes that are not readily amenable to removal by coagulation or adsorption-based treatment processes. However, from the standpoint of practical ME applications,

the levels of As in the ME treated LFG condensate are sufficiently low so as not to require any additional removal of arsenic.

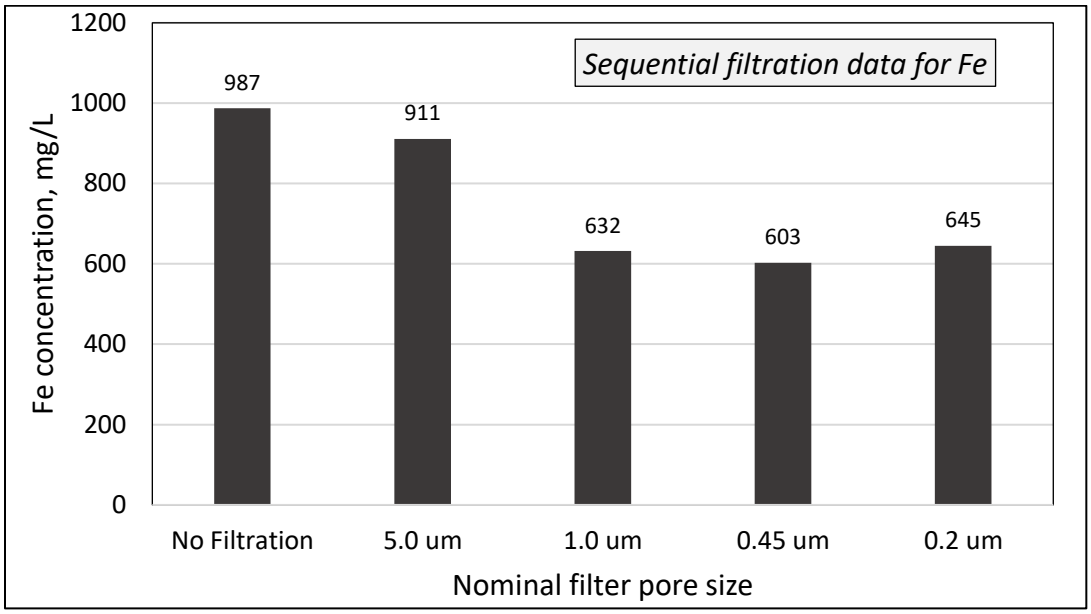

Fig 4-26 Effects of sequential filtration of Fe concentrations in pH-adjusted and air oxidized ME-treated LFG condensate. SR19 typical ME treatment, Cycle1, GAC/ZVI Top Offs 08-27-23 - 2L, BC3, 50 gL ZVI CR - GACcoco 2to1 w 2 gL GAC/ZVI top offs, pH 3 1M H2SO4, CO2flush, ContMix

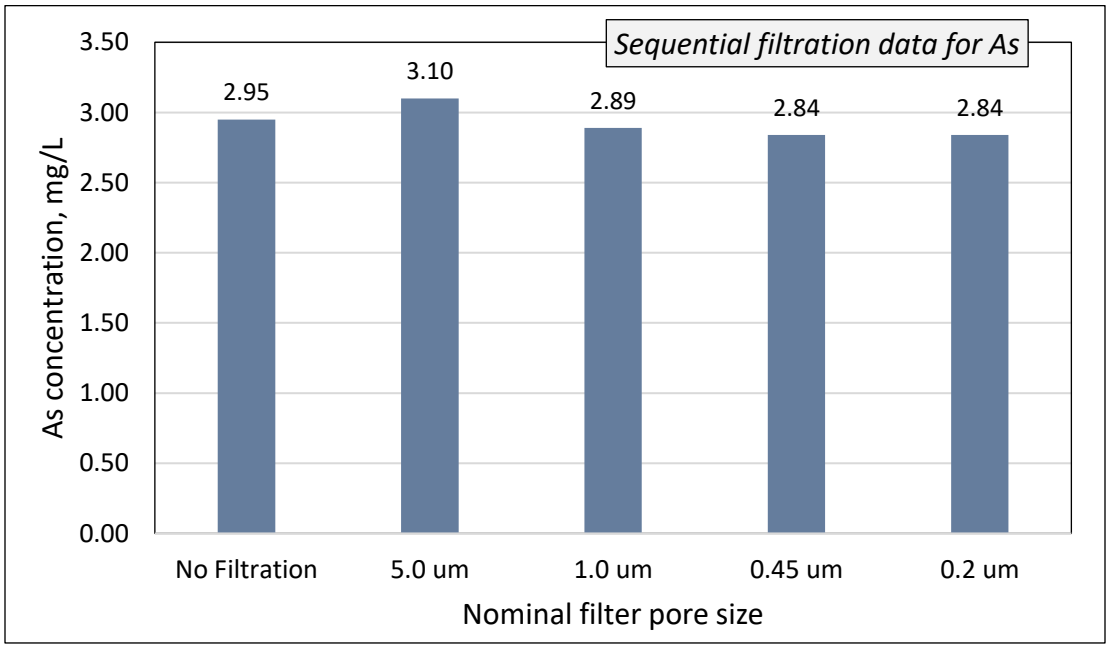

Fig 4-27 Effects of sequential filtration of As concentrations in pH-adjusted and air oxidized ME-treated LFG condensate. SR19 typical ME treatment, Cycle1, GAC/ZVI Top Offs 08-27-23 - 2L, BC3, 50 gL ZVI CR - GACcoco 2to1 w 2 gL GAC/ZVI top offs, pH 3 1M H2SO4, CO2flush, ContMix

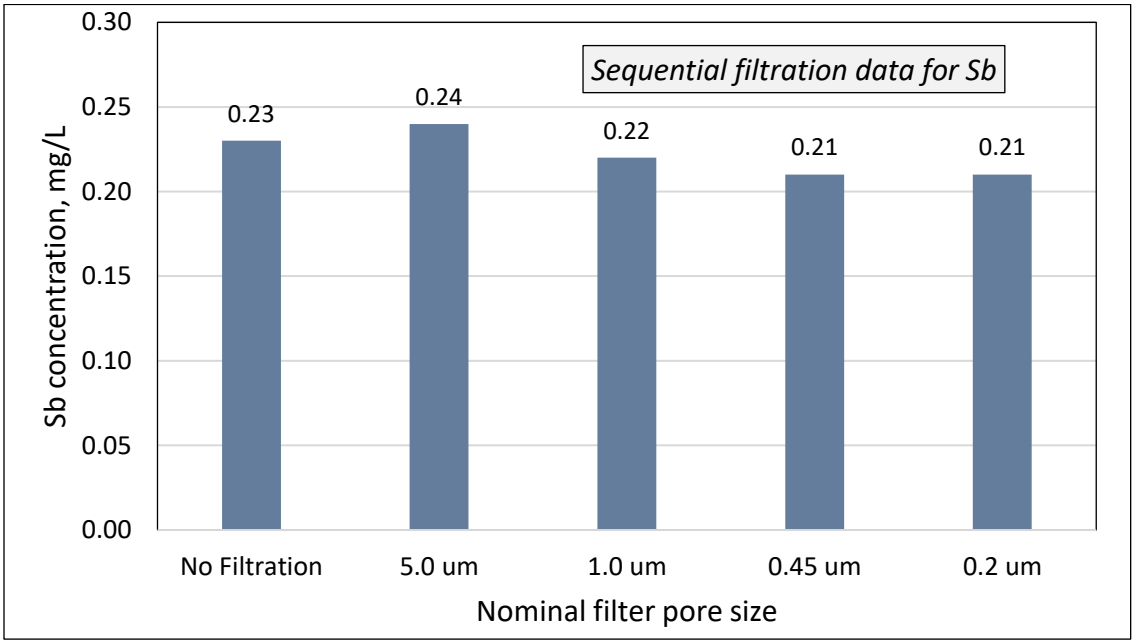

Fig 4-28 Effects of sequential filtration of Sb concentrations in pH-adjusted and air oxidized ME-treated LFG condensate. SR19 typical ME treatment, Cycle1, GAC/ZVI Top Offs 08-27-23 - 2L, BC3, 50 gL ZVI CR - GACcoco 2to1 w 2 gL GAC/ZVI top offs, pH 3 1M H2SO4, CO2flush, ContMix

The obtained results indicate that approximately 5g of iron compounds are generated per every two liters of treated effluent. The estimated weight of iron does not show a significant variation as the reaction cycles progress. Moreover, the comparison between filtered and unfiltered effluent reveals no substantial disparity, implying that the ferrous ions are not effectively filtered by the filter tips.

However, as was observed during the experiment, there's a pronounced reduction in solids content as the cycles advance. The reason for the lack of substantial weight difference with increasing cycles remains to be investigated and clarified. These observations collectively suggest the need for further experimentation, specifically exploring the impact of different top-off cycles.

5. Conclusions and future work suggestions

This thesis concludes with a synthesis of the experimental findings and recommendations for future research. The presented data emphasize the significance of Fe release as a useful surrogate parameter of As removal efficacy in ME treatment. This study also evaluated the performance of a relatively simple analytical approach, the standard 1,10-Phen spectrophotometric method, that can be used to quantify Fe concentrations in ME-treated solutions. This method and its applicability were tested using several analytical approaches. Additionally, this study investigated the impact of various system parameters on Fe release which is important in the context of establishing and using the relationship between Fe release and As removal.

5.1. Quantitation of Fe release in ME treatment

A series of experiments was undertaken to quantify weight loss of the ZVI media and formation of suspended solids in ME treatment. Results of these experiments showed that the weight of air-dried solids separated from pH-adjusted ME-treated effluents ranged from 2.1 to 3.1 g/L across different ME treatment cycles. Despite the observed variations of the mass of Fe-based solids formed in sequential ME cycles, little difference was observed in the behavior of Fe species remaining in ME-treated effluent after its pre-filtration in the absence of pH adjustment. Sequential filtration experiments confirmed that the Fe species present in ME treated effluents were mostly ferrous compounds whose concentration decreased by about 40% as the filter pore size decreased. However, Fe concentrations passing 0.2 μm filters remained high.

While Fe concentrations in prefiltered ME-treated effluents decreased with the filter pore size, concentrations of As and Sb species remaining in LFG condensate after its treatment were unaffected by filtration. This suggests that these species were solutes that were not readily removed by filtration, nor were they sorbed of Fe colloidal particles or amenable to removal by coagulation. While the residual As and Sb species can be removed by further ME treatment, this is not necessary practically, once the target level of As removal, for instance 90%, is achieved.

These findings also highlight the need for careful consideration of post-treatment handling and disposal requirements for ME-treated effluents and their byproducts. The estimated weight of Fe-based formed post-treatment in pH-adjusted ME-treated effluents may be considerable thus necessitating further research on best practices needed for appropriate handling and disposal of these treatment byproducts.

5.2. Effects of ME treatment conditions on Fe release

The influence of various treatment parameters such as pH, mixing intensity and other conditions on Fe release was explored in this study. The data show that low pH levels, e.g., 3.0 to 3.5, result in higher rates of Fe release, which also corresponds to higher rates of removal of As and Sb from LFG condensate. However, excessively low pH levels, for instance those below 3, were deemed impractical due to the instability of ZVI surfaces and potentially increased As volatilization which needs controlled or even suppressed or eliminated in practical ME operations. These results confirm that pH 3.0 is the most optimal condition for ME treatment, ensuring efficient contaminant removal while minimizing operational challenges.

We also investigated the effects of variable top-offs and mixing intensity on Fe release and treatment efficiency. The combination of ZVI and GAC as top-offs was found to be accompanied by higher rates of Fe release and better maintenance of ME treatment. Experiments using variable mixing conditions showed that higher mixing speeds promote greater Fe release and faster removal of As and Sb from LFG condensate.

These findings underscore the importance of optimizing operational parameters in ME treatment. By understanding the factors influencing Fe release, it is possible to fine-tune ME treatment processes practically in real time to ensure ME treatment' consistent and effective performance across various conditions.

5.3. Fe release in ME treatment as a surrogate parameter for As removal estimates

The investigation into the significance of correlations between As/Sb removal and Fe release during ME treatment resulted in gaining further insights and development of practical approaches to estimate the efficacy of ME treatment. All experiments carried out in this study show that Fe release can be employed as a surrogate parameter for tracking the progress and efficiency of ME treatment. The reliability and reproducibility of Fe detection techniques, combined with the relative simplicity of the 1,10-Phen method and the intrinsic relationship between Fe release and As or Sb removal result in multiple advantages of this approach over the alternative of ORP

measurements which were deemed in prior studies carried out by our group to be a suitable surrogate for the efficiency of ME treatment.

The relationship between As removal and Fe release during ME treatment depends in some extent on ME treatment cycle number and pH, with Fe release tending to be higher for the initial cycle of ME treatment and lower pHs. Despite these differences, As removal vs. Fe release correlations can serve as actionable predictors of arsenic removal. By establishing typical ranges of Fe release correlated with specific As removal objectives, a practically implementable metric for monitoring the progress of ME treatment in field conditions can be developed.

5.4. Future work

5.4.2. Enhanced understanding of system conditions affecting Fe release and As removal

- **Type and Characteristics of GAC/ZVI:** Investigating the influence of different types and characteristics of GAC and ZVI on Fe release can provide insights into their reactivity and suitability for ME treatment. Variations in pore size, surface area, and surface chemistry may affect the speciation, redox and adsorptive reactions of Fe solutes, ultimately influencing overall Fe release and As/Sb removal.
- **Interference Analysis:** It is necessary to conduct additional experiments to investigate the effects of potentially interfering compounds (e.g., Ni, Mn & Cr) whose release from the active media can vary significantly between different types of ZVI, its concentrations, ME treatment cycle number and other treatment conditions. This will help to better understand and mitigate any factors that may impact the accuracy of Fe determinations using the 1,10-Phen method when it is used in field conditions.
- **Model Refinement:** The data presented above demonstrate a need to develop separate correlations for different ME treatment cycles. This will allows developing more precise cycle-specific estimates of ME treatment efficiency in field conditions.
- **Cycle Number:** Examining the effects of treatment cycle number and media aging on Fe release can help assess the long-term performance and stability of ME treatment systems. Over successive treatment cycles, ZVI/GAC media may undergo changes in the structure and reactivity of their surfaces, potentially impacting Fe release kinetics and treatment efficiency. The nature of such changes must be understood in sufficient detail.

- **Hydraulic Conditions:** Exploring the influence of hydraulic conditions, such as mixing flow direction and mixing rates on Fe release can help optimize ME reactor design and practical ME operations.
- **Integration of Advanced Characterization Techniques**: Integrating advanced characterization techniques, for instance scanning electron microscopy (SEM), X-ray diffraction (XRD) and others, can provide valuable insights into the mechanisms governing Fe release and As/Sb removal during ME treatment. By characterizing the morphology and composition of media particles before and after treatment, we can elucidate the mechanisms underlying Fe release and identify factors contributing to treatment efficiency.

5.4.3. Suggestions of future work for ME treatment

- **Use of model systems:** Utilizing a typical ME treatment with a DMA model offers a valuable opportunity to gain deeper insights into the kinetics and mechanisms of As removal and Fe release in ME treatment.
- **Extension of media cycling:** To enhance the recycling capacity of active media, it is imperative to further optimize supplementary dosages and explore alternative catalysts. Given that GAC has demonstrated significant As retention, the efficiency of media cycling may be constrained by factors such as available GAC surface area or fouling of ZVI/GAC surfaces during ME treatment. Considering GAC's non-selectivity and its potential to retain numerous constituents present in LFG condensate beyond As and Sb alone, there is merit in investigating the efficacy of larger top-off doses, particularly those containing higher quantities of GAC.
- **Media regeneration:** Exploration of media regeneration techniques, such as the application of strong acids to the ZVI phase, is essential to prolong the useful lifespan of ME treatment media. This endeavor holds promise for mitigating media costs and reducing the volume of hazardous waste generated.

6. Appendix

6.1. Materials for ME treatment

6.1.1. Personal protection equipment (PPE)

- Laboratory coats
- Safety goggles
- Carbon activated masks
- KN95 masks
- Safety nitrile gloves
- Sampling pants
- Sampling gloves

6.1.2. Column reactors

Fabrication of the microelectrolysis reactors requires both commercially available materials and tailor designed 3D pieces. All the materials used are listed below:

a) Materials:

- PVC columns
- Plastic barbed tube fittings
- Marine Weld adhesive
- Silicone 100% waterproof
- Spray on protective enamel
- Electric tools: 20V cordless drill, variable-speed Dremel
- Common tools: saw, hammer, screwdrivers, pliers, tweezers, and scissors.
- Regular and sealant tape
- Tygon® tubing
- Ender Pro 5 3D and Flashforge Adventurer 4 3D printers
    - The printers were used to fabricate selected components of ME reactors that would be difficult to make or order conventionally.
- Silk Polylactic Acid (PLA) 3D printing filament 1.75 mm

b) Instrumentation and sensors:

- Advanced electrochemistry multimeters

- Data acquisition kit
- ORP electrodes
- pH meters
- pH controllers
- Gas flowmeters
- Digital timer outlets

c) Software:

- AutoCAD Autodesk student version

6.1.3. Experiments equipment and materials

a) Equipment:

- Electric mixer JJ-1, permanent magnet DC motor 60W
- Cartridge Filter
- Grooved sediment water filter cartridge
- Positive displacement pumps
- Air pumps
- Anton Paar Multiwave 3000 Microwave digestor
- Mettler Toledo Compact titrator G20
- Magnetic agitators
- Scale
- Voltage converter
- Autosampler

b) Materials:

- Glass beakers
- Glass bottles
- Plastic bottles
- Funnels
- Vacuum filters
- Pipettes
- One-way valves
- Rubber stoppers

- Grommets and washers

c) Consumables:

- MilliQ and DI water
- Filter papers and membranes
- Pipette tips
- Syringes
- Plastic weighing containers
- In-line filters (0.45 um)
- Disposable spatulas
- Glass beads
- Vacuum grease
- Disposable bags
- Disposable bottles
- Paper towels

d) Reagents

Table 6-1 Reagents used for ME experiments

Reagent	CAS Number	Supplier
LC Plus Fine (Zero Valence Iron)	7439-89-6	Hoganas
LC Plus (Zero Valence Iron)	7439-89-6	Hoganas
Powder Activated Carbon	7440-44-0	Fisher Chemical
Granular Activated Charcoal (12-40 mesh)	7440-44-0	Acros Organics
Sulfuric Acid	7664-93-9	VWR analytical
Hydrochloric Acid	7647-01-0	Supelco
Sodium Hydroxide	1310-73-2	Fisher Scientific
USP Grade Carbon Dioxide	124-38-9	Linde Gas
Potassium permanganate	7722-64-7	Fisher Chemical
Sodium sulfite	7757-83-7	Fisher Chemical
Nitric Acid, Trace Metal Grade	7697-37-2	Fisher Chemical
Arsenic (III)	ICP-151	Agilent

Reagent	CAS Number	Supplier
Antimony	ICP-033	Agilent
ICP-MS Yttrium standard	IMS-115	Ultra Scientific

6.2. Experiments with SR21 landfill gas condensate: results of ME treatment

Due to the extreme turbidity and high levels of suspended solids in SR21, we filtered 1 liter from bottle 6 to separate the solids from the sample. Bottle 6 was specifically chosen as it was collected from the bottom of the sampling well, where a higher concentration of suspended solids is likely present. This allows for a greater quantity of solids for subsequent experiments (Section 6.3). This filtration process not only enhances the treatment conditions but also mitigates some post-treatment challenges.

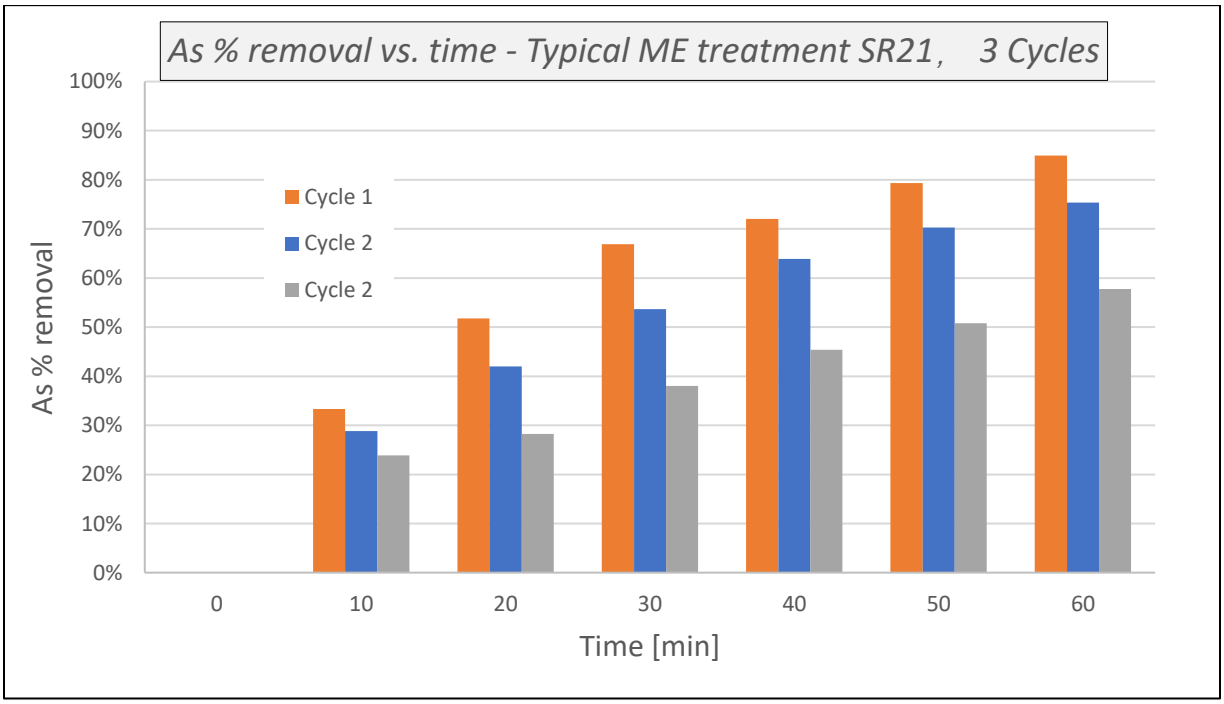

Fig 6-1 Arsenic removal vs. treatment time for three consecutive cycles of ME treatment of SR21 LFG condensate (experiment carried out on 24/05/07). 0.25 L Mini Column 1 ME reactor, 50 g/L active media, ZVI/GAC weight ratio 2:1, 2 g/L cycle top offs, pH 3 (0.5M H2SO4), pre-treatment CO_2 flush, 1000 rpm mixing rate.

Fig 6-1 illustrates the percentage of As removal over time during a typical ME treatment in SR21 across three 1-hour cycles. In Cycle 1, an 85% As removal rate was achieved, while Cycles 2 and 3 achieved 76% and 58% removal rates, respectively. However, the As removal efficiencies in all three cycles were lower compared to experiments conducted under the same conditions with SR19 and SR20.

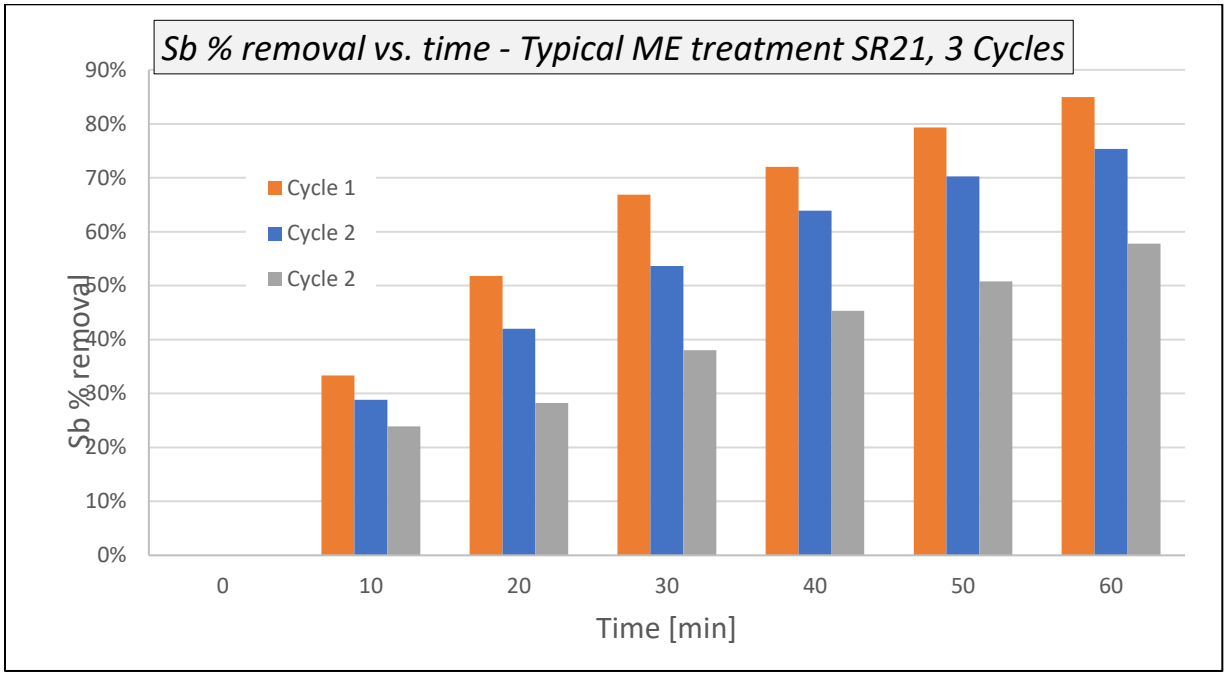

Fig 6-2 Antimony removal vs. treatment time for three consecutive cycles of ME treatment of SR21 LFG condensate (experiment carried out on 24/05/07). 0.25 L Mini Column 1 ME reactor, 50 g/L active media, ZVI/GAC weight ratio 2:1, 2 g/L cycle top offs, pH 3 (0.5M H2SO4), pre-treatment CO_2 flush, 1000 rpm mixing rate.

A similar trend is observed for Sb removal, with SR21 achieving only 85% removal for cycle1, which is 5% to 8% lower than previous data. Cycle 2 achieves 75% removal and cycle 3 achieves only 57%, which is much less removal compared to the results in SR20. Additionally, the removal rate is noticeably slower. In SR20, ME treatment achieved more than 70% Sb removal within the first 10 minutes, which is twice the rate observed in SR21. This discrepancy suggests that the composition of SR21 differs from that of SR20 and SR19. Furthermore, the filtration process may have impacted the removal efficiency, as this step was not performed for SR19 and SR20.

6.3. Characterization of SR21 landfill gas condensate: metal release from particulates isolated from SR21

SR21 is the latest sample obtained from the landfill, having remained in the waste tank for several months. Characterized by extreme turbidity and the presence of grey suspended solids, this sample is of particular interest. It comprises six bottles in total, with bottle 1 obtained from the upper level of the tank and bottle 6 is retrieved from the bottom of the tank. As the samples we got is from different water level, it's not clear to us if each level has the same compounds and same amount of TDS. Each bottle of sample is fully shake before pouring out. 50 mL of each bottle's sample is filtered through 0.2 um membrane. Redox potential, pH, TDS (Total Dissolved Solids) and conductivity are tested both before and after filtration, and Fe is determined by 1,10-Phen method.

Table 6-2 pH, ORP, conductivity and TDS of SR21(pre and post filtration), 6 bottles

		SR21			
		pH	ORP [mV]	Conductivity [µS/cm]	TDS [ppm]
Bottle 1	Pre-filtration	8.2	-233.9	16204	8102
	Post-filtration	8.2	-208.3	17040	8520
Bottle 2	Pre-filtration	8.2	-278.8	16578	8280
	Post-filtration	8.2	-229.9	17280	8640
Bottle 3	Pre-filtration	8.1	-229.2	17160	8580
	Post-filtration	8.3	-73.3	17460	8730
Bottle 4	Pre-filtration	8.2	-252.8	16800	8280
	Post-filtration	8.2	-215.2	17640	8820
Bottle 5	Pre-filtration	8.2	-251	16324	8162
	Post-filtration	8.3	-52.5	18600	9300
Bottle 6	Pre-filtration	8.2	-103.7	18180	9090
	Post-filtration*	8.3	72.6	19436	9718

Table 6-2 shows that SR21 LFG condensate had an average pH of 8.2. Typically, the pre-filtration pH was slightly lower than the post-filtration pH. The ORP measurement experiences significant fluctuations between each bottle, both before and after filtration. The ORP reading for post-

filtration bottle 6 registers at 72.6 mV, representing the sole positive reading among all samples. This variability in ORP levels may be attributed to the duration of sample exposure to air. Additionally, conductivity increase with the bottle number, suggesting a correlation between depth and conductivity. TDS also exhibit a similar trend, increasing with bottle number, indicating that deeper samples contain higher concentrations of settled solids.

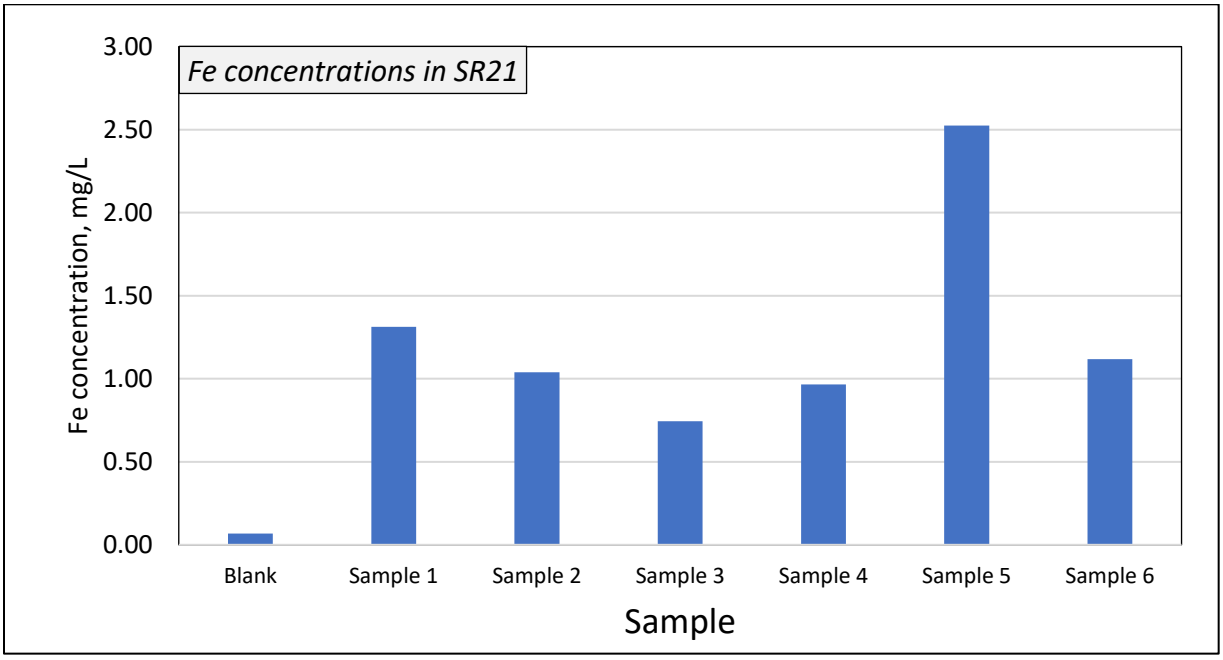

Fig 6-3 Fe concentrations in six consecutively taken samples of SR21 LFG condensate.

Fig 6-3 shows Fe concentrations in the six container with SR21 gas condensate filtered through a 0.2 um membrane. Concentrations of Fe tend to relatively low at ca. 1 mg/L, with sample 5 exhibiting the highest Fe concentration at 2.5 mg/L. Given the absence of only 1g/L of Fe in all six filtered SR21 samples, an investigation is underway to determine whether the suspended solids may contain Fe, in addition to As and Sb.

The suspended solids which separated from bottle 6 were air-dried for three days. To examine the effect of pH on Fe and As release, we prepared three bottles each containing 100 g of Milli-Q water and 100 mg of the dried solids (solid concentration = 1 g/L), supplemented with 0.01 M $NaNO_3$ as a background salt. The pH of each bottle was adjusted to 2, 3, and 4 respectively using HNO_3. Samples were periodically taken using syringes and filtered through 0.45 µm filters for both 1,10- Phen method and ICP-MS analysis.

6.3.1. Fe release

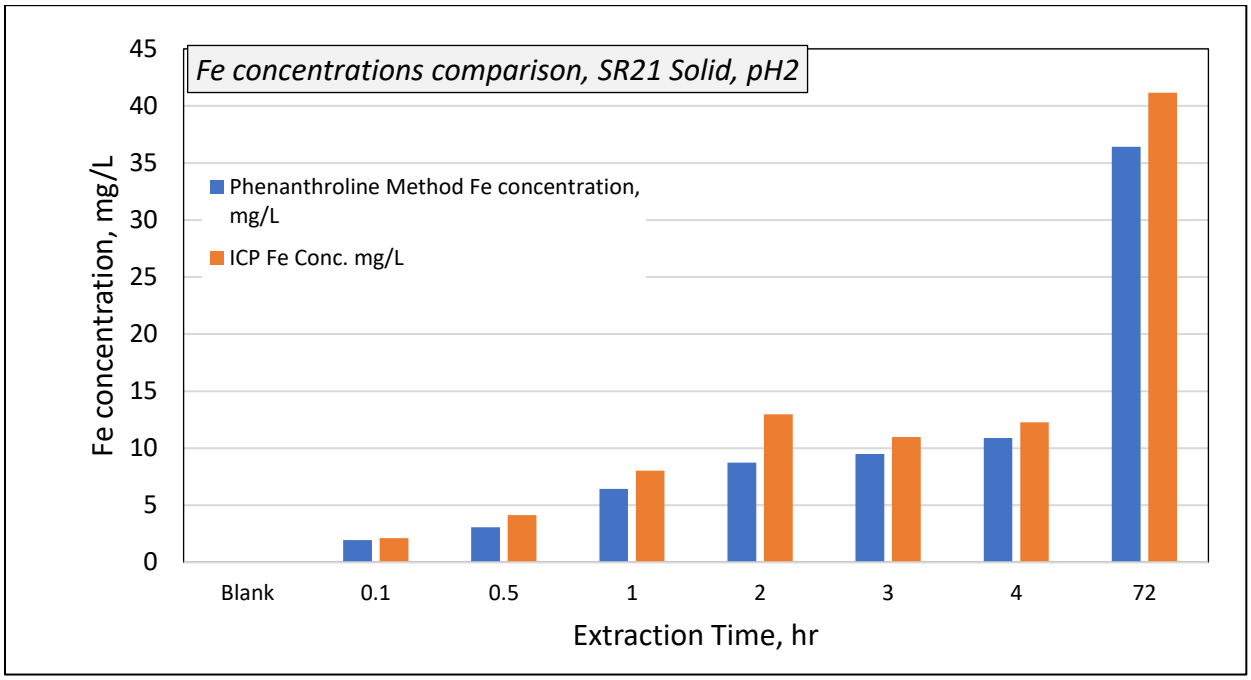

Fig 6-4 Comparison of Fe concentrations determined using the 1,10-Phen method and ICP-MS measurements using UW equipment, Experimental conditions: 1g/L SR 21 solids, pH 2, adjusted by HNO_3, 0.01M $NaNO_3$.

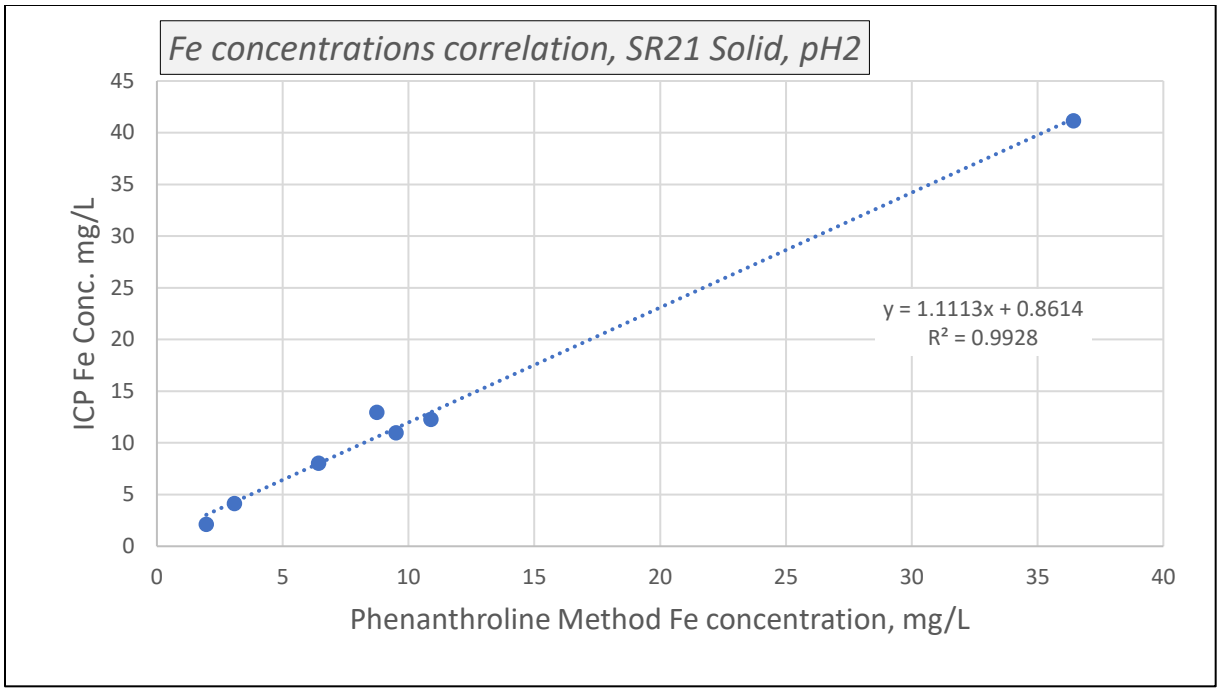

Fig 6-5 Correlation between Fe concentrations determined with the 1,10-Phen method and ICP-MS measurements using UW equipment, Experimental conditions: 1g/L SR 21 solid exposure, pH2, adjusted by HNO_3, 0.01M $NaNO_3$.

Fig 6-4 shows Fe release over three days of exposure of 1g/L SR21 solids at pH 2. The Fe concentration increases gradually over time, with minimal change during the first 4 hours, eventually reaching approximately 40 mg/L after 3 days' exposure. The ICP data shows a 10% higher Fe concentration compared to the Phenanthroline method. This discrepancy is likely due to the delay in sending the samples for ICP analysis, which may have allowed additional Fe to be reduced over the week. However, the correlation between the two measurements remains reliable, with an R^2 of 0.99, indicating high accuracy and consistency between the two methods. (Fig 6-5)

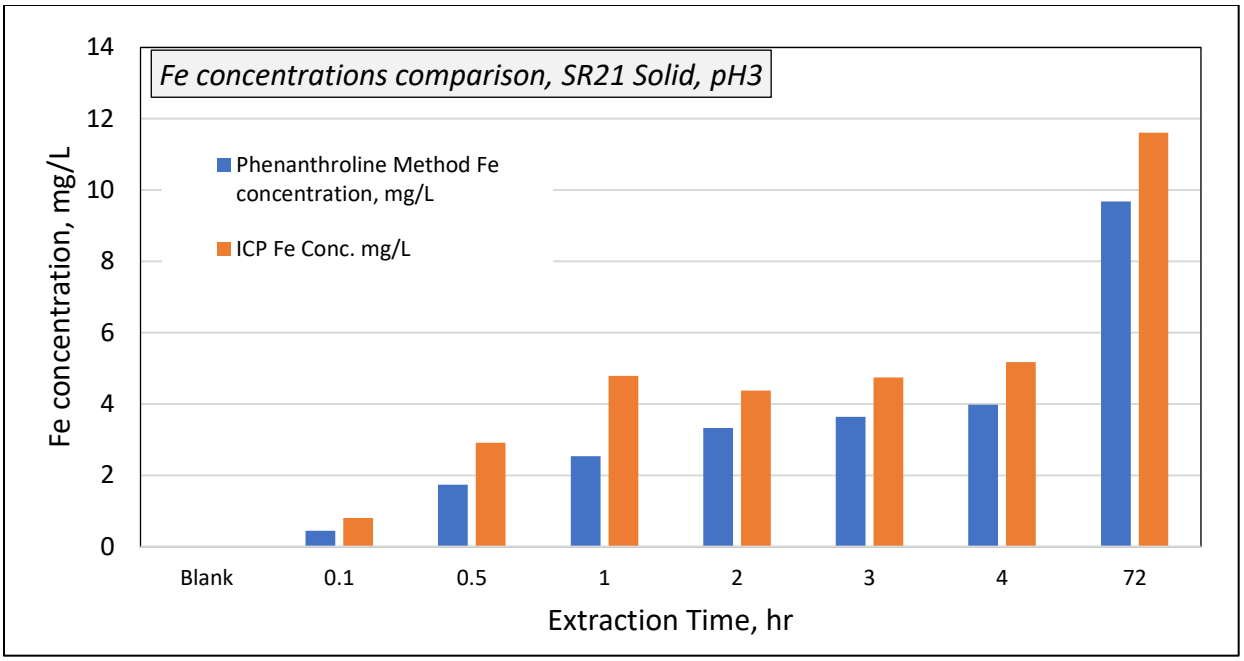

Fig 6-6 Comparison of Fe concentrations determined using the 1,10-Phen method and ICP-MS measurements in UW, Experimental conditions: 1g/L SR 21 solid exposure, pH3, adjusted by HNO_3, 0.01M $NaNO_3$.

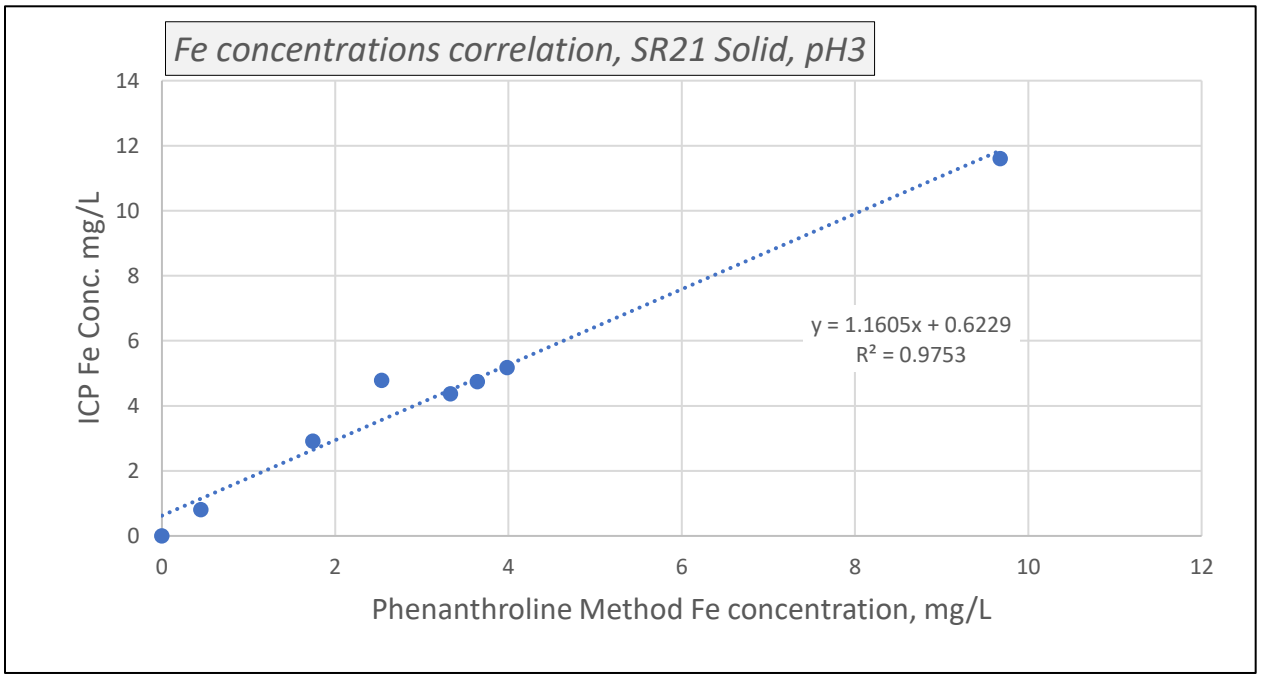

Fig 6-7 Fe concentrations correlation determined using the 1,10-Phen method and ICP-MS measurements in UW, Experimental conditions: 1g/L SR 21 solid exposure, pH3, adjusted by HNO_3, 0.01M $NaNO_3$.

In Fig 6-6, a similar trend is observed at pH 3, with increasing Fe release over time. At pH 3, approximately 10 mg/L of Fe is released after 3 days. Although more Fe is detected by ICP, the correlation between the two measurement methods remains reasonable, with an R^2 of 0.97 (Fig 6-7).

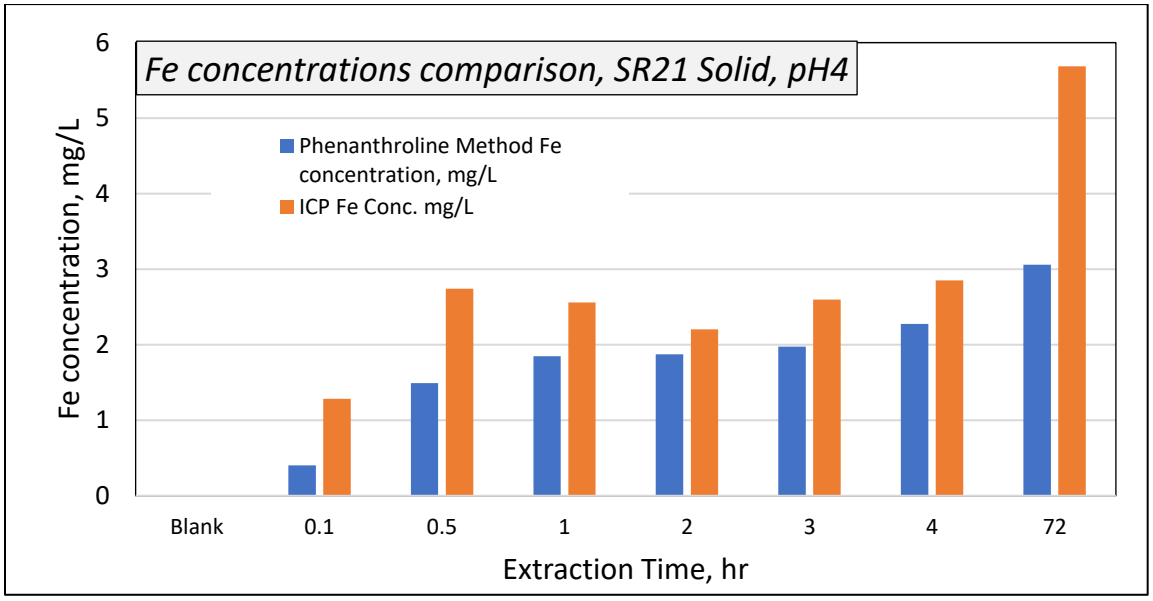

Fig 6-8 Comparison of Fe concentrations determined using the 1,10-Phen method and ICP-MS measurements in UW, Experimental conditions: 1g/L SR 21 solid exposure, pH4, adjusted by HNO_3, 0.01M $NaNO_3$

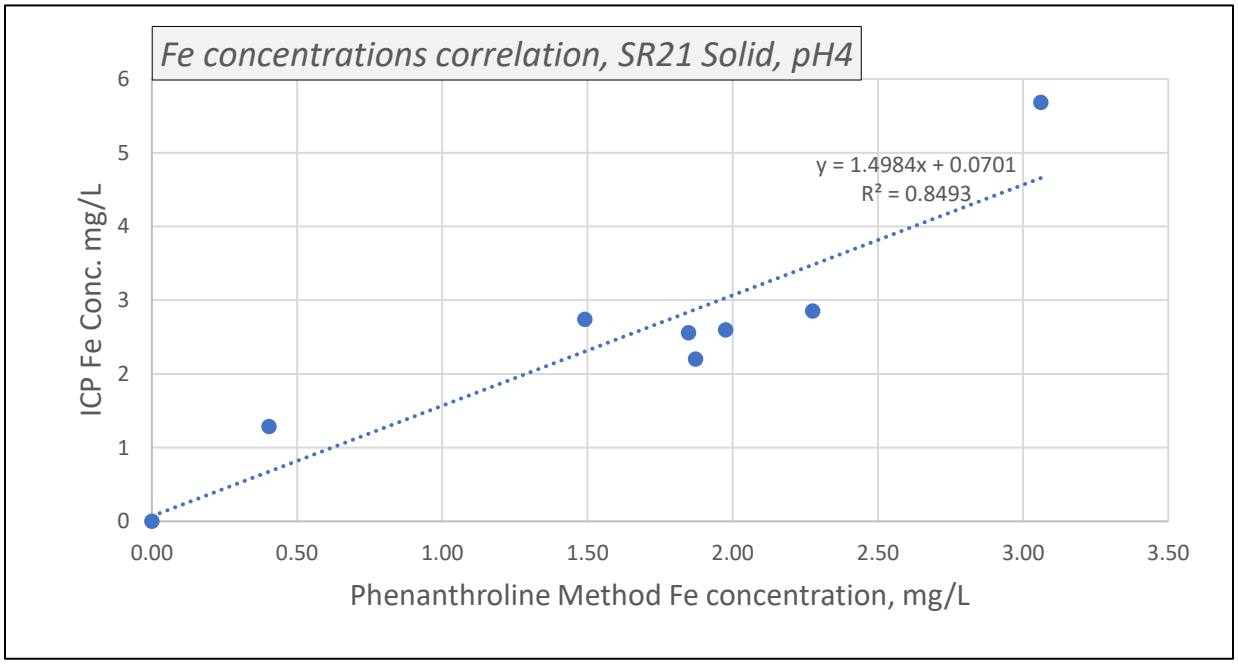

Fig 6-9 Fe concentrations correlation determined using the 1,10-Phen method and ICP-MS measurements in UW, Experimental conditions: 1g/L SR 21 solid exposure, pH3, adjusted by HNO_3, 0.01M $NaNO_3$.

In Fig 6-8, the Fe concentration shows a 50% discrepancy after 3 days of exposure at pH 4, with 3 mg/L measured by the 1,10-Phenanthroline method and 6 mg/L measured by ICP. The correlation between the two methods is poorer than at previous pH conditions, with an R^2 of only 0.84. (Fig 6-9)

The trends across the three different pH levels indicate that higher pH conditions lead to greater discrepancies between the measurements of the two methods. This is likely because lower pH levels better maintain the chemical environment for Fe, as Fe tends to remain in its soluble ionic form rather than precipitating as insoluble hydroxides under acidic conditions.

6.3.2. As & Sb release

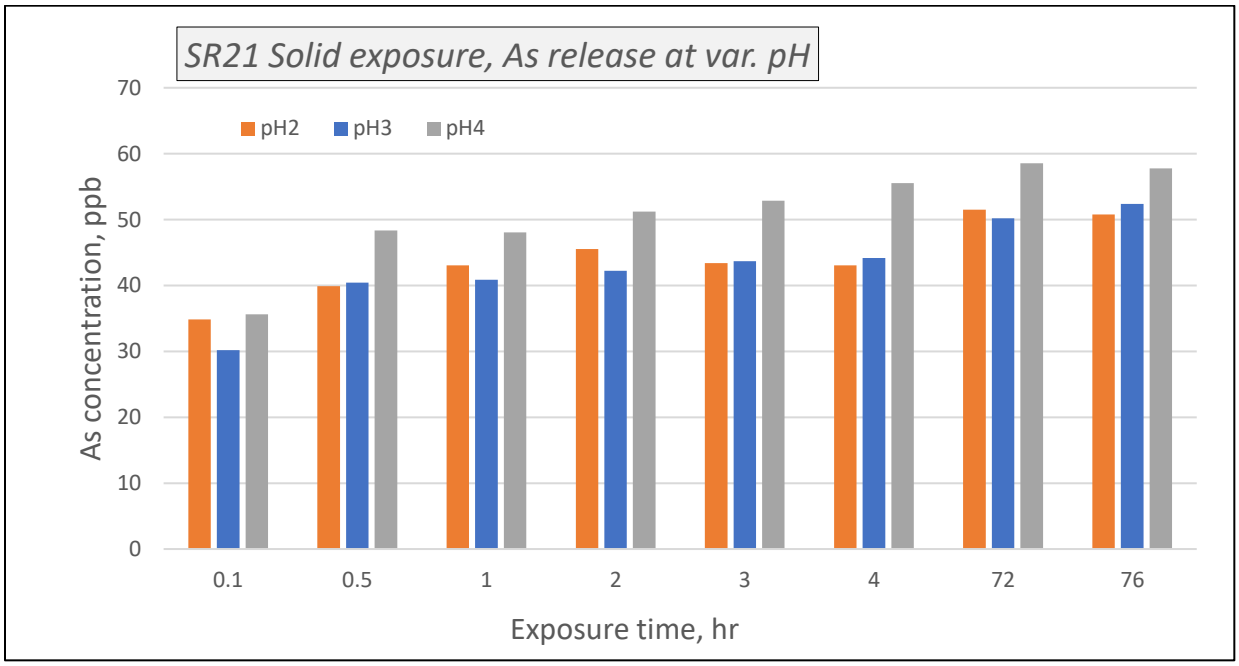

Fig 6-10 Comparison of As release at var. pH, Experimental conditions: 1g/L SR 21 solid exposure, adjusted by HNO_3, 0.01M $NaNO_3$.

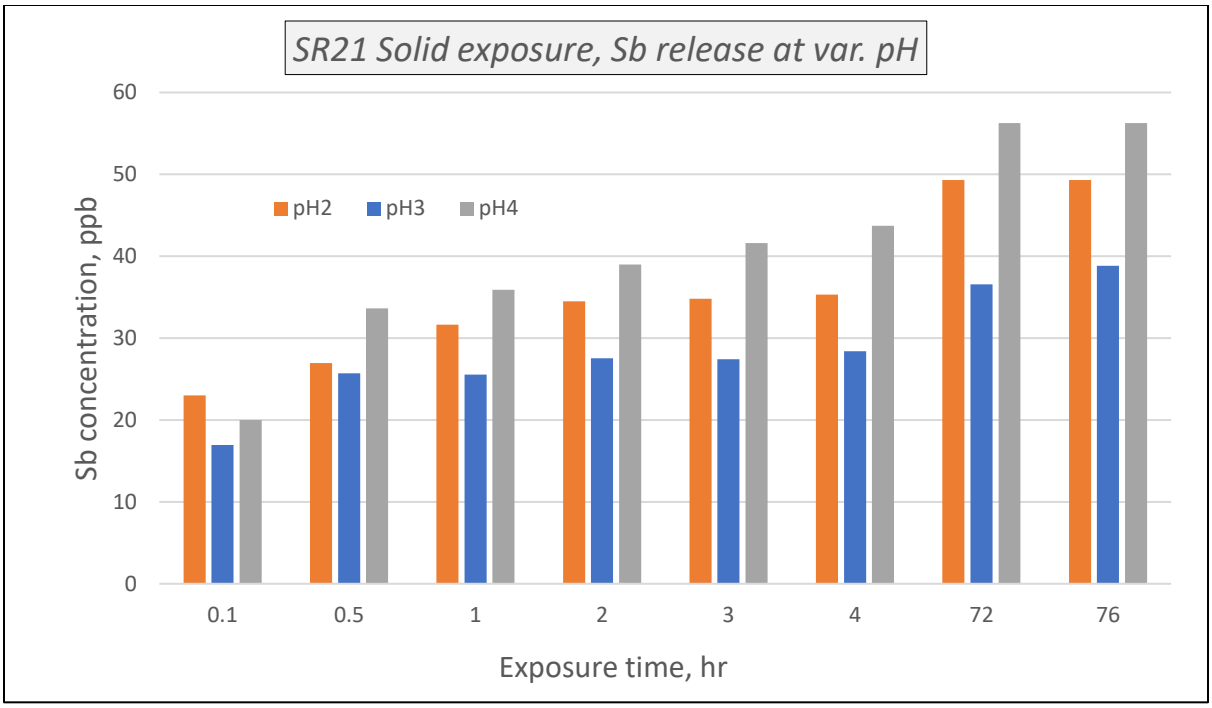

Fig 6-11 Comparison of As release at var. pH, Experimental conditions: 1g/L SR 21 solid exposure, adjusted by HNO_3, 0.01M $NaNO_3$.

From Fig 6-10, there is no significant difference in As release between pH 2 and pH 3. However, it is surprising that approximately 15% more As is released at pH 4 compared to pH 2 and pH 3.

However, the trend for Sb is different; most Sb is released at pH 4, followed by pH 2, with the least Sb release occurring at pH 3. (Fig 6-11)

Both As and Sb show the highest release at pH 4, suggesting that pH 4 may be the optimal condition for exposure experiments. However, compared to the original concentrations of As and Sb in SR21, the release observed is relatively small.

Due to the limited time, we only got one set of data from this type of experiment. Further experiments are needed to confirm and validate the reliability of this result.

References

Al-Ghouti, M.A., Razavi, M.M., 2020. Water reuse: brackish water desalination using Prosopis juliflora. Environ. Technol. Innov. 17, 100614.

American Cancer Society. (2023, June 1). Arsenic and Cancer Risk. https://www.cancer.org/cancer/risk-prevention/chemicals/arsenic.html

Anderson, D.L., 1989. Theory of the Earth. Blackwell Scientific Publications, Boston (pp. 289–305)

APHA Standard Methods, 22nd ed., Method 3500-Fe B (1997). ASTM D 1068-77, Iron in Water, Test Method A

Arsenic. (1977). National Academy of Sciences. https://www.ncbi.nlm.nih.gov/books/NBK231016/

Cheney-Irgens, A. (2022) Mass Balance of Arsenic in Microelectrolysis Treatment of Arsenic-Containing Landfill Gas Condensate and Initial Study of Formation of Volatile Arsenic Species[Master's thesis, University of Washington]. ProQuest Dissertations Publishing.

Cullen, W.R., Reimer, K.J., 1989. Arsenic speciation in the environment. Chem. Rev. 89, 713–764.

de Oliveira, F. D. G., Robey, N. M., Smallwood, T. J., Spreadbury, C. J., & Townsend, T. G. (2022). Landfill gas as a source of anthropogenic antimony and arsenic release. Chemosphere (Oxford), 307, 135739–135739. https://doi.org/10.1016/j.chemosphere.2022.135739

Determination of Landfill Gas Composition and Pollutant Emission Rates at Fresh Kills Landfill. U.S. Environmental Protection Agency, Region II: New York, 1995; EPA 902-R-95-001.

Dhaliwal, S.S., Singh, J., Taneja, P.K., Mandal, A., 2020. Remediation techniques for removal of heavy metals from the soil contaminated through different sources: a review. Environ. Sci. Pollut. Res. 27, 1319–1333. https://doi.org/10.1007/s11356-019-06967-1.

Elemental Analysis Core. (n.d.). ICP-MS as a Technique. Oregon Health & Science University. https://www.ohsu.edu/elemental-analysis-core/icp-ms

technique#:~:text=Mass%20Spectrometer%20(MS)%20separates%20the,concentration%20of%20each%20chosen%20element.

Environmental Protection Agency. (2003, July). Arsenic Treatment Technology Evaluation Handbook for Small Systems. Environmental Protection Agency. https://cfpub.epa.gov/safewater/arsenic/arsenictradeshow/Pubs/handbook_arsenic_treatment-tech.pdf

Environmental Protection Agency. (2023, November 22). National Overview: Facts and Figures on Materials, Wastes and Recycling. Environmental Protection Agency. https://www.epa.gov/facts-and-figures-about-materials-waste-and-recycling/national-overview-facts-and-figures-materials

Environmental Protection Agency. (2024, July). Inductively Coupled Plasma – Mass Spectrometry (Method 6020B). Environmental Protection Agency. https://www.epa.gov/sites/default/files/2015-12/documents/6020b.pdf

Ferguson, J. F.; Anderson, M. A. Chemical forms of arsenic in water supplies and their removal. In Chemistry of water supply, treatment, and distribution; Rubin, A. J., Ed.; Ann Arbor Science, Ann Arbor, MI, 1974; pp 137-158

Fu, F.L., Dionysiou, D.D., Liu, H., 2014. The use of zero-valent iron for groundwater remediation and wastewater treatment: a review. J. Hazard. Mater. 267, 194e205.

Gillham, R.W., O'Hannesin, S.F., 1994. Enhanced degradation of halogenated aliphatics by zero-valent iron. Ground Water 32(6), 958e967.

Hao, L., Wang, N., Wang, C., Li, G., 2018. Arsenic removal from water and river water by the combined adsorption-UF membrane process. Chemosphere 202, 768e776.

Hu, Y., Boyer, T.H., 2018. Removal of multiple drinking water contaminants by combined ion exchange resin in a completely mixed flow reactor. J. Water Supply Res. Technol. - Aqua 67 (7), 659e672.

Huang, P.P., Cao, C.Y., Wei, F., Sun, Y.B., Song, W.G., 2015. MgAl layered double hydroxides with chloride and carbonate ions as interlayer anions for removal of arsenic and fluoride ions in water. RSC Adv. 5 (14), 10412e10417.

Hughes MF, Beck BD, Chen Y, Lewis AS, Thomas DJ. 2011. Arsenic exposure and toxicology: a historical perspective. Toxicol. Sci. 123(2):305–32

J.A. Tetlow and A.L. Wilson, "The Absorptiometric Determination of Iron in Boiler Feed-Water", Analyst, Vol. 89, p. 442 (1964)

Karakurt, S., 2019. Removal of carcinogenic arsenic from drinking water by the application of ion exchange resins. Oncogen J. 2 (1), 5

King County. (2024). Environmental Lab. King County. https://kingcounty.gov/en/legacy/depts/dnrp/wlr/sections-programs/environmental-lab

King County. (n.d.). Facts about arsenic. King County. https://kingcounty.gov/en/legacy/depts/health/environmental-health/toxins-air-quality/arsenic-lead/about-arsenic#:~:text=Arsenic%20has%20a%20long%20history,quantities%20in%20semi%2Dconductor%20manufacturing.

Korte, N. E.; Fernando, Q. Crit. Rev. Environ. Control 1991, 21, 1-39.

L.F. Greenlee, J.D. Torrey, R.L. Amaro, J.M. Shaw, Kinetics of zero valent iron nanoparticle oxidation in oxygenated water, Environ. Sci. Technol. 46 (2012)12913–12920.

Laatikainen, M., Sillanpaa, M., Sainio,T..2016.Comparison of ion exchange process configurations for arsenic removal from natural waters. Desalination and Water Treatment 57(29),13770-13781.

Liu, S., Kuznetsov, A. M., Han, W., Masliy, A. N., & Korshin, G. V. (2022). Removal of dimethylarsinic acid (DMA) in the Fe/C system: roles of Fe (II) release, DMA/Fe (II) and DMA/Fe (III) complexation. Water Research, 213, 118093.

Long, H., Zheng, Y.J., Peng,Y.L., Jin, G.Z., Deng, W.H., Zhang,S.C.,2019.Comparison of arsenic (V) removal with different lead-containing substances and process optimization in aqueous chloride solution.Hydrometallurgy 183,199-206.

Maitlo, H.A., Kim, J.H., Kim, K.H., Park, J.Y., Khan, A, 2019. Metal-air fuel cell electrocoagulation techniques for the treatment of arsenic in water. J. Clean. Prod. 207, 67-84.

Mari Pantsar-Kallio , Anu Korpela. (2000). Analysis of gaseous arsenic species and stability studies of arsine and trimethylarsine by gas chromatography-mass spectrometry. Analytica Chimica Acta Volume 410, Issues 1–2, 20, Pages 65-70

Matschullat J (2000) Arsenic in the geosphere—a review. SciTotal Environ 249:297–312. doi:10.1016/S0048-9697(99)00524-0

Mohan, D., Dey, S., Dwivedi, S.B., Shukla, S.P., 2019. Adsorption of arsenic using low cost adsorbents: guava leaf biomass, mango bark and bagasse. Curr. Sci. 117 (4), 00113891.

Mosier, D.L., Beger, V.I. & Singer, D.A. (2009). Volcanogenic massive sulfide deposits of the world: database and grade and tonnage models. U.S. Geological Survey Open- File Report 2009-1034. Available from http://pubs.usgs.gov/of/2009/1034.

Panico, A. (2023). [Master's thesis, Università degli Studi di Napoli Federico II].

Parris, G. E., & Brinckman, F. E. (1976). Reactions which relate to environmental mobility of arsenic and antimony. II. Oxidation of trimethylarsine and trimethylstibine. Environmental Science & Technology, 10(12), 1128–1134. https://doi.org/10.1021/es60122a010

PerkinElmer. (n.d.). *NexION 2000B ICP Mass Spectrometer*. PerkinElmer. https://www.perkinelmer.com/product/nexion-2000b-icp-ms-configuration-n8150044

Pinel-Raffaitin, P.; Ponthieu, M.; Le He´cho, I.; Amouroux, D.; Mazeas, L.; Donard, O. F. X.; Potin-Gautier, M. Evaluation of the analytical strategies for the determination of metal concentrations to assess landfill leachate contamination.J. Environ. Monit. 2006, 8, 1069-1077.

Pinochet-Troncoso, I. (2023). Optimization of Microelectrolysis Treatment to Remove Arsenic from Landfill Gas Condensate and Correlations Between Changes of Redox Potential and Arsenic Removal [Master's thesis, University of Washington]. ProQuest Dissertations Publishing.

Rifkin, G. (2021). Arsenic in Landfill Gas Condensates and Gas Treatment Solids: A Study of Removal by Alternative Treatment Approaches and Mobilization [Master's thesis, University of Washington]. ProQuest Dissertations Publishing.

Sahoo, P. K., & Kim, K. (2013). A review of the arsenic concentration in paddy rice from the perspective of geoscience. Geosciences Journal, 17, 107-122.]

Sarkar, A., Paul, B., 2016. The global menace of arsenic and its conventional remediation-a critical review. Chemosphere 158, 37e49.

Schlepp, G. (2024). Continued optimization of a microelectrolysis treatment process for removal of arsenic from landfill gas condensate, characterization of materials, and evaluation of Fe as a predictor of treatment monitoring [Master's thesis, University of Washington]. ProQuest Dissertations Publishing.

Shih, M. C. (2005). An overview of arsenic removal by pressure-driven membrane processes. Desalination, 172(1), 85-97.

T.Z. Liu, P.H. Rao, M.S.H. Mak, P. Wang, I.M.C. Lo, Removal of co-present chromate and arsenate by zero-valent iron in groundwater with humic acid and bicarbonate, Water Res. 43 (2009) 2540–2548.

Ungureanu, G., Santos, S., Boaventura, R., Botelho, C., 2015. Arsenic and antimony in water and wastewater: overview of removal techniques with special reference to latest advances in adsorption. J. Environ. Manag. 151, 326e342.

Walters, S. (2022). A study of removal techniques for arsenic species in landfill gas condensate. [Master's thesis, University of Washington]. ProQuest Dissertations Publishing.

Wang, P., Sun, G., Jia, Y., Meharg, A. A., & Zhu, Y. (2014). A review on completing arsenic biogeochemical cycle : Microbial volatilization of arsines in environment. Journal of

Environmental Sciences (China), 26(2), 371–381. https://doi.org/10.1016/S1001-0742(13)60432-5

WHO. Guidelines for Drinking Water Quality, Vol 1: Recommendations, 2nd ed.; WHO: Geneva, 1993.

Yan, X., Fan, X., Wang, Q., Shen, Y., 2017. An adsorption isotherm model for adsorption performance of silver-loaded activated carbon. Therm. Sci. 21 pp. 48-48. ynnyk, K., Hojjati, B.,

Yokogawa. (2014, March). Basics of ORP. Yokogawa. https://www.yokogawa.com/us/library/resources/white-papers/basics-of-orp/

Zhao, R., Novak, J. T., & Douglas Goldsmith, C. (2013). Treatment of organic matter and methylated arsenic in landfill biogas condensate. Waste Management (Elmsford), 33(5), 1207–1214. https://doi.org/10.1016/j.wasman.2013.01.013